Prince Edward Island, Canada

LINKING STRUCTURAL, FUNCTIONAL AND CLINICAL INISHGT GAINED FROM IMAGING

2019 IWOAI

INTERNATIONAL WORKSHOP ON OSTEOARTHRITIS IMAGING

June 26-28, 2019
Rodd Charlottetown Hotel
75 Kent Street
PEI
iwoai.org / isoai.org
info@isoai.org

13th Annual International Workshop on Osteoarthritis Imaging

Contents

A message from our organizers

Dear Workshop Attendees,

Welcome to beautiful Prince Edward Island and the 13th International Workshop on Osteoarthritis Imaging. We hope you are as excited about the scientific and social program as we are!

This year we are focussing our osteoarthritis lens towards the theme of 'Linking Structural, Functional & Clinical Insight Gained From Imaging'. We will approach this theme from several angles and we hope this will allow us to see the 'links' in different ways throughout the meeting. The first day will focus on novel analytics and computational approaches with the pre-workshop machine learning segmentation challenge in the morning and then related machine learning talks in the afternoon. In these talks, our invited speakers will demystify the topics of machine learning for image classification and segmentation. Day 2 will highlight what imaging has taught us on the topics of tissue and joint function in the morning and early detection and phenotyping in the afternoon. On the final day, our invited speakers provide us with an update of OA clinical trials and population studies and then we will end off the meeting with a head-to-head with a debate on the need for biomarkers in OA research.

Of course throughout the workshop we will be hearing from you, the attendees, through abstract presentations at the oral and poster sessions; your contribution and varying expertise is essential so that we can see the links in our field. It is our hope that you will keep the linking theme at the forefront of your thoughts throughout the workshop and maybe even identify some connections that you hadn't noticed before.

Thank you for making the trip so that we can come together as trainees, clinicians and scientists to listen, learn and inspire one another. In Anne of Green Gables, a teacher once says to Anne 'I'm hoping that you'll be enthusiastic enough about my classes that you'll pepper me with questions'; we too hope that you will pepper each other with questions and generate some lively discussion!

Your workshop chairs,

JD Johnston
Emily McWalter

Summary of Our New Society By-laws

The purpose of the International Society of Osteoarthritis Imaging (ISOAI), Inc. (the "Society") is to coordinate, develop, promote and foster the advancement of scientific research and clinical practice in osteoarthritis imaging through education and research. Imaging is critical in both the diagnosis and management of osteoarthritis. Clinical trials and epidemiological studies characteristically utilize imaging-derived inclusion/exclusion criteria as well imaging based outcome measures.

The Society seeks to provide researchers, physicians, allied health professionals and scientists with educational programs and materials of the highest quality, and to constantly improve the content and value of these educational activities. We seek to promote research in all aspects of osteoarthritis imaging and related research and sciences, including basic clinical research in the promotion of quality healthcare for the billions of people suffering from osteoarthritis.

The Society will bring together a closer fellowship among all branches of medicine, research, science, and industry allowing for greater cooperation among the osteoarthritis community dedicated to the furtherance of the understanding, diagnosis, management and cure of osteoarthritis. We deem it necessary in our mission to stimulate the exchange of knowledge and ideas among Society members and between Society members and non-members by providing meetings and digital forums for the presentation and discussion of clinical case studies, scientific papers, and reviews on all aspects of osteoarthritis imaging, related pathology and clinical management. To foster the development of groups or societies in and outside of the United States where the diagnosis and clinical management of osteoarthritis remains subordinate. Additionally, we seek to establish and maintain a Journal, in the year 2020, that will be the official publication of the Society.

Current Board of Directors

Ali Guermazi, President
Felix Eckstein, Vice President
Christoph Ladel, Member
Colin Miller, Member
Tuhina Neogi, Member
Frank Roemer, Member
Julie O'Malley, Treasurer
Shannon Desmond, Executive Director

Currently Accepted Advisory Board

Akshay Chaudhari
Michel Crema
Olga Kubassova
James MacKay

Patrick Omoumi
Jos Runhaar
Peter Steiger
Tom Turmezei

Our Sponsors

This workshop would not have been possible without financial support from our industry and academic partners. Please, notice their name tags indicating SPONSOR and thank them for their continued support of our workshop.

Diamond Level

Platinum Level

Gold Level

Our Sponsors

Silver Level

KOLON TISSUEGENE

parexel.

samumed

SYMICBIO

Bronze Level

chondrometrics

imorphics

SCANCO MEDICAL

General Conference information

General Conference Questions:

Point Persons: J.D. Johnston and Shannon Desmond.
Please ask them any questions.
Email: info@isoai.org.
This will be monitored at all times during the conference.
Mobile via call or text: +1 857 324-3940
This is the Society number and will go to
Shannon Desmond during the conference.

Scientific Questions

Besides asking questions orally, we will be monitoring a
Slack page where attendees can ask questions.
To install Slack on your device, please go to www.slack.com.
Information regarding the specific page(s) will be provided at
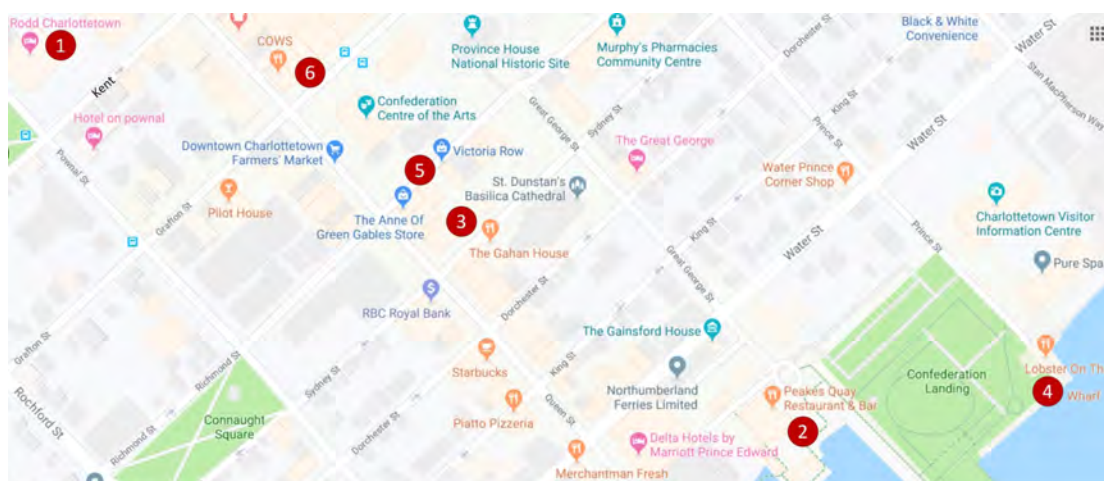*the meeting.*

Emergency

Emergency Services   911
Ambulance, Fire Department, Police

Conference Hotel

Rodd Charlottetown   75 Kent Street
+1 902-894-7371

Walking Routes

Thursday Morning Walk (07:00-07:45) – Walk from Rodd Charlottetown along waterfront to the lighthouse at Brighton Beach, and return. The walk, in total, should take approximately 45 minutes (22.5 minutes out, 22.5mm back).

The route at the end of Pownal St might be closed. If so, take the route indicated by the dotted red line.

Friday Morning Walk (07:00:07:45) – Walk from Rodd Charlottetown along waterfront, ending at Receiver Coffee in Vic Row. Attendees partaking in the Tuesday Dinner / Boat Trip may also consider taking this route as it goes thru Peakes Quay. It's a 32 minute walk, with 13 minutes to walk back to Rodd Charlottetown.

1. Rodd Charlottetown – Pownal & Kent - Conference Location
2. Peakes Quay – end of Great George St – Tuesday dinner at Chip Shack, Cow's Ice Cream & Boat Tour with Peakes Wharf Boat Tour
3. Olde Dublin / Claddagh Room – Queen & Sydney - Wednesday dinner. The Gahan House, a local brewery, is also in this area
4. Lobster on the Wharf – end of Prince St - Friday dinner. Enjoy deck and make way to Peakes Quay for live entertainment.
5. Victoria Row – Queen & Richmond - Popular pub/restaurant area. Receiver Coffee, a great little indie coffee shop, is also in this area
6. Cow's Ice Cream – Queen & Grafton – PEI Institution. There's also a Cow's location at Peakes Quay (#2)

13th International Workshop on Osteoarthritis Imaging

Linking Structural, Functional & Clinical Insight Gained From Imaging

26-28 June, 2019
Rodd Charlottetown, Charlottetown,
Prince Edward Island, Canada

Day 0 — Tuesday, 25th June

18:00-21:30

Pre-Congress Dinner & Harbour Boat Tour at Sunset (Optional)
Dinner at The Chip Shack on Peakes Wharf
Main: Fish & Chips / Lobster Roll & FriesDessert: Cow's Ice Cream

Day 1 — Wednesday, 26th June

09:00-16:00 Registration desk open (Victorian Foyer)
10:00-10:30 Refreshments (Victorian Foyer)
Snacks: Fruit / Yogurt / Granola Bars / Coffee / Tea / Juice

10:30-11:45
Pre-Course – Workshop: Machine Learning Segmentation Challenge
Organizer: *Akshay Chaudhari*

11:45-12:45
Lunch (Georgian Ballroom)
Buffet: Baked Haddock with Dill Sauce / Roast Chicken Chasseur

12:45-13:00
Welcome
Co-chairs: *J.D. Johnston, Emily McWalter*

13:00-13:15
Promotion of International Society on Osteoarthritis Imaging (ISOAI) Inc.
Ali Guermazi

13:15-14:45
Session 1: Novel Analytics and Computational Approaches 1
Moderators: *Richard Kijowski & Lauren Watkins*

13:15-14:00
Keynote
Valentina Pedoia: Machine Learning for Image Classification

Three abstracts selected for oral presentations
13:45-14:00 *Akshay Chaudhari:* Deep learning enables rapid quantitative MRI of OA with automatic analysis
14:00-14:15 *Hayato Aoki:* Learning times and segmentation accuracy of U-Net Convolutional Neural Networks on automatic segmentation for MRI of knee
14:15-14:30 *Arjan Desai:* Streamlining quantitative musculoskeletal MRI analysis with DOSMA

14:30-15:00
Break (Victorian Foyer)
Snacks: Biscuits / Scones / Cookies / Coffee / Tea / Juice / Pop

Day 1   Wednesday, 26th June continued

15:00-16:15   **Session 2: Novel Analytics and Computational Approaches 2**
Moderators: *Jeff Duryea & Arjun Desai*

15:00-15:30   **Keynote**
Erik Dam: Machine Learning for Scan Segmentation

Three abstracts selected for oral presentations
15:30-15:45   *Amparo Ruiz:* Imaging low-grade inflammation with hyaluronan mimetic peptides
15:45-16:00   *Arash Panahifar:* How can high resolution x-ray imaging help to understand the etiology of OA?
16:00-16:15   *Don Anderson:* 3D joint space width measures from weight bearing CT detect early joint changes after treatment of intra-articular fracture

16:15-16:25   **Young Investigator Award Session**
Christoph Ladel (MerckSerono) & Emily McWalter

16:25-16:30   Activity info: Evidence-based activities for people with OA
Saija Kontulainen

16:30-17:30   **Poster session (ODD) & Wine/Beer Reception**

18:30-22:00   **Dinner at Claddagh Room / Olde Dublin Pub (Optional)**
Pre-appetizer: Various choices of oysters
Appetizer: PEI Seafood Cake with baked beans and tomato jam
Main: PEI Boiled Dinner with Fixin's (chow, pickled beets, mustard pickles)
Dessert: Sticky Date Pudding with Irish whiskey brown sugar sauce
Entertainment: Guiness

Day 2   Thursday, 27th June

07:00-07:45   **Activity: Nordic Walking / Walking along seaside (Westside)**
08:00-16:00   **Registration desk open (Victorian Foyer)**
08:00-09:00   **Speaker & Sponsor Breakfast (Invited) (Georgian Terrace)**

09:00-10:15   **Session 3: Linking Imaging with Tissue / Joint Function 1**
Moderators: *Rebecca Moyer & Carly Jones*
Keynote
09:00-09:30   *David Wilson:* Tissue property insight gained from imaging

Three abstracts selected for oral presentations
09:30-09:45   *Sven Nebelung*: Serial T1ρ mapping to study cartilage tissue functionality and its relation to degeneration
09:45-10:00   *Jane Desrochers:* Depth-dependent changes in T2 and strain in compressed knee cartilage
10:00-10:15   *Hayden Atkinson:* T2 relaxation response of knee articular cartilage to a challenging dynamic loading stimulus in patients at-risk for OA and healthy controls

Break (Victorian Foyer)
10:15-10:45   *Snacks: Fruit / Yogurt / Granola Bars / Coffee / Tea / Juice*

10:45-12:00   **Session 4: Linking Imaging with Tissue / Joint Function 2**
Moderators: *Sven Nebelung & Marianne Black*

Keynote
10:45-11:15   *Sarah Manske:* Joint function insight gained from imaging

Three abstracts selected for oral presentations
11:15-11:30   *Steve Boyd:* The effects of acute ACL tears on human knee bone microarchitecture in the 1st year post-injury
11:30-11:45   *Lauren Watkins:* Sodium PET-MRI detects regions of abnormal bone response to acute exercise
11:45-12:00   *Jessica Küpper:* Dynamic cartilage contact maps integrated with T2 imaging

Lunch (Georgian Ballroom)
12:00-13:00   *Buffet: Stuffed Sole with Hollandaise / Beef & Mushroom Pie*

13:00-14:15   **Session 5: Imaging Early OA**
Moderators: *David Hunter & Jos Runhaar*
Keynote
13:00-13:30   *Frank Roemer:* Can we identify early OA patients based on imaging?

Three abstracts selected for oral presentations
13:30-13:45   *Kent Kwoh:* MRI-detected structural abnormalities and development of incident radiographic knee OA over 10 years of follow-up
13:45-14:00   *Carly Jones:* dGEMRIC is reduced in hips with bone marrow lesions
14:00-14:15   *Marianne Black:* Detecting early superficial and deep changes in cartilage of ACL-reconstructed knees using cluster analysis of T2 relaxation times

14:15-14:45   **Coffee Break (Victorian Foyer)**
Treats: Biscuits / Scones / Cookies / Coffee / Tea / Juice / Pop

Thursday, 27th June Continued

14:45-16:00

Session 6: Phenotypes/Subgroups of OA
Moderators: *Christoph Ladel & Hayden Atkinson*

Keynote

14:45-15:15

Erwin Van Spil: Can we offer feasible solutions to phenotype patients based on imaging?

Three abstracts selected for oral presentations

15:15-15:30

Mohamed Jarraya: Prevalence of intra-articular mineralization on knee dual-energy computed tomography: The Multicenter Osteoarthritis Study

15:30-15:45

Sarah Kennedy: Optimizing subject selection in knee osteoarthritis clinical trials by radiographic joint space width: post-hoc clinical response analysis from a Phase 2B trial of WNT pathway inhibitor SM04690

15:45-16:00

Frank Roemer: MRI-based screening for structural definition of eligibility in clinical DMOAD trials: Rapid OsteoArthritis MRI Eligibility Score (ROAMES)

16:00-17:00

Poster session (EVEN) & Wine/Beer Reception

18:00-22:00

Gala Dinner (Optional)
Bus trip to New Glasgow Lobster Suppers
Appetizer: Salad, Mussels & ChowderMain: 1.5lb Lobster
Dessert: Mile-high Lemon Meringue Pie
Entertainment: Ceilidh with Richard Wood Trio

Day 3 — Friday, 28th June

07:00-07:45	**Activity: Nordic Walking / Walking along seaside (Southside)**
08:00-09:00	**Young Investigator Breakfast Panel (Optional) (Georgian Terrace)**
	Organizer: *Jamie MacKay*

09:00-10:15 — **Session 7: Clinical Research 1**
Moderators: *Ali Guermazi & Feliks Kogan*

Keynote
09:00-09:30 — *Stefan Lohmander:* Which patients should participate in a DMOAD trial? Clinical & Imaging Parameters

Three abstracts selected for oral presentations
09:30-09:45 — *Richard Kijowski:* Deep Learning approach to predict pain progression in knee OA
09:45-10:00 — *Wolfgang Wirth:* Radiographic selection criteria for knee OA trials determine sensitivity to change and progressor rates in medial compartment cartilage thickness loss
10:00-10:15 — *Tom Turmezei:* 3D structural parameters predict future total hip replacement better than current 2D radiographic standards: an AGES-Reykjavik study

10:15-10:45 — **Break (Victorian Foyer)**
Snacks: Fruit / Yogurt / Granola Bars / Coffee / Tea / Juice

10:45-12:00 — **Session 8: Clinical Research 2**
Moderators: *Frank Roemer & Jessica Küppe*r

Keynote
10:45-11:15 — *David Hunter:* Summary of ongoing DMOAD trialsThree abstracts selected for oral presentations
11:15-11:30 — *Ali Guermazi:* History of acute knee injury as an indicator for the protective effect of bisphosphonates on knee OA: a longitudinal propensity score-matched study from the OAI cohort
11:30-11:45 — *Jos Runhaar:* The association between meniscal volume and the development of knee OA in subjects at high-risk for OA development
11:45-12:00 — *Jamie MacKay:* Utility of MRI quantitative biomarkers for experimental studies of knee OA

12:00-13:00 — **Lunch (Georgian Ballroom)**
Buffet: *Seafood Casserole / BBQ Chicken with Scalloped Potatoes*

13:00-14:30 — **Session 9: Updates & Insight from APPROACH / OAI / MOST**
Moderators: *Wolfgang Wirth & Mohamed Jarraya*
13:00-13:30 — *Christoph Ladel:* APPROACH
13:30-14:00 — *Tuhina Neogi:* OAI/MOST

Two abstracts selected for oral presentations
14:00-14:15 — *Neil Segal:* 24-month responsiveness of tibiofemoral 3D joint space narrowing measured with standing CT in the MOST study
14:15-14:30 — *Jeff Duryea:* A novel method to characterize topography of cartilage change on MRI
14:30-15:00 — **Break (Victorian Foyer)**
Snacks: Biscuits / Scones / Cookies / Coffee / Tea / Juice / Pop

Friday, 28th June Continued

15:00-16:00	**Session 10: Debate – Do we have enough biomarkers?**
	Moderators: *David Wilson & Hollis Crowder*
	Keynote Speaker in Favour
15:00-15:20	*Jamie Collins*: "We have enough biomarkers and need to focus on standardizing/validating/qualifying existing biomarkers"
15:20-15:40	**Keynote speaker (against)**
	Garry Gold: "Existing biomarkers are not enough and we need more"
15:40-16:00	Questions & Discussion
16:00-16:15	**Poster Competition Awards**
	J.D. Johnston
16:15-16:30	**Segmentation Challenge Awards**
	Organizer: *Akshay Chaudhari*
16:30-16:45	**Promotion of next year's Workshop in the Netherlands**
	Edwin Oei & Jos Runhaar
16:45-17:15	**Session 11: General Discussion**
	Moderators / Facilitators: *Ali Guermazi, David Hunter, Frank Roemer*
	This free-form session will give attendees an opportunity to discuss thoughts and ideas arising from the meeting, potential directions for the ISOAI and IWOAI, and/or other aspects not addressed during the meeting.
17:15-17:30	**Closing**
	J.D. Johnston & Emily McWalter
18:30-22:00	**Dinner at Lobster on the Wharf (Optional)**
	Appetizer: Lobster Poutine
	Main: Halibut with Mustard Pickle Sauce
	Dessert: Strawberry Rhubarb Crumble Pie

Day 4

Saturday, 29th June

11:30-22:30	Post-Congress Activity: Bike/Beach Trip (Optional)
11:30-12:00	Bus trip to Mount Stewart (bus leaves from Rodd Charlottetown)
12:00-13:00	**Lunch at Trailside Music Cafe**
	Main: Lobster Roll
	Dessert: Raspberry Cheesecake
13:00-15:00	Bike from Mount Stewart to St. Peters along protected PEI trails & coastline
15:00-15:15	Bus trip to Greenwich Beach
15:15-17:45	Beach visit & explorations of dunes and wetlands
17:45-18:00	Bus trip to Lin's Takeout
18:00-19:45	**Supper at Lin's Takeout**
	Main: Fried Fish/Scallops/Clams & Fries
	Dessert: Ice Cream
19:45-20:00	Bus trip back to Greenwich Beach
20:00-22:00	Bonfire at Greenwich Beach
22:00-22:30	Bus trip to Charlottetown (bus ends at Rodd Charlottetown)
	Note: Individuals desiring a longer bike ride will have options to bike additional routes at the end of the group ride between Mount Stewart and St. Peters

Oral Presentations

Program Committee

Co-chair: J.D. Johnston, PhD, University of Saskatchewan

Co-chair: Emily McWalter, PhD, University of Saskatchewan

Saija Kontulainen, PhD, University of Saskatchewan

Scientific Committee:

Akshay Chaudhari, PhD, Stanford

Ida K. Haugen, MD, PhD, Diakonhjemmet Hospital

Richard Kijowski, MD, University of Wisconsin

Saija Kontulainen, PhD, University of Saskatchewan

Christoph Ladel, PhD, Merck

Eveliina Lammentausta, PhD, University of Oulu

Jamie MacKay, MD, Cambridge Univrsity

Rebecca Moyer, MPT, PhD, Dalhouse University

Tuhina Neogi, MD, PhD, Boston University

DEEP LEARNING ENABLES RAPID QUANTITATIVE MRI OF OA WITH AUTOMATIC ANALYSIS

*Chaudhari A., *Grissom M., *Stevens K., **Fang Z., *Desai A., *Kogan F., ***Lee J.H., *Gold G., *Hargreaves B.

*Radiology, Stanford University, Stanford CA
**LVIS Corp., Palo Alto, CA
***Neurology, Stanford University, Stanford CA

INTRODUCTION: The quantitative double-echo steady-state (qDESS) sequence offers compositional and structural qMRI measures to study the multi-factorial nature of knee OA[1]. However, the multi-contrast qDESS generates thick slices that hampers semi-quantitative assessment (WORMS, MOAKS, etc) due to lack of high-quality 3D analysis. Moreover, qDESS requires manual segmentation of tissues, which is a time-consuming and variable process. Deep-learning can enable super-resolution (DLSR) to retrospectively enhance lower-resolution MRI[2], and can also automate cartilage segmentation for T2 analysis, where automatic-manual T2 variations are lower than scan-rescan variations[3].

OBJECTIVE: We use DLSR to enhance the slice-resolution of a 5-minute multi-contrast qDESS scan twofold to detect knee abnormalities. We compare these findings to a routine diagnostic knee MRI protocol and to arthroscopy. Lastly, we exhibit automated segmentation and sub-regional analysis of automatically generated qDESS T2 maps[4].

METHODS: A 5-minute 3D qDESS sequence[1] with a slice thickness of 1.6mm was enhanced to 0.7mm thickness using DLSR[2] in 51 patients referred for a diagnostic knee MRI. Two musculoskeletal radiologists evaluated findings from the qDESS (with and without a T2 map) and conventional protocols for the 51 patients, and arthroscopy for 43 patients using the following criteria[3-5]: *Ligaments* (cruciate and collateral): low, moderate, or high grade sprain; *Menisci*: degeneration or tear; *Cartilage*: Grade 1, 2A, 2B, or 3 lesions; *Bone*: bone marrow lesion (BML), subchondral cyst, or fracture; *Extensor Mechanism*: partial or complete tear; *Synovium*: effusion or synovitis. Arthroscopic results were computed for cartilage, meniscal, and cruciate ligament injuries. The agreement between qDESS and the conventional imaging protocols was compared. Sensitivity and specificity were evaluated for both imaging protocols compared to arthroscopy. Cohen's linearly-weighted Kappa was used to evaluate inter-observer agreement. The utility of adding a 2min coronal intermediate-weighted (IW) fast spin echo scan to the qDESS protocol was also assessed. Radiographs for KL grades were available in 34 patients who were stratified into groups of 15 (KL 0/1) and 19 (KL 2/3/4). Sub-regional analysis of femoral cartilage (deep/superficial layers, with anterior/central/posterior regions in medial/lateral condyles) using automated[4] and manual segmentation was compared using Mann-Whitney U-Tests.

RESULTS: qDESS had high agreement with the conventional imaging protocol and excellent inter-reader agreement (Table 1). Both protocols had similar sensitivity and specificity compared to arthroscopy (Table 2). The IW scan increased BML sensitivity to 71%. The qDESS T2 map increased cartilage lesion sensitivity ($p<0.05$) from 54% to 73% (56% for conventional imaging). The T2 maps were beneficial in detecting subtle grade 1 and 2a cartilage lesions (46%, 61% qDESS sensitivity compared to 35% and 29% for conventional imaging) and added additional diagnostic value in 41/51 patients and in 30% of all cartilage regions studied. Using the automated segmentation, significant cartilage T2 differences ($p<0.05$) were found between KL 0/1 and 2-4 groups in the deep and superficial T2 in the medial and lateral posterior condyles, and deep T2 in the femoral trochlea.

	Kappa	+ Agreement	- Agreement
Meniscus	0.73	87%	92%
Cruciate Ligaments	0.85	74%	99%
Collateral Ligaments	0.71	59%	98%
Cartilage	0.73	87%	86%
Extensor Mechanism	0.92	50%	99%
Marrow	0.83	47%	98%
Synovium	0.85	94%	89%
Total	**0.82**	**74%**	**97%**

Table 1: Agreement between qDESS and conventional diagnostic imaging protocol.

DISCUSSION: DLSR enhanced image resolution without compromising scan time or signal to noise ratio, while T2 maps were obtained concurrently with morphological images. The automatic qDESS T2 measures detected the earliest chondral degenerative changes with significantly higher sensitivity than conventional imaging methods. Paired with the fully-automated segmentation and sub-regional analysis method, T2 was useful in stratifying KL groups. qDESS also showed efficacy for detecting tissue damage for WORMS/MOAKS scoring, compared to conventional imaging and arthroscopy. The addition of a rapid 2-minute IW sequence enhanced BML sensitivity (from 47% to 71%). Simultaneous bilateral knee imaging can be performed for both sequences to further enhance efficiency[5].

CONCLUSION: The 5-minute qDESS method with DLSR and T2 mapping paired with automatic segmentation can characterize quantitative structural and compositional changes along with semi-quantitative tissue analysis in OA. This is a promising, inexpensive, and efficient method to monitor disease progression and for rapid screening in clinical studies.

	Seq	Sens.	Spec.
Meniscus	C	0.93	0.79
	D	0.9	0.8
Cruciate Ligaments	C	0.91	0.87
	D	0.86	0.91
Cartilage	C	0.56	0.71
	D	0.73*	0.66
Total	C	**0.65**	**0.78**
	D	**0.74***	**0.73**

Table 2: qDESS (D) and conventional (C) imaging vs arthroscopy. * $p<0.05$

REFERENCES: [1] Chaudhari 2018 [2] Chaudhari 2018 [3] Barbieri 2019 [4] Desai 2019 [5] Kogan 2018
DISCLOSURE: AC has consulted for Skope MR, Subtle Medical, Chondrometrics.
CORRESPONDENCE: akshaysc@stanford.edu

LEARNING TIMES AND SEGMENTATION ACCURACY OF U-NET CONVOLUTIONAL NEURAL NETWORKS ON AUTOMATIC SEGMENTATION FOR MRI OF KNEE

*Aoki H., *Ozeki N., *Hyodo A., **Suzuki K., **Masumoto J., *Sekiya I.

*Center for Stem Cell and Regenerative Medicine, Tokyo Medical and Dental University, Tokyo, Japan
**Fujifilm Corporation, Tokyo, Japan

INTRODUCTION: Three-dimensional (3D) qMRI of the knee has been useful in osteoarthritis studies, but the method has not been commonly used due to the complicated and time-consuming procedure required to reconstruct the 3D images. We have developed a 3D MRI analysis software that uses a convolutional neural network algorithm (Fig. 1) to enable automatic reconstruction of these 3D images of the cartilage and meniscus in the knee joint.

OBJECTIVE: The purpose of this study was to analyze the learning times and segmentation accuracy of U-Net convolutional neural networks on automatic segmentation of the MRI of knee cartilage and of the MRI of the meniscus region.

METHODS: A deep learning model based on the U-Net was developed to perform automatic segmentation, and soft Dice loss was used as the loss function (Fig. 2). PDWI and SPGR MRI data sets of the knee in 10 healthy and 40 patients with knee pain were analyzed, retrospectively. The data sets used pixel spacing of 0.31mmX0.31mm with a slice thickness of 0.6mm and included 320 slices. The patients with knee pain were all graded ≤ 2 on the Kellgren-Lawrence scale. Morphological imaging of cartilage was manually segmented with SPGR while meniscus and bone were manually segmented with PDWI (Fig. 3). Knee data was randomized, and 45 sets of knee data were selected and used for training, and another five were used for the test. The software was constructed to learn 50 epoch and 200 epoch with training data. We compared the segmentation accuracy of 50 epoch software with 200 epoch software. Performance of the automatic segmentation was evaluated based on the overlap between the Dice similarity coefficient (DSC) and the manual segmentation. Then, Wilcoxon signed-rank test was used to compare the two groups.

RESULTS: Automatic segmentation of cartilage, meniscus, and bone took approximately 1.5 minutes with the trained network. The DSC was 0.90 ± 0.02 (average $\pm$ standard deviation) for the femoral cartilage and 0.88 ± 0.03 for the tibial cartilage on both epoch networks. The DSC of the meniscus was 0.86 ± 0.03 on the 50 epoch network and 0.88 ± 0.02 on the 200 epoch network (n=5, p<0.01). The training time in the 50 epoch network was 6 hours 48 minutes for cartilage and 6 hours 4 minutes for meniscus. Training time in the 200 epoch network was 27 hours 34 minutes for cartilage and 24 hours 36 minutes for meniscus.

CONCLUSION: This study demonstrated the feasibility of using our automatic segmentation system create 3D qMRI of the knee. The system needs to run more iterations of meniscus to learn compared to the iterations of cartilage that need to be run. The high segmentation accuracy of our network will be useful for evaluation and intervention with early knee osteoarthritis.

Fig 1. Meniscus and cartilage are reconstructed 3-dimensionally

Fig 2. U-Net convolutional neural network
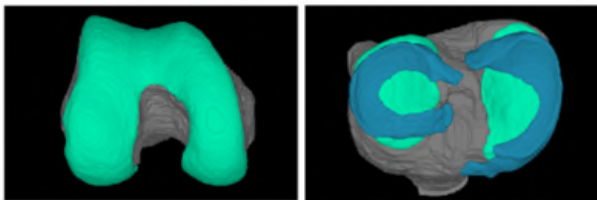
Fig 3. Cartilage and meniscus area segmented automatically.
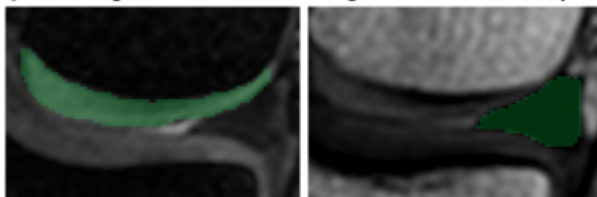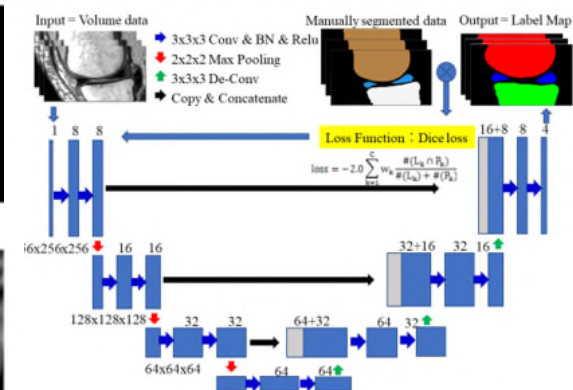
STREAMLINING QUANTITATIVE MUSCULOSKELETAL MRI ANALYSIS WITH DOSMA

*Desai A.D., *Barbieri M., *Mazzoli V., *Rubin E.B., *Black M.S., *Watkins L.E., *Gold G.E., *Hargreaves B.A., *Chaudhari A.S.

*Radiology, Stanford University, Stanford, USA

INTRODUCTION: Recent advancements in qMRI have enabled capturing quantitative image-based biomarkers for early detection of OA using a variety of MRI sequences[1,2]. However, to obtain such quantitative biomarkers, regions of interest must be segmented; volumes from different protocols must be registered to each other; and quantitative calculations must be performed in a standardized manner to generate reproducible results. While automatic, machine learning-based methods have been developed to replace tedious manual tasks, most methods are either not publicly available or are not seamlessly compatible with existing image processing tools.

OBJECTIVE: To establish a streamlined, open-source musculoskeletal MRI analysis framework, termed DOSMA, to consolidate automatic MR image processing techniques and to facilitate automatic quantitative and morphological analysis of musculoskeletal tissues.

FEATURES: To facilitate the processing of MR scans, DOSMA currently supports the analysis and visualization of femoral/tibial cartilage and the meniscus using multi-echo spin-echo and multi-echo gradient-echo sequences. These sequences include, but are not limited to, quantitative double-echo in steady-state (qDESS)[3], $T_{1\rho}$-prepared Cubequant[4], T_2^*-weighted UTE-Cones[5], and $T_{1\rho}/T_2$ MAPSS[6]. Each scan sequence is associated with a set of plausible *actions*, such as automatic segmentation and registration, and *quantitative value* analysis and visualization methods. The framework abstracts these *actions* and *quantitative analysis* techniques to enable generalizability and ease of extension to other protocols. DOSMA also supports both Dicom/NIfTI I/O, auto-sequence search, and multi-vendor compatibility. The framework is accessible via the command line and a graphical user interface.

METHODS: In this proof-of-concept study, we demonstrate the efficacy of DOSMA to perform automatic segmentation and quantitative T_2 analysis of qDESS in femoral cartilage. In a cohort of healthy participants (n=10) and OA patients (n=10, KLG $\geq$ 1), T_2 in femoral cartilage was measured using manual and automatic segmentation in the anterior, central, and posterior regions in both the medial and lateral condyles. Statistical comparisons between automatic and manual T_2 estimates were assessed using pairwise Kruskal-Wallis tests and corresponding Dunn posthoc tests (α=0.05).

RESULTS & DISCUSSION: Among the healthy cohort, the difference in estimated T_2 from automatic and manual segmentations in all six femoral cartilage regions was insignificant (p=0.13). T_2 estimation differences were also negligible in the OA cohort for five regions (p=0.174), but auto-segmentation T_2 estimates were significantly overestimated (p<0.05) in

Figure 1: T_2 estimates between manual and automatic segmentations in (A) healthy and (B) diseased subjects

the lateral-anterior region. However, the range of differences in T_2 were comparable to the error range of scan/rescan T_2 estimates[5] (Fig. 1). Additionally, higher T_2 estimates for OA patients were observed. The mean computation time per subject was 3.1 CPU minutes.
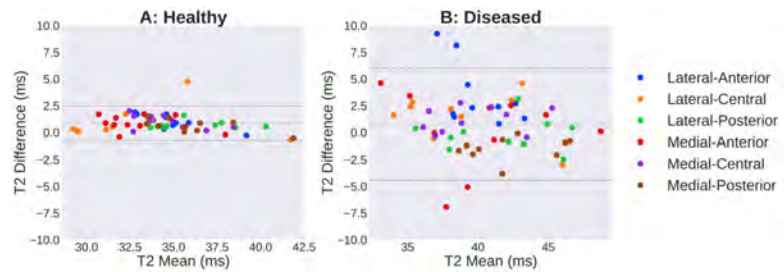
CONCLUSION: DOSMA is a one-shot image-processing environment with support for features such as segmentation, registration, and quantitative value estimation and visualization. It is designed to automate tedious MR post-processing and to facilitate reproducible quantitative analysis of musculoskeletal tissues. We encourage collaborators and the OA imaging community to contribute to the GitHub repository (https://github.com/ad12/DOSMA) to add functionality.

REFERENCES: [1] Li, MRM, 2009 [2] Williams, OAC, 2012 [3] Chaudhari, JMRI, 2018 [4] Nguyen, ISMRM, 2012 [5] Qian, MRM, 2010 [6] Li, MRM, 2008 [7] Barbieri, ISMRM, 2019

IMAGING LOW-GRADE INFLAMMATION WITH HYALURONAN MIMETIC PEPTIDES

*Ruiz A., *Duarte A., *Ramos E., **Bravo D., *Raya J.G.

*Center for Biomedical Imaging, Dpt. of Radiology, New York University Langone Health
**Department of Orthopedic Surgery, New York University School of Medicine

INTRODUCTION: One driving factor in the progression to PTOA is the perpetuation of the inflammatory response to injury into low-grade chronic inflammation. MRI is limited in the assessment of low-grade inflammation in vivo. Contrast-enhanced MRI can measure inflammatory vasodilation but lacks molecular specificity and ability to assess inflammation in low-perfused tissues such as ligaments and cartilage. Molecular imaging offers many opportunities to complement the sensitivity of MRI, with molecular specificity. An important pathway for activation of the immune response is by degradation fragments of the extracellular matrix such as low molecular weight hyaluronan fragments (LMWHA). LMWHA act as damage-associated molecular patterns (DAMPS) to TLR2/4, RHAMM and CD44 receptors, triggering an immune response and producing inflammatory mediators that further stimulate the production of DAMPS.

OBJECTIVE: To develop contrast agents to image hyaluronan (HA)-mediated inflammatory signaling through interactions with HA-cell receptors CD44 and RHAMM.

METHODS: We have developed two imaging probes based in HA-mimetic peptides, A6 that targets monomeric CD44 and P15-1 with homology to HA binding sequences of RHAMM, thus blocking HA interactions. The two peptides were labeled with near infrared (NIR) fluorophores Cy5.5 and Cy7.5, so that they can be measured simultaneously. We also conjugated both peptides to a Gd-DOTA chelating complex, so that we can perform MRI and use fluorescence for histology validation. We induced OA in mature male SD rats by surgical transection of the ACL and perform experiments eight weeks after surgery. First, we tested pharmacokinetic of the contrast agents. Rats were injected intraarticularly (IA) with $10\mu g/50\mu l$ of Cy5.5-P15-1 and Cy7.5-A6 tracers (n=8 ACLT, n=8 Sham, n=8 control). NIR imaging was acquired before injection, 5 min after injection and 3, 6, 12, 24, 48 and 72 h after injection. Average radiance was measured in each joint. After confirmation of retention, we explored their use in MRI. Bilateral knee MRI was performed 24 h before injection, and 5, 24 and 48 h after injection on a Bruker 7T magnet using a 4-element receive surface coil. We injected IA both limbs of six rats with either DOTA-Gd-P15-1 or DOTA-Gd-Cy7.5-A6 (1 mM). MRI protocol included an inversion recovery turbo-spin echo sequence (IR-TSE) with (resolution=$100\times100\times750\mu m^3$, TE/TR=12.5/5343ms, turbo-spin factor=5, echo spacing=6.25s, inversion times=0.05, 0.1, 0.15, 0.2, 0.3, 0.4, 0.5, 0.75, 1, 1.5, 2, 3, 4, 5 s, 8 slices, total acquisition time=35min/knee). T1 maps were calculated from IR-TSE images and cartilage was segmented to calculate average T1 value. After the last imaging session, limbs underwent histology with cryosectioning and fluorescence microscopy. Finally, we performed competitive binding to test specificity of contrast agents. Group differences were assessed with paired test after confirmation of data normality with the K-S test.

RESULTS: Analysis of average radiance showed a window of opportunity between 12 and 72 h to detect changes in the ACLT with significantly higher ($p<0.05$) accumulation than in control limbs. Fluorescence microscopy showed accumulation on menisci and more predominantly in articular cartilage for P15-1. A6 accumulated on synovium and fat pad. For P15-1 tracer, T1 on an ACLT knee showed a significant decrease in the femoral trochlea and the patella at 48 h: -10% (patella) to -25% (trochlea) and an -18% globally. There was no difference in control groups (2% globally).

CONCLUSIONS: P15-1 represents a promising contrast agent to image chronic low-grade inflammation in PTOA, thus with potential to provide new insight into the pathophysiology of OA.

HOW CAN HIGH RESOLUTION X-RAY IMAGING HELP TO UNDERSTAND ETIOLOGY OF OSTEOARTHRITIS?

*,**Panahifar A., *,**Chapman L.D., **Wiebe S., *,**Cooper D.M.L.

*Canadian Light Source, Saskatoon, Canada
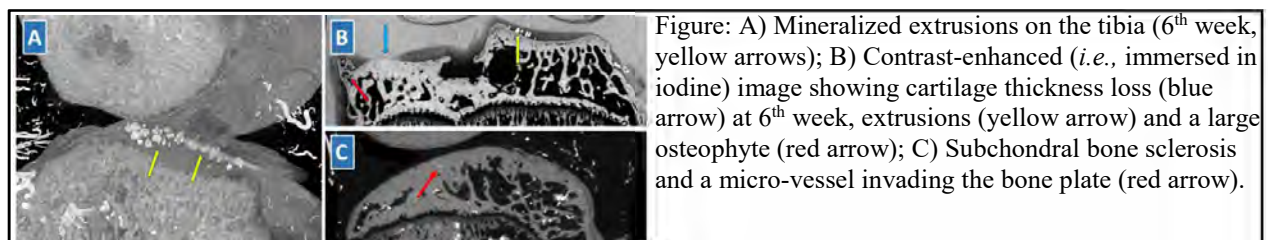**University of Saskatchewan, Saskatoon, Canada

INTRODUCTION: Despite knowing many risk factors, the etiology of OA is not completely understood. In recent years the consensus has achieved that OA is a whole organ disease. Many clinical imaging modalities while being sensitive in diagnosing OA in medium to late stages, come short of detecting early changes. In addition, investigating the spatial and temporal connection of pathological changes in various tissues involved in OA have been challenging due to the lack of sufficient resolution and sensitivity.

OBJECTIVE: To explore the types of micro-structural changes detectable with high resolution X-ray.

METHODS: Post traumatic OA was induced in 18 skeletally mature (6-month old) male rats by medial meniscectomy on right knee. Left knee was considered as contralateral control. At 2, 6, and 8 weeks post-surgery 6 animals were euthanized. µCT was performed at the BioMedical Imaging and Therapy (BMIT) beamline at the Canadian Light Source synchrotron because of its high resolution (up to 0.9µm pixel size), high X-ray flux, and precise tunability of X-ray energy (eV range). Active bone remodeling was imaged by using barium as bone-seeking contrast agent. Micro-angiography was performed, *in-vivo* and *ex-vivo*, to detect early vascular changes in the bone. Cartilage lesions were imaged *ex-vivo* with the aid of iodine. Cellular imaging was carried out to investigate the detectability of individual chondrocytes, and osteocytes. All imaging was carried out at 6.5µm resolution with the exception of cellular imaging (0.9µm pixel size).

RESULTS: Starting at 2 weeks post-surgery, formation of pseudo-calcified osteophytes, hypertrophy of chondrocytes at the joint margins, and degeneration of cartilage were already in place. In later stages, sclerosis of subchondral bone plate along with vascular invasion to the bone plate were detected. Individual osteocyte and chondrocyte porosities in the subchondral bone plate and osteophytes were readily detected. Metabolic bone changes including subchondral bone sclerosis and osteophytes formation incorporated the barium tracer and were visualized. Moreover, micro-scale highly mineralized extrusions within hyaline cartilage were detected in both the operated and non-operated knee joints.

CONCLUSION: The 3D nature of µCT enables investigating inter-relation of micro-structural changes among various tissues and compartments over time and space. *Ex-vivo* imaging allowed for infusion of high concentration of the contrast agent, leading to detection of micro-vessels within bone (up to 20-30µm in diameters). The micro-mineralizations in the hyaline cartilage are under reported in the literature. They may degrade the cartilage from within and contribute to the initiation and progression of OA due to their spike shape. Synchrotron high resolution X-ray imaging provides powerful tools for characterizing pathological changes in OA. While the high radiation dose and limited field of view of µCT limits its applicability to human patients, the additional information it delivers can be utilized in preclinical studies as well as biopsies and TKA samples to broaden the insight on why OA is happening in humans.

Figure: A) Mineralized extrusions on the tibia (6th week, yellow arrows); B) Contrast-enhanced (*i.e.,* immersed in iodine) image showing cartilage thickness loss (blue arrow) at 6th week, extrusions (yellow arrow) and a large osteophyte (red arrow); C) Subchondral bone sclerosis and a micro-vessel invading the bone plate (red arrow).

DISCLOSURE STATEMENT: None.
CORRESPONDENCE ADDRESS: Arash.Panahifar@lightsource.ca

3D JOINT SPACE WIDTH MEASURES FROM WEIGHT BEARING CT DETECT EARLY JOINT CHANGES AFTER TREATMENT OF INTRA-ARTICULAR FRACTURE

*Ho M., *Dibbern K., *Willey M., *Marsh J.L., *Anderson D.D.

*Department of Orthopedics and Rehabilitation, University of Iowa, Iowa City, IA, USA

INTRODUCTION: Clinical monitoring for post-traumatic OA (PTOA) development after treatment of intra-articular fracture of the distal tibial pilon presently involves serial acquisition of weight-bearing radiographs.[1] However, radiographs capture an obscured 2D projection of a complex 3D structure and pathology. Our working hypothesis is that a low-dose weight-bearing CT (WBCT) scanner for the foot and ankle provides more sensitive and responsive measures of joint degeneration, without an increase in cost or time and without a significant increase in radiation.[2] WBCT would provide much greater diagnostic value, not only because of its 3D nature, but also because patients are imaged in a functional weight-bearing position. Clinically, the JSW is most often measured manually in a single plane from these inherently 3D data, failing to use a majority of the feature-rich data in these scans.

OBJECTIVE: The goal of this project was to more fully investigate data available from these WBCTs by measuring 3D JSW across the entire joint surface after intra-articular fracture treatment.

METHODS: 15 patients with operatively fixed tibial pilon fractures were prospectively enrolled. Six months after injury, all subjects underwent bilateral ankle WBCT. A semi-automated segmentation protocol generated triangulated surface meshes of both the tibia and talus. The intact talar dome was split into a 3-by-3 grid. 3D JSW was computed as the normal distance from the center of each triangulated face on the talus subchondral bone to that of the opposing tibia. The mean, minimum, and standard deviation of 3D JSW was computed for each of the 9 regions and across the whole surface for comparison between the injured and uninjured contralateral ankles.

RESULTS: Mean 3D JSW was insignificantly smaller on the injured side for 11 of 15 patients (2.2 ± 0.5mm vs. 2.4 ± 0.4mm; $p=0.21$). Minimum 3D JSW was significantly smaller on the injured side for 12 of the 15 patients (0.6 ± 0.5mm vs. 1.3 ± 0.4mm; $p<0.001$). Standard deviation in 3D JSW was significantly larger on the injured side for 13 of the 15 patients (0.5 ± 0.2mm vs. 0.2 ± 0.1mm; $p<0.001$). Examining the 9 anatomical regions, minimum 3D JSW was significantly smaller on the injured side for six of the nine regions ($p<0.05$: Figure 1), while none of the 9 regions showed a significant difference in the mean 3D JSW. Most cases showed a smaller 3D JSW in the anterior and lateral portions of the joint for the injured ankle relative to the uninjured, which was accompanied by a slightly larger 3D JSW in the posterior medial portion of the joint. The standard deviation in 3D JSW (an indicator of surface irregularity) was at least 120% greater for the injured ankles opposed to their uninjured counterparts.

CONCLUSION: WBCT scans enable 3D JSW analysis that can detect early changes indicating PTOA as soon as 6 months following operative treatment of tibial pilon fractures. Measures derived from these data provide insight into both the location and magnitude of potential JSN, as well as less obvious signs of surface incongruity like increases in the JSW variability across the surfaces. The subjects of this study are being followed longitudinally so that any progression of these changes can be assessed.

Figure 1. % difference in minimum JSW between intact and fractured ankles.

REFERENCES: [1] Kellgren & Lawrence, Ann Rheum Dis, 1957 [2] Kokkonen, J Orthop Res, 2014
CORRESPONDENCE ADDRESS: don-anderson@uiowa.edu

SERIAL T1ρ MAPPING TO STUDY CARTILAGE TISSUE FUNCTIONALITY AND ITS RELATION TO DEGENERATION

*Nebelung S., *Post M., *Kuhl C., *Truhn D.

*Department of Diagnostic and Interventional Radiology, Aachen University Hospital, Aachen, Germany

INTRODUCTION: Detection of early cartilage degeneration by clinical standard diagnostic tools remains elusive. Quantitative MRI (qMRI) techniques such as T1ρ mapping provide information on the extracellular matrix beyond structure and morphology. However, as these parameters have failed to reliably diagnose early cartilage degeneration, biomechanical stimuli have been combined with qMRI to assess tissue functionality as a potential surrogate marker of the tissue's status in health and disease.

OBJECTIVE: The aim of this study was to investigate changes in response to sequential pressure-controlled loading and unloading in human articular cartilage of variable histological degeneration using serial T1ρ mapping. We hypothesized that loading induces distinctly different changes in T1ρ in intact as opposed to degenerative cartilage (as controlled by histology).

METHODS: This was an institutional review board-approved prospective comparative *ex-vivo* imaging study. 42 cartilage samples of variable degeneration were obtained from the medial femoral condyles of 42 patients undergoing total knee replacement at our institution. Samples were placed in a standardized artificial knee joint within an MRI-compatible whole knee-joint compressive loading device (Fig. 1a, b) and imaged before (δ_0), during (δ_{ld1}, δ_{ld2}, δ_{ld3}, δ_{ld4}, δ_{ld5}) and after (δ_{rl1}, δ_{rl2}, δ_{rl3}, δ_{rl4}, δ_{rl5}) pressure-controlled loading to 0.66 ± 0.02 kN (95% body weight) using serial T1ρ mapping (spin-lock multigradient echo sequence of 7.4 min duration each; clinical 3.0T MRI system [Achieva, Philips]) (Fig.1c). Reference assessment included histological grading of cartilage degeneration (according to the Mankin classification, Fig. 1d). Sample dichotomization into *intact* (n=21) and *degenerative* (n=21) was based on histological findings, i.e. Mankin grade 0 (*intact, int*) versus Mankin grade $\geq$ I (*degenerative, deg*). Data were analyzed using Mann Whitney and Kruskal Wallis tests.
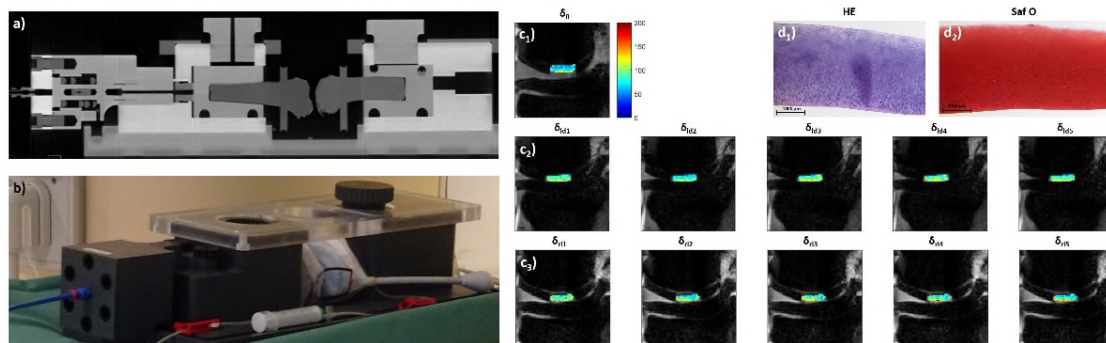
Fig. 1: a) Sagittal cross-sectional CT view and b) photograph of the pressure-controlled whole-knee joint loading device positioned within the 3T MRI scanner. c) Serial T1ρ maps (unloaded, δ_0 [c_1]) in response to sequential loading (δ_{ld1-5} [c_2]) and unloading (δ_{rl1-5} [c_3]) of a histologically intact cartilage sample (d).

RESULTS: At δ_0, no significant differences between *int* and *deg* samples were determined, while the response-to-loading patterns were distinctly different. In *int* samples, T1ρ increases were consistent and non-significant, while in *deg* samples, T1ρ increases were significantly higher (p=0.004, δ_0 vs. δ_{ld1}, δ_0 vs. δ_{ld3}), yet undulating and variable. With unloading, T1ρ increases subsided, yet were persistently elevated beyond δ_0 levels.

CONCLUSION: Cartilage mechanosensitivity is related to histological degeneration and assessable by serial T1ρ mapping. Unloaded, T1ρ characteristics are not significantly different in *int* versus *deg* cartilage. Load bearing is organized in *int* cartilage and disorganized in *deg* cartilage.

DEPTH-DEPENDENT CHANGES IN T2 AND STRAIN IN COMPRESSED KNEE CARTILAGE

*Desrochers J., **Yung, A.C., *Wilson D.R.

*Center for Hip Health and Mobility and Department of Orthopedics, UBC, Vancouver Canada
**Center for Hip Health and Mobility and MRI Research Center, UBC, Vancouver Canada

INTRODUCTION: Associations of quantitative T2 with loading have been shown in both clinical and *ex vivo* MRI studies, but the exact relationship and mechanistic understanding of T2 vs. strain have yet to be defined. A direct analysis of local, depth dependent changes in T2 with local, depth dependent strain is required to better understand how and why T2 changes in cartilage under load.

OBJECTIVE: The specific objective of this work was to directly measure the relation between local, *in situ* changes in cartilage T2 and strain using high resolution 7T MRI.

METHODS: Osteochondral blocks from the medial compartment of four cadaveric knees were prepared and mounted in a custom designed, MR compatible loading rig. MR image volumes of tibial and femoral cartilage were acquired in the sagittal plane using the DESS sequence on a Bruker Biospec 7T MRI at applied strain levels of approximately: 0% (unloaded), 10, 25 & 35%. All images were acquired with the image plane oriented at 0° with respect to the external magnetic field B_0. Cartilage strain and T2 were analyzed from tibiofemoral cartilage-cartilage contact regions from a central volume that included 11 central image slices, each of which was between 25 – 51 voxels wide. Sample and acquisition data are further described below.

Sample Data		**Image Data**		**DESS parameters**	
Age (mean ± SD)	83 ± 5 years	Voxel height (loading)	60 µm	Flip angle	30°
KL Grade (mean ± SD)	0.75 ± 0.4	Voxel width (⊥ to load)	250 µm	Repetition time (TR)	17 ms
		Voxel thickness	800 µm	Echo time (TE)	4.5 ms

Local measurements of *in situ* cartilage strain were calculated by fitting applied strains to a decaying exponential model for depth-dependent cartilage strain[1]. Loaded cartilage datasets were then non-linearly warped to match their unloaded image volumes and voxel-wise changes in cartilage T2 were calculated from image subtraction of warped, loaded – unloaded T2 data.

RESULTS: Relationships between ΔT2 and cartilage strain were different between superficial and full-depth cartilage and between femoral and tibial cartilage. We found no significant correlation between ΔT2 and strain for bulk tibial or femoral cartilage (i.e., averaged through full depth) (Table 1), but found a strong linear relation between ΔT2 and strain for the surface zone (i.e., within 15% of the articular surface) for both tibial and femoral cartilage ($0.68 < R < 0.82$, $p < 0.05$), (Figure 1).

Average   Cartilage   T2

		Tibia	**Femur**
Bulk	Unloaded	12.6 ± 2.1	13.5 ± 2.1
	Loaded	13.3 ± 2.2	13.9 ± 2.2
Surface	Unloaded	16.4 ± 1.8	14.0 ± 2.4
	Loaded	13.3 ± 1.3	13.7 ± 2.1

Table 1: Grouped averages for unloaded and loaded T2 tibial and femoral cartilage (mean ± SD, ms)

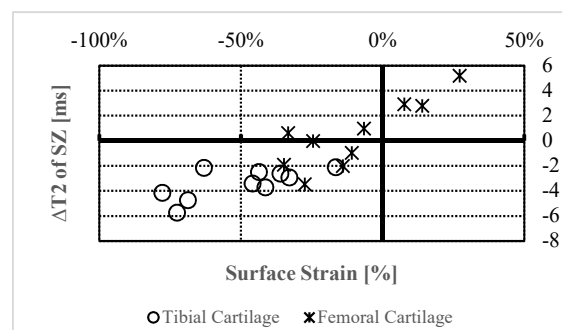**Figure 1: ΔT2 vs. Strain for Surface Cartilage**

CONCLUSION: ΔT2 is a promising indirect measure of cartilage surface strain.

REFERENCE: [1] Chen, OAC, 2001
CORRESPONDENCE ADDRESS: david.wilson@ubc.ca

T2 RELAXATION RESPONSE OF KNEE ARTICULAR CARTILAGE TO A CHALLENGING DYNAMIC LOADING STIMULUS IN PATIENTS AT-RISK FOR OA AND HEALTHY CONTROLS

*Atkinson H.F., *Birmingham T.B., **Moyer R.F., ***Milner J.S., *,***Holdsworth D.W., ****Thiessen J.D., ****Thompson R.T., *Giffin J.R.

*Bone and Joint Institute, Western University, London, Canada
**Faculty of Health, School of Physiotherapy, Dalhousie University, Halifax, Canada
***Robarts Research Institute, Western University, London, Canada
****Imaging Program, Lawson Health Research Institute, London, Canada

INTRODUCTION: Permeability of articular cartilage may be compromised in people at risk for knee OA, lessening the ability of cartilage to accept loads and predisposing it to damage. Load-bearing, functional exercises, such as walking and hiking are promoted for these individuals, but their effect on articular cartilage is unclear. Compositional MRI measures such as T2 relaxation time are sensitive to acute and long-term changes in articular cartilage composition and collagen orientation, and may detect early alterations in articular cartilage response to loading in patients at risk for knee OA.

OBJECTIVE: To evaluate the acute T2 relaxation response of knee articular cartilage to a standardized challenging dynamic loading stimulus in patients with risk factors for knee OA and healthy controls.

METHODS: We recruited 16 patients from the Fowler Kennedy Sport Medicine Clinic with risk factors for knee OA based on the Osteoarthritis Initiative incidence Cohort criteria (previous knee injury, surgery, frequent symptoms) and 16 healthy controls. All participants were scanned using a 3T Siemens Magnetom Trio magnet and a 15-channel Siemens PRISMA knee coil. Pulse sequences included 3D Dual Echo Steady State and Multi-Echo Spin Echo T2 Mapping (TR 2700 ms/TE 11.1-77.7 ms, ETL 7). Participants were seated 30 minutes prior to the scan to reduce effect of loading earlier in the day. Following the baseline scan, all participants completed the same standardized loading stimulus, consisting of 25 minutes of challenged walking on an instrumented, dual-belt treadmill capable of moving with 6 degrees of freedom. We subjected participants to changes in speed (110-120% self-selected speed), inclines and declines (±10°), lateral sways (1 m/s, 15 cm left/right), and random pre-specified perturbations in the form of rapid belt slips, sagittal plane pitches, and frontal plane sways. Immediately following challenged walking, participants completed a post-loading MRI with the same sequences as the baseline scan. We generated T2 relaxation maps using software developed in-house by fitting image intensities of the T2 weighted images pixel-by-pixel to the equation $S(TE) \propto \exp(-TE/T2)$ using a Levenberg-Marquardt mono-exponential fitting algorithm implemented using Insight Toolkit. One reader blinded to scan order and group manually segmented load-bearing regions of the medial and lateral femur and tibia using a standardized anatomical atlas using 3D Slicer software. Segmentations were divided into equal sized superficial and deep layers based on each pixel's minimum Euclidean distance to the articular surface and bone cartilage interface. Two primary outcome measures used for statistical analysis were the mean T2 relaxation time of the four load-bearing tibiofemoral compartments for the superficial and the deep layers. Patients and controls were compared before and after the loading stimulus using two-factor group (between) by time (within) analysis of variance.

RESULTS: For the superficial compartments, there was a significant main effect for time ($p<0.001$), but no significant main effect for group ($p=0.6$) and no group-by-time interaction ($p=0.9$). The mean decrease in T2 relaxation for the patients was -3.8 ms, 95%CI: [-2.9;-4.7], and -3.9 ms, 95%CI: [-3.0;-4.8] for the healthy controls. The mean difference between groups in the change (response to loading) was -0.1 ms, 95%CI: [-1.1;1.3]. For the deep compartments, there was no main effect for time ($p=0.07$) or group ($p=0.9$) and no group-by-time interaction ($p=0.5$). The mean decrease for healthy controls was -0.5 ms [-1.2;0.2] and for the at-risk group was -1.1 ms [-2.8;0.5]. The mean difference between groups in the change was -0.6 ms, 95%CI: [-2.3;1.1].

CONCLUSION: The present results suggest patients at risk for knee OA and healthy controls have the same T2 relaxation response in knee articular cartilage following a challenging dynamic loading stimulus.

CORRESPONDANCE ADDRESS: hatkins5@uwo.ca

THE EFFECTS OF ACUTE ACL TEARS ON HUMAN KNEE BONE MICROARCHITECTURE IN THE FIRST YEAR POST-INJURY

*,**Kroker A., *,**Besler B.A., *,**Bhatla J.L., *,**Shtil M., *,**Salat P., *,***Mohtadi N., *,**Walker R.E., *,**Manske S.L., *,**Boyd S.K.

*McCaig Institute for Bone and Joint Health, University of Calgary, Calgary, AB, Canada
**Department of Radiology, Cumming School of Medicine, University of Calgary, Canada
***Sport Medicine Centre, University of Calgary, Canada

INTRODUCTION: ACL tears are a common knee injury and are associated with an elevated risk of developing OA. Bone plays an important role in OA development, and bone mass has been shown in animal models and human studies to decrease immediately following injury before partially recovering. ACL transection models have confirmed this bone loss is driven by trabecular structure degradation, however, this has not been confirmed in humans due to limited *in vivo* image resolution.

OBJECTIVE: To describe the detailed bone microarchitectural changes in the human knee within the first year following a unilateral acute ACL tear, using high-resolution peripheral quantitative computed tomography (HR-pQCT).

METHODS: Participants with unilateral ACL tears (n=15, 22-44 years of age, 10 female and 5 male) were followed with HR-pQCT with up to four time points (baseline, +2 months, +4 months, +8months). The baseline measurement occurred within 6 weeks of injury. Both the ACL deficient and uninjured contralateral knees were imaged at 61µm isotropic voxel size (XtremeCTII, Scanco Medical). Bone microarchitecture was assessed up to 7.5 mm below the weight bearing surfaces of the medial and lateral tibia and femur. The subchondral bone plate (density, thickness), and trabecular bone (density, thickness, number, separation) were quantified. Longitudinal bone changes within each knee were assessed using quadratic temporal mixed effects models, which were compared to linear and intercept-only mixed effects models using chi-squared tests (level of significance: $p<0.05$). 95% confidence intervals for each model parameter were assessed using bootstrapping (200 samples with replacement).

RESULTS: Bone loss occurred throughout the injured knee (-4.6% to -15.8%; Fig 1). Bone loss occurred in a non-linear manner, with loss occurring within the first 7 to 8 months post-injury before indicating the start of a recovery phase. The loss was driven by trabecular structure degradation as reflected by an increase in trabecular separation (6.4% to 10.6%) and decrease in number (-3.1% to -7.8%) of trabecular elements. The subchondral bone plate of the lateral femur significantly decreased in thickness (-9.0%). The contralateral knee was mostly unaffected.

CONCLUSION: Bone loss in the injured knee during the first year following ACL tears is driven by loss of trabecular elements. This likely cannot be reversed as for any future 'recovery' of bone mass there is no known mechanism to re-establish the original bone structure. Thus, permanent structural changes may persist, which indicates there may be a short window for intervention to reduce the risk of long-term OA development.
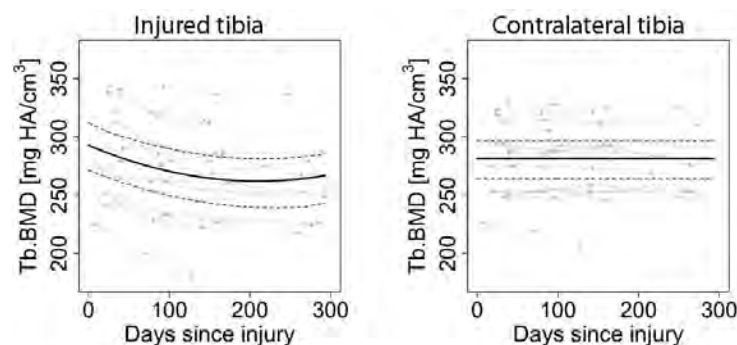
FIGURE 1: Bone mass of the LT (injured and contralateral knee) – example region of interest.

SODIUM PET-MRI DETECTS REGIONS OF ABNORMAL BONE RESPONSE TO ACUTE EXERCISE

*Watkins L., **Haddock B., *Uhlrich S., *Mazzoli V., *Gold G.E., *Kogan F.

*Stanford University, Stanford, USA
**Rigshospitalet, Copenhagen University Hospital, Denmark

INTRODUCTION: [18F]-sodium fluoride (18F-NaF) is a well-established bone-seeking agent which has shown promise as a marker to study bone metabolism in a variety of bone and joint disorders. Acute loading of the knee during exercise may act as a stimulus for bone remodeling.

OBJECTIVE: Here, we investigate bone metabolic activity in healthy and osteoarthritic knees in response to acute knee loading from exercise.

METHODS: Both knee joints of 12 healthy subjects (7 females, 5 males; age: 34 +/- 7 years; body-mass index: 23.1 +/- 3.3 kg/m^2) were scanned using [18F]NaF PET/MRI before and after performing one-legged step up and drop-land exercises. We identified focal areas with abnormally high increases in post-exercise uptake, defined as ROIs consisting of 4 or more adjacent voxels with an absolute SUV increase after exercise greater than two standard deviations above the mean SUV increase (0.83 ± 0.4). These abnormal focal ROIs (ROI_{focal}) were applied to pre- and post-exercise SUV maps for analysis. A second cohort of 5 osteoarthritic subjects (female; age: 62 +/- 7 years; body-mass index 28.8 +/- 4.6 kg/m^2) was scanned before and after performing one-legged squats to fatigue (58 +/- 17 squats) on an exercise machine using 50% body weight. Subjects performed the exercise on the affected knee, or on the knee with moderate pain if bilateral knee pain was reported. For these subjects, ROI_{focal} were recorded in the exercised knee where SUV increased by 3 or more.

RESULTS: In healthy subjects, eight ROI_{focal} were identified in the post exercise [18F]NaF PET images of six subjects (Fig 1a,b). Of these, three of the focal points already had significantly higher activity than the surrounding subchondral tissue at baseline, while five were unremarkable at baseline (Fig 1a,b). The relative mean increase in SUV_{max} was 342% (209 - 518%) for the focal points appearing normal at baseline and 111% (82–180%) for the focal points which were identifiable at baseline. In the OA cohort, 42 ROI_{focal} were identified in the post-exercise images of all five subjects (Fig 1c). Seven appeared unremarkable (SUV_{max}<3) at baseline with a relative mean increase in SUV_{max} of 297% (168 - 427%); 36 were abnormal (SUV_{max}>3) at baseline and had a mean increase of 95% (28 - 268%).
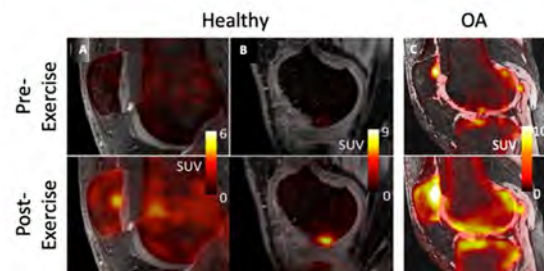
Fig 1: Representative [18F]]NaF PET images for healthy and OA subjects.

CONCLUSION: We sought to examine bone metabolic activity using an exercise protocol to acutely load the knee joint. After exercise, numerous focal regions of increased 18F-NaF uptake were observed in the subchondral bone. These were observed in higher proportion in the OA cohort, predominantly in subchondral regions where abnormally increased uptake was observed at baseline. Further, many of the ROI_{focal} regions in both healthy and OA subjects showed no abnormalities in 18F-NaF uptake compared to adjacent regions at baseline pre-exercise or structural subchondral bone abnormalities on MRI. Together, these findings suggest that 18F-NaF PET may identify regions where there are functional abnormalities in joint response to acute load. Areas of increased 18F-NaF uptake at baseline often correspond to structural abnormalities such as bone marrow lesions and osteophytes which often form in response to improper joint function. Even more interesting, subchondral regions showing high focal uptake only after acute loading suggest that 18F-NaF may detect functional abnormalities in areas that appear structurally normal on MRI.

CORRESPONDENCE ADDRESS: lewatkin@stanford.edu, (260) 243-1712

DYNAMIC CARTILAGE CONTACT MAPS INTEGRATED WITH T2 IMAGING

*,**Küpper J.C., **Kline A., **Felfeliyan B., *,**Ronsky J.L.

*Mechanical and Manufacturing Engineering, University of Calgary, Calgary, AB, Canada
**McCaig Institute for Bone and Joint Health, University of Calgary, Calgary, AB, Canada

INTRODUCTION: The complex relationship between the locations of contact in the knee during a dynamic task and the regional cartilage health status has not been fully characterized to date. Many approaches to explore variations in T2 over the joint divide the cartilage into static anatomical subregions [1] or investigate specific regions of interest [2]. However, linking the T2 values with the dynamic cartilage contact over the movement of interest [e.g., phases of walking (gait cycle)] may help to clarify how the cartilage contact patterns relate to areas of differing cartilage health that may occur with aging, following injury, or with OA progression.

OBJECTIVE: To demonstrate a methodology for linking cartilage contact mechanics during a dynamic task to static MRI T2 values in a healthy knee joint during the early stance phase of the gait cycle. It was hypothesized that T2 values during stance phase would be higher than during swing phase as higher habitual loading is sustained during this phase of the gait cycle [3]. The medial compartment was explored first since medial OA is more common [4].

METHODS: High-speed biplanar videoradiographic data was collected for one healthy participant (male, age 25) while walking on a treadmill at 1.2 m/s. The gait cycle was analyzed from 74%-100% (swing) and 0%-26% (stance). Cartilage contact regions (Fig. 1) were determined based on proximity of the tibiofemoral surfaces closer than a threshold of 1 mm. Vertices of the contact mesh were aligned with a point cloud of T2 values over the entire segmented tibiofemoral cartilage volume using an iterative closest point algorithm. The T2 values were determined from MRI scans of the knee, unloaded for at least one hour prior to scanning (T2 weighted fat suppressed FSE Multislice Multiecho Carr-Purcell Meiboom-Gill; ST 3mm; SS 1 mm; FOV 24 × 24 cm; 256 × 256 pixels; 33 slices; 16 echos with TE 7.5, 15,… 120 ms; TR 1733 ms; FA 90º; TA approx. 1'43"). To assign an average T2 value to each face of the contact mesh, a local volume above and below (20 mm) each face in the normal direction was searched for T2 points (i.e., over the entire cartilage depth) and averaged. The value for each frame was the T2 average over the contact surface.
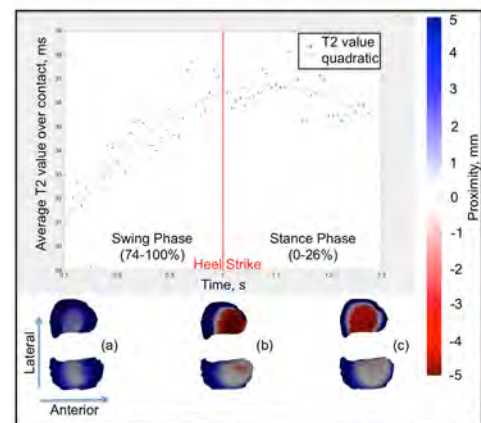
Figure 1: Average T2 values (ms) for tibial medial compartment (graph) over contact region (tibial surfaces with proximity in mm) during (a) swing phase (b) heel strike and (c) stance phase

RESULTS: The T2 values in the medial tibial compartment (Fig.1) increase (range of 5.8 ms) during swing phase to a maximum (36.8 ms) at approximately 1.1 s (10% gait cycle) and then decrease thereafter over a range of 1.8 ms.

CONCLUSION: The findings of higher T2 values during stance compared to swing support the hypothesis. The maximum point was 10% past heel strike, which could be explained by the fact that a local maximum vertical ground reaction force higher than body weight is typically observed at this point of the gait cycle [3]. The higher T2 is likely a result of the joint motion in this healthy subject rather than the cause. Stance phase is a region of sustained higher loading compared to swing phase. T2 values relate to the water content of the cartilage and in general higher T2 values may indicate a reduction in the cartilage quality in a region [1], or initiation of early changes to the joint (not observed in this participant based on MOAKS). Next steps include investigating T2 values over all compartments for multiple steps in additional participants, and a comparison to cartilage thickness.

REFERENCES: [1] Liu, Radiology, 2015 [2] Chang, Magn Reson Mater Phy, 2013 [3] Rose and Gamble, Human Walking 3rd Edition, 2006 [4] Felson, Arthritis Rheum, 2013
CORRESPONDENCE ADDRESS: johnsojc@ucalgary.ca

MRI-DETECTED STRUCTURAL ABNORMALITIES AND DEVELOPMENT OF INCIDENT RADIOGRAPHIC KNEE OA OVER 10 YEARS OF FOLLOW-UP

*Kwoh C.K., **,***Roemer F.W., ****Sharma L, *Ashbeck E.L., *Hu C., **Guermazi A.

* University of Arizona Arthritis Center, Tucson, AZ, USA
** Boston University School of Medicine, Boston, MA, USA
*** University of Erlangen-Nuremberg, Erlangen, Germany
**** Northwestern University, Chicago, IL, USA

INTRODUCTION: Structural joint pathology on MRI has been found in knees without radiographic evidence of osteoarthritis (OA). We have previously shown that structural abnormalities on MRI may be precursors of disease and associated with the detection of incident radiographic knee OA (ROA) up to 2 years later, and in some circumstances up to seven years later. The prognostic value of structural abnormalities on MRI for knee OA, however, is unknown.

OBJECTIVE: Estimate the probability of incident ROA over 10 years of follow-up, according to structural abnormalities detected on baseline MRIs.

METHODS: A subcohort of OAI participants (862 knees, one knee/person) with at least one knee at risk of developing ROA (i.e., KL 0,1 at baseline) was randomly selected. MRI-detected structural features of the knee were assessed by expert readers using MOAKS. Participants underwent bilateral posteroanterior fixed-flexion weight-bearing knee radiographs at baseline and annually through year 4, and then every two years until year 10. Radiographs were centrally read for KL grade, with ROA defined as KL$\geq$2. Survival was estimated with the Turnbull non-parametric maximum likelihood estimator, a generalization of Kaplan Meier curves for interval censored data. Survival curves were compared using a log rank permutation test available in the R package interval. Hazard ratios were estimated using Cox models fit using the R package icenReg, designed for interval censored data.

RESULTS: Knees with any of the following structural abnormalities had significantly higher estimated probabilities for the development of ROA over 10 years of follow-up: effusion-synovitis, bone marrow lesions (BMLs) in the whole knee, surface area cartilage damage in the whole knee, and medial meniscal extrusion (Table 1); as well as Hoffa-synovitis, lateral meniscal extrusion, medial and lateral meniscal tears/macerations, cartilage damage in the patellofemoral (PF), medial, and lateral compartments, and BMLs in the PF and medial regions (data not shown).

CONCLUSION: Our results demonstrate the prognostic value of MRI-detected effusion-synovitis, Hoffa-synovitis, BMLs, cartilage damage, and meniscal extrusion and morphology for the development of ROA up to 10 years later. Future directions include developing a predictive model that incorporates multiple features.

Table 1. Baseline MRI-Detected Structural Abnormalities and Incident Radiographic Osteoarthritis

MRI-detected abnormalities at baseline	Knees	Estimated Probability of Radiographic OA			P value*	Hazard Ratio	(95% CI)
		Within 2 years	Within 4 years	Within 10 years			
Effusion-Synovitis					<.0001		
Physiologic amount	692	0.06	0.10	0.27		1.00	ref
Small	146	0.15	0.31	0.46		2.11	(1.81, 2.46)
Medium/Large	24	0.48	0.62	0.67		5.10	(3.55, 7.34)
BML, Whole knee Max Score					<.0001		
0: none	339	0.06	0.10	0.21		1.00	ref
1: <33%	333	0.08	0.13	0.33		1.43	(1.22, 1.67)
2: 33-66%	143	0.14	0.25	0.41		2.14	(1.78, 2.57)
3: >66%	47	0.24	0.41	0.56		3.25	(2.49, 4.24)
Cartilage Damage, Surface Area, Whole Knee Max Score					<.0001		
0: none	146	0.04	0.06	0.13		1.00	ref
1: <10%	235	0.03	0.06	0.16		1.41	(1.05, 1.90)
2: 10-75%	454	0.13	0.21	0.43		3.67	(2.81, 4.80)
3: >75%	27	0.43	0.43	0.66		8.66	(5.40, 13.86)
Meniscus Extrusion, Medial					<.0001		
0: <2 mm	677	0.06	0.12	0.24		1.00	ref
1: 2-2.9 mm	141	0.19	0.32	0.55		2.51	(2.15, 2.92)
2/3: >3 mm	44	0.20	0.25	0.55		2.88	(2.27, 3.66)

*Asymptotic Logrank k-sample test (permutation form), Sun's scores

DISCLOSURE STATEMENT: CKK, grant/research support from EMD Serono, consultant for EMD Serono, TissueGene, Taiwan Liposome Co., Astellas and Thusane; FWR and AG, shareholders BICL, LLC; LS, None; ELA, consultant for EMD Serono; CH, None; AG, consultant to Pfizer, EMD Serono, AstraZeneca, TissueGene and Roche.
CORRESPONDENCE ADDRESS: kwoh@arthritis.arizona.edu

dGEMRIC IS REDUCED IN HIPS WITH BONE MARROW LESIONS

*Jones C.E., **Qian H., *Zhang H., ***Guo Y., ****Russell D., ****Forster B.B., **Wong H., ***Esdaile J.M., *Wilson D.R., ***Cibere J., and the IMPAKT-HiP study team

*Centre for Hip Health and Mobility, Vancouver, BC, CAN
**Centre for Health Evaluation and Outcome Science, Vancouver, BC, CAN
***Arthritis Research Canada, Richmond, BC, CAN
****Department of Radiology, Faculty of Medicine, Univ. of British Columbia, Vancouver, BC, CAN

INTRODUCTION: Bone marrow lesions (BML) are associated with painful and progressive OA. Quantitative MRI has been used to study early cartilage degeneration in knees with BML, but similar work has not been done in the hip. Further work is needed to understand the connection between BML and cartilage degeneration in the hip.

OBJECTIVE: The purpose was to compare mean dGEMRIC relaxation values (T_{1Gd}) in hips with BML to mean T_{1Gd} in hips without BML in a population-based study. Reduced T_{1Gd} suggests depleted GAG. Our hypothesis was: mean T_{1Gd} is lower in hips with BML compared to hips without BML.

METHODS: Study participants (n=128) were recruited from the Investigations of Mobility, Physical Activity, and Knowledge Translation in Hip Pain (IMPAKT-HiP) study, which is a cross-sectional population-based study of 500 subjects aged 20-49 years with and without hip pain and femeroacetabular impingement (FAI) in Vancouver, Canada. dGEMRIC and proton-density (PD) weighted MRI scans of one hip from each of the 128 participants who completed the dGEMRIC protocol were used for this analysis. BML were identified from PD-weighted fat-suppressed images by a MSK radiologist using the Hip OA MRI Scoring System (HOAMS). BML were graded semi-quantitatively (grade 0-3: absent, small ($\leq$33%), moderate (33-66%), and severe (>66%)) in 15 regions. Hips with at least one BML of any grade in any region were treated as the BML group. Acetabular and femoral cartilage were manually segmented as a single object by an imaging scientist to determine mean T_{1Gd}. We applied a sampling-weighted linear regression model to determine the association of the presence of BML with mean cartilage T_{1Gd} (significance: p<0.05). The model was adjusted for age, sex, BMI and physical activity. Sampling weights accounted for non-response of eligible participants and for poststratification to match the population of a large city (n=1,016,990).

RESULTS: 36 of the 128 participants (28%) had at least one BML. Subjects with BML, compared to those without BML, had similar weighted characteristics on age, BMI, physical activity levels, and frequency of hip pain. In the BML group 57% were male and 81% had FAI compared to 45% and 37%, respectively, in the no-BML group. From the crude weighted regression model mean T_{1Gd} was 79ms (95% CI: [-140, -18], p=0.01) (9%) lower in the BML group compared to the no-BML group. After adjustment for age, sex, BMI, and physical activity, mean T_{1Gd} was 83ms (95% CI: [-152, -14], p=0.02) (10%) lower in the BML compared to the no-BML group (Table 1).

CONCLUSION: Our result that the estimated difference in overall mean T_{1Gd} between the BML and no-BML groups was 11.2% suggests cartilage in hips with BML have a lower GAG content than hips without BML, which is consistent with previous studies. These results suggest that BML are associated with cartilage degeneration in the hip. This work motivates further study of BML in the hip and the relationship between BML and cartilage degeneration.

Table 1: Difference in mean T1Gd between BML and no-BML adjusted for age, sex, BMI, and physical activity.

Model Adjustments	Estimated difference (ms) [95% CI]	p-value
Crude	-79.34 [-140.54, -18.15]	0.01
Age, sex	-85.09 [-152.06, -18.13]	0.01
Age, sex, BMI	-84.46 [-152.19, -16.73]	0.01
Age, sex, BMI, physical activity	-83.15 [-152.06, -14.24]	0.02

DETECTING EARLY SUPERFICIAL AND DEEP CHANGES IN CARTILAGE OF ACL-RECONSTRUCTED KNEES USING CLUSTER ANALYSIS OF T2 RELAXATION TIMES

*,**Black M.S., **Young K., **Chaudhari A.S., **Kogan F., **Gold G.E., *,**Levenston M.E., **Hargreaves B.A.

*Mechanical Engineering, Stanford University, Stanford, CA, USA
**Radiology, Stanford University, Stanford, CA, USA

INTRODUCTION: Individuals who have experienced anterior cruciate ligament (ACL) tears have a significantly elevated risk of developing osteoarthritis, whether the ACL has been surgically reconstructed or not[1,2]. Cluster analysis of cartilage T2 relaxation times has been shown to detect differences between healthy and ACL-injured knees as early as 6 months post-surgery in femoral cartilage[3]. Superficial and deep layers of cartilage exhibit different properties and are affected differently during OA development; thus, separate analysis of both layers may allow for additional sensitivity to changes that may otherwise be undetected using full-thickness cartilage analysis.

OBJECTIVE: The objective of this study was to evaluate if changes in deep and superficial cartilage following ACL-reconstruction surgery can be observed using cluster analysis to detect elevated T2.

METHODS: 10 ACL-injured subjects undergoing ACL-reconstruction surgery (5W/5M, 39±12 yrs, BMI: 23 ± 1.5) and 10 matched controls (5W/5M, 37±13 yrs, BMI: 23 ± 1.5) were included in this study. Both knees of the ACL-reconstructed subjects and the right knee of the control subjects were scanned in a 3T MRI scanner using a quantitative DESS sequence to obtain T2 relaxation times[4] at: 3-weeks (baseline), 3-months, 9-months and 18-months post-ACL reconstruction surgery. Femoral and tibial cartilage was manually segmented and T2 projections were created[3] and further separated into superficial and deep layers based on the thickness midpoint. T2 difference maps were created by subtracting the baseline projection from each timepoint (Fig.1a). Clusters in difference maps were quantified as adjoining sets of pixels with an area > 12.4mm^2 consisting of values greater than 2x the standard deviation of control subjects' difference maps[3] (Fig.1a). Cluster maps were divided into anatomical regions (medial, lateral and anterior, central, posterior) for further analysis. Our outcome was reported as the change in T2 percent cluster area (ΔT2%CA, area fraction covered by clusters) in each region. We used a general linear model with Bonferroni's correction to test for differences in ΔT2%CA.

RESULTS: The ΔT2%CA of the ACL-reconstructed knee progressively increased in the femoral cartilage (Fig 1). The ΔT2%CA in femoral cartilage for even the early 3-month time-point was significantly higher than that of both the contralateral knee (p=0.001) and the control knee (p<0.001). While ΔT2%CA in tibial cartilage did not significantly differ from controls at 3-months (p=0.692), by 9-months the ΔT2%CA was significantly higher than the control (p=0.007). Trends in the deep vs superficial zones were apparent, including slightly decreasing ΔT2%CA in the tibial superficial layer, as opposed to progressively increasing ΔT2%CA in the deep zone (Fig 1c).
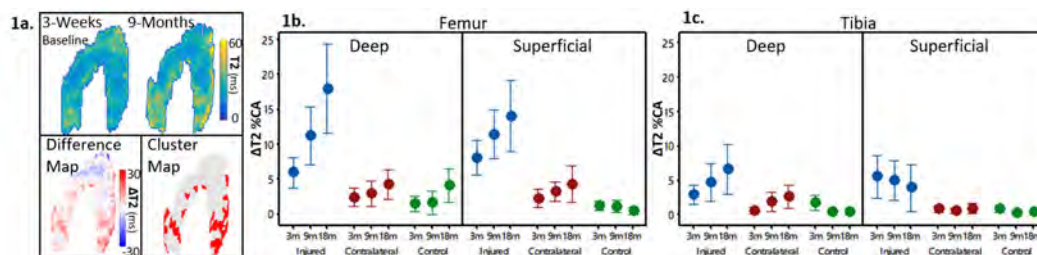

Figure 1: (a) Sample projection maps of T2 at 3-weeks (baseline) and 9-months post-surgery, resulting difference map (ΔT2), and resulting cluster maps indicating elevated T2. ΔT2%CA results for femoral (b) and tibial (c) cartilage in both deep and superficial layers at 3-months (3m), 9-months (9m) and 18-months (18m) post-surgery.

CONCLUSION: The higher ΔT2%CA for ACL-reconstructed compared to the contralateral and control knees is indicative of early cartilage changes occurring following ACL-reconstruction surgery. The ΔT2%CA is representative of local, elevated T2 and could represent specific areas within cartilage where degeneration first occurs. It appears that these earliest changes may be occurring in the femoral cartilage as soon as 3-months post-surgery. Early detection of cartilage changes is necessary to stop the progression of OA, and the T2 cluster analysis method may be ideal for detecting early cartilage degeneration and monitoring OA progression.

REFERENCES: [1] Simon 2015 [2] Meuffels 2009 [3] Monu 2017 [4] Sveinsson 2017
DISCLOSURE STATEMENT: BAH and GEG receive research support from GE Healthcare. ASC consults for Subtle Medical, Skope MR, Chondrometrics GmBH.
CORRESPONDENCE ADDRESS: mblack32@stanford.edu

PREVALENCE OF INTRA-ARTICULAR MINERALIZATION ON KNEE DUAL-ENERGY COMPUTED TOMOGRAPHY: THE MULTICENTER OSTEOARTHRITIS STUDY

*Jarraya M., **Neogi T., ***Lynch J.A., **Clancy M., **Felson D., ***Nevitt M., ****Lewis C.E., *****Torner J., *Guermazi A.

*Department of Radiology, Boston University School of Medicine, Boston, MA
**Department of Medicine, Boston University School of Medicine, Boston, MA
***Department of Epidemiology, University of California San Francisco, San Francisco, CA
****Department of Epidemiology, University of Alabama at Birmingham, AL
*****Department of Epidemiology, College of Public Health, University of Iowa, IA

INTRODUCTION: Computed tomography (CT) has a higher sensitivity for the detection of intraarticular (i.a.) mineralization in comparison with commonly used imaging technique in knee OA including radiographs and MRI. The role of i.a. mineralization in knee OA is unclear, yet worth investigating.

OBJECTIVE: to report the prevalence of CT-detected i.a. mineralization in older adults with or at risk of knee OA.

METHODS: The Multicenter Osteoarthritis (MOST) Study is an NIH-funded longitudinal cohort study of persons with or at risk of knee OA. In the current visit, bilateral knee CT scans, PA knee radiographs and standard questionnaires to ascertain frequent knee pain are being obtained. A musculoskeletal radiologist scored multiplanar CT images using an ordinal score (0-3) for degree of mineralization in each of the WORMS subregions of cartilage and menisci, as well as ligaments, capsule, and vasculature. Prevalence of i.a. mineralization was computed for the total sample, and stratified by age, sex, and presence of frequent knee pain and radiographic knee OA (ROA) (Kellgren and Lawrence grade ≥ 2).

RESULTS: To date, 621 subjects (1242 knees) have been scored during the ongoing study visit (58% female, mean age 71.8, mean BMI 29.8). Overall, 12% of knees had calcium crystal deposition on radiograph, while CT-detected mineralization was present in 24% of knees in either cartilage, meniscus, and/or capsule. The prevalence in specific locations was: 17% articular cartilage, 20% meniscus, and 12% capsule (figure). Of the knees with CT-detected articular cartilage mineralization, the majority had it in 1-4 WORMS cartilage subregions (out of 14), and 81% also had meniscal mineralization. For the knees with meniscal mineralization, the majority had it in 5 or 6 WORMS meniscus subregions (out of 6), and 41% also had articular cartilage mineralization. Articular and meniscal mineralization increased with age, was similar among men and women, and was more prevalent in those with ROA. Prevalence of CT-detected i.a mineralization was comparable in subjects with and without frequent knee pain (Figure). Capsular mineralization was similar across age and gender, but more prevalent in those with ROA. Overall, 52% of knees had vascular calcification, which increased with age and was more prevalent in men.

CONCLUSION: CT of the knee provides greater visualization of i.a. mineralization than radiographs, including locations within the hyaline articular cartilage, meniscus, and soft tissue, as well as its co-localization. These data will provide opportunity to evaluate the longitudinal relation of i.a. mineralization to adjacent articular tissue pathology and overall OA progression.

DISCLOSURE STATEMENT: AG (President: BICL, LLC. Consultant: Merck Serono, Ortho-Trophix, Genzyme and TissueGene). Other authors have nothing to disclose.
CORRESPONDENCE: mohamedjarraya@gmail.com

Figure: Prevalence of intra-articular mineralization on knee CT
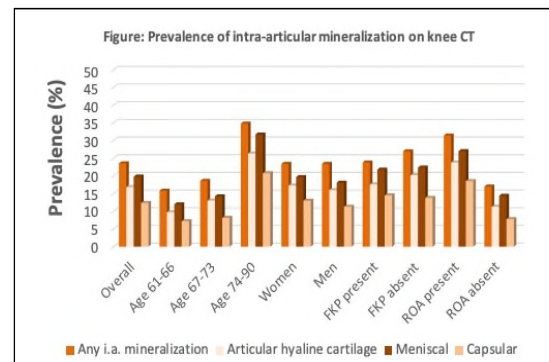
OPTIMIZING SUBJECT SELECTION IN KNEE OSTEOARTHRITIS CLINICAL TRIALS BY RADIOGRAPHIC JOINT SPACE WIDTH: POST-HOC CLINICAL RESPONSE ANALYSIS FROM A PHASE 2B TRIAL OF WNT PATHWAY INHIBITOR SM04690

*Kennedy S., *Swearingen C.J., *Tambiah J., **Conaghan P.

*Samumed, LLC, San Diego, CA, USA
**University of Leeds, Leeds, UK

INTRODUCTION: Knee osteoarthritis (OA) trial radiographic inclusion criteria usually comprises Kellgren-Lawrence (KL) grading, which mixes features such as osteophytes and joint space narrowing and leads to study population heterogeneity. Selecting subjects with baseline medial joint space width (mJSW) 2-4 mm has been shown to reduce heterogeneity and improve responsiveness to radiographic change in comparison to broader knee OA populations.[1,2] However, effects of baseline-fixed mJSW on symptom responsiveness are unknown.

OBJECTIVE: To evaluate the impact of baseline mJSW 2-4 mm on patient-reported outcomes (PROs) as measured by effect size in a 24-week phase 2b trial of SM04690, a Wnt pathway inhibitor in development as a potential disease-modifying OA drug (DMOAD).

METHODS: Knee OA subjects with KL grades 2-3 and Pain Numerical Rating Scale (NRS, [0-10]) ≥4 and ≤8 in the target knee and <4 in the contralateral knee received a single IA 2 mL SM04690 injection (0.03, 0.07, 0.15, 0.23 mg), vehicle placebo (PBO), or sham (dry needle) in the target knee at baseline. PRO 24-week endpoints included change from baseline in weekly average of daily OA target knee pain by NRS, Western Ontario and McMaster Universities Osteoarthritis Index (WOMAC) Pain [0-100], WOMAC Physical Function [0-100], and Patient Global Assessment (PtGA) [0-100]. Primary results are presented elsewhere.[3] A post-hoc completer analysis of subject results with baseline mJSW 2-4 mm is reported.

RESULTS: 635 subjects (91.4%) completed the study (mean age 59.0 [±8.5] years, BMI 29.0 [±4.0] kg/m^2, female 58.4%, KL3 57.3%). In both full analysis set (FAS, all dosed subjects) and mJSW 2-4 mm subjects, significant improvements compared to PBO (P<0.05) were seen in Pain NRS, WOMAC Pain, WOMAC Function, and PtGA for 0.07 mg and 0.23 mg SM04690 dose groups at Week 12 (Figure). The effect sizes were improved in the mJSW 2-4 mm group in comparison to FAS for most doses at Weeks 12 and 24.

CONCLUSION: In this post-hoc analysis of SM04690-treated knee OA subjects, those with baseline mJSW 2-4 mm showed increased PRO effect sizes compared to those in the FAS. Previous data also demonstrated SM04690-treated subjects with mJSW 2-4 mm had improved radiographic sensitivity to change. Data from SM04690 studies suggest mJSW 2-4 mm should be considered as an inclusion criterion for trials of potential knee DMOADs.

Figure. Ladder plot of effect size and treatment estimates (with 95% confidence intervals) for improvement in Pain NRS over PBO

δ: Effect size   *: $P < 0.05$
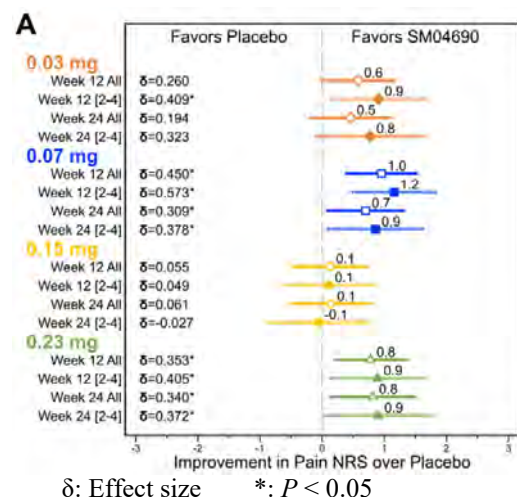
REFERENCES:
[1] Bowes, ARD, 2017
[2] Yazici, Arthritis Rheumatol, 2017
[3] Yazici, Arthritis Rheumatol, 2018

MRI-BASED SCREENING FOR STRUCTURAL DEFINITION OF ELIGIBILITY IN CLINICAL DMOAD TRIALS: RAPID OSTEOARTHRITIS MRI ELIGIBILITY SCORE (ROAMES)

*,**Roemer F.W., ***Collins J.E., ****Kwoh C.K., *****Hannon M.J., ******Neogi T., ******Felson D.T., *******Hunter D.J., ********Lynch J.A., *Guermazi A.

*Quantitative Imaging Center (QIC), Department of Radiology, Boston University School of Medicine, Boston, MA
**Department of Radiology, University of Erlangen-Nuremberg, Erlangen, Germany
***Orthopaedics and Arthritis Center of Outcomes Research, Brigham and Women's Hospital, Harvard Medical, School, Boston, MA, USA
****University of Arizona Arthritis Center & University of Arizona College of Medicine, Tucson, AZ USA
*****Pinney Associates, Pittsburgh, PA, USA & Division of Rheumatology and Clinical Immunology, University of Pittsburgh School of Medicine, Pittsburgh, PA, USA (former affiliation at time of study)
******Boston University School of Medicine, Section of Rheumatology, Boston, MA, USA.
*******Department of Rheumatology, Royal North Shore Hospital and Institute of Bone and Joint Research, Kolling Institute, University of Sydney, St Leonards, NSW, Australia.
********Department of Epidemiology and Biostatistics, University of California San Francisco, San Francisco, CA, USA

INTRODUCTION: Although a number of potential disease-modifying molecules have been investigated in recent years, there is still no pharmacological agent that has been approved by regulatory agencies. There are several reasons for failure of clinical trials in the past, including the commonly applied definition of structural eligibility based on radiographic assessment. In the context of precision medicine it will be of increasing relevance to find the appropriate patient for a specific treatment approach. Phenotypical stratification by imaging at eligibility will be paramount in the future and cannot be achieved using radiography alone. Furthermore, joints at high risk for faster progression need to be identified, as these may allow a more efficient DMOAD trial design. In addition, joints at high risk of joint collapse should to be excluded at screening. MRI may be able to offer solutions in this context, and commonly perceived hurdles in the application of MRI at eligibility assessment may potentially be overcome as a result of technological advances and simplified image assessment.

OBJECTIVE: Our aim was to introduce a simplified MRI instrument, Rapid OsteoArthritis MRI Eligibility Score (ROAMES), for defining structural eligibility of patients for inclusion in disease-modifying osteoarthritis drug trials using a tri-compartmental anatomic approach that enables stratification of knees into different structural phenotypes and includes diagnoses of exclusion. We also aimed to define overlap between phenotypes and determine reliability.

METHODS: 50 knees from the Foundation for National Institutes of Health Osteoarthritis Biomarkers study, a nested case-control study within the Osteoarthritis Initiative, were selected within pre-defined definitions of phenotypes as either inflammatory, subchondral bone, meniscus/cartilage, atrophic or hypertrophic. A focused scoring instrument was developed covering cartilage, meniscal damage, inflammation and osteophytes. Diagnoses of exclusion were meniscal root tears, osteonecrosis, subchondral insufficiency fracture, tumors, malignant marrow infiltration and acute traumatic changes. Reliability was determined using weighted kappa statistics. Descriptive statistics were used for determining concordance between the a priori phenotypic definition and ROAMES and overlap between phenotypes.

RESULTS: ROAMES identified 43 of 50 (86%) pre-defined phenotypes correctly. Of the 50 participants, 27 (54%) had no additional phenotypes other than the pre-defined phenotype. 18 (36%) had one and 5 (10%) had two additional phenotypes. None had three or four additional phenotypes. All features of ROAMES showed almost perfect agreement. One case with osteonecrosis and one with a tumor were detected.

CONCLUSION: ROAMES is able to screen and stratify potentially eligible knees into different structural phenotypes and record relevant diagnoses of exclusion. Reliability of the instrument showed almost perfect agreement.

DEEP LEARNING APPROACH TO PREDICT PAIN PROGRESSION IN KNEE OSTEOARTHRITIS

*Kijowski R., *Guan B., *Liu F., **Mirzaian A., **Demehri S., ***Neogi T., ***Guermazi A.

*University of Wisconsin School of Medicine, Madison, Wisconsin, USA
**John Hopkins School of Medicine, Baltimore, Maryland, USA
***Boston University School of Medicine, Boston, Massachusetts, USA

BACKGROUND: Pain progression in individuals with knee osteoarthritis (OA) is poorly understood and difficult to predict. Developing improved methods for predicting the progression of knee pain could identify individuals at high risk for pain progression who would be best suited for early intervention.

OBJECTIVE: We hypothesize that a deep learning (DL) approach could be used to predict knee pain progression in subjects with knee OA.

METHODS: The study group consisted of 600 subjects from the FNIH Biomarkers Consortium with Kellgren Lawrence (KL) grades 1, 2, or 3 knee OA at baseline. Two-hundred ninety-seven subjects showed pain progression and 303 subjects did not show pain progression over a 48-month follow-up period. Pain progression was defined as a 9 point or greater increase in WOMAC score between baseline and 2 or more follow-up time-points. Six-fold cross-validation was used for training and evaluation of the DL models for predicting knee pain progression. For each fold, the study group was randomly divided into a training dataset (247 subjects with and 253 subjects without pain progression) used to train the models and a testing dataset (50 subjects with and 50 subjects without pain progression) used to evaluate model performance. A fully connected neural network was used to create a clinical model to provide a probability score for pain progression using demographic and radiographic risk factors including age, gender, body mass index, history of knee trauma, baseline KL grade, and varus or valgus alignment. The convolutional neural network DenseNet was used to assess the baseline standing posterior-anterior knee radiographs of subjects and provide a probability score for pain progression. A combined clinical and DL model was also created by integrating both clinical data and DL analysis of baseline radiographs to provide a probability score for predicting pain progression. The combined model used DenseNet to extract radiographic information as a feature vector, which was further concatenated with the clinical data vector. The combined feature vector was then fed to a fully connected neural network for joint model training. Receiver operation characteristic (ROC) and area under the curve (AUC) analysis was performed using the testing dataset to evaluate the diagnostic performance of the clinical, DL, and combined clinical and DL models for predicting pain progression. Delong's method was used to compare the AUCs of the models. The optimal sensitivity and specificity of the models were determined using the Youden index.

RESULTS: The AUC for the clinical model, DL model, and combined clinical and DL model was 0.692 (95% CI 0.653-0.729), 0.794 (95% CI 0.759-0.826), and 0.857 (95% CI 0.827-0.884) respectively. The DL model had significantly higher ($p<0.01$) AUC than the clinical model, while the combined model had significantly higher ($p<0.01$) AUC than the DL and clinical models. The standard deviation of the AUCs for the combined model for the six folds of training and testing was 0.023, indicating high model stability. The optimal sensitivity for the clinical model, DL model, and combined clinical and DL model was 66.3% (95% CI 60.7%-71.7%), 78.0% (95% CI 72.9%-82.6%), and 85.5% (CI 81.1%-89.3%) respectively. The optimal specificity for the clinical model, DL model, and combined clinical and DL model was 62.0% (95% CI 56.2%-67.5%), 79.0% (95% CI 73.9%-83.4%), and 72.3% (95% CI 66.8%-77.3%) respectively.

CONCLUSION: Our study demonstrated the feasibility of using a combined clinical and DL model for predicting pain progression in subjects with knee OA using baseline knee radiographs. The combined clinical and DL model showed a significant improvement in diagnostic performance for predicting pain progression when compared to a clinical model and DL model alone.

RADIOGRAPHIC SELECTION CRITERIA FOR KNEE OA TRIALS DETERMINE SENSITIVITY TO CHANGE AND PROGRESSOR RATES IN MEDIAL COMPARTMENT CARTILAGE THICKNESS LOSS

*,**Wirth W., ***Nevitt M.C., ****Hunter D.J., *****Kwoh C.K., *,**Maschek S., *,**Eckstein F.

*Chondrometrics GmbH, Ainring, Germany
**Paracelsus Medical University Salzburg & Nuremberg, Salzburg, Austria
***Univ. of California San Francisco, San Francisco, CA
****Rheumatology Dept., Inst. of Bone and Joint Res., Univ. of Sydney, Sydney, Australia
*****Univ. of Arizona Arthritis Ctr., Tucson, AZ

INTRODUCTION: OARSI JSN grades allow to specifically select knees with structural progression in the affected compartment and are therefore superior to whole-knee KLG when relying on compartment-specific outcome measures. Baseline minJSW was suggested to be a more objective alternative to JSN grades for participant selection, but the minJSW-based participant selection may be confounded by body height and sex.

OBJECTIVE: a) To explore the impact of body height and sex on minJSW; b) to report the sensitivity to change and % progressor rates in medial compartment cartilage thickness over one year for strata of OARSI medial JSN and minJSW; c) to provide an informed recommendation on selection criteria for DMOAD trials

METHODS: The analysis was based on 866 OAI participants (59% females, age: 62±9 years, BMI: 30±5 kg/m²) with radiographic OA (KLG 2-4) at baseline. They were required to have baseline OARSI JSN grades from central readings, baseline minJSW measurements with reasonable tibial alignment (rim distance <6.5mm), and medial femorotibial compartment (MFTC) cartilage thickness measurements at baseline and year 1 follow-up. Mean change and sensitivity to change (SRM = standardized response mean = mean change / SD) and MFTC % progressor rates were calculated for each stratum. For progressor rates, the change observed in healthy reference knees was used as reference (80% confidence level: mean change ± 1.28 x SD [104 µm])[1].

RESULTS: For both men and women, baseline minJSW differed significantly between those below vs above the sex-specific median height (men: 3.1±1.7mm vs. 3.5±1.7mm, women: 3.2±1.3mm vs. 3.5±1.5mm; both p < 0.05). Women with medial JSN 0-2 had lower baseline minJSW than men (JSN 0: 4.7±0.8mm vs. 5.5±1.0mm; JSN 1: 4.0±0.7mm vs. 4.4±0.8mm; JSN2: 2.5±0.7mm vs. 2.8±0.8mm; all p<0.001). Longitudinally, the greatest SRM amongst JSN strata was observed in knees with medial JSN 3 (-0.71), and for minJSW strata in knees with 1-2mm minJSW (Table). The percentage of knees with progression was greatest for knees with medial JSN 2, and for knees with 1-2mm minJSW (Table). When combining JSN strata, the SRMs were -0.60 for knees with JSN 2&3, -0.48 for knees with JSN 1-3, -0.45 for knees with JSN 1-2. For combined minJSW strata, the SRMs were -0.76 for 0-2mm minJSW, -0.60 for 0-3mm minJSW, and -0.59 for 1-2mm minJSW.

Table: Mean change ±SD (in µm), standardized response mean (SRM) and % progressor knees

	medial JSN (N=178/261/336/91)				minJSW (N=117/182/223/177/107/60)					
	Grade 0	Grade 1	Grade 2	Grade 3	>=5mm	4-5mm	3-4mm	2-3mm	1-2mm	0-1mm
Mean±SD	-6±129	-32±122	-109±187	-100±142	-7±115	-31±136	-55±157	-84±178	-150±187	-89±121
SRM	-0.05	-0.26	-0.58	-0.71	-0.06	-0.23	-0.35	-0.47	-0.80	-0.74
% Progr.	17.4	24.9	45.5	40.7	20.5	22.5	32.7	38.4	54.2	36.7

CONCLUSION: Baseline minJSW was associated with body height and sex, but still allowed selecting subgroups with high sensitivity to change. Knees with high JSN grades or low minJSW showed the greatest SRMs of one-year cartilage thickness change and greatest progressor rates. However, the specificity of radiographic selection criteria needs to be balanced against the screening efficacy. Knees with medial JSN 1-2 (or 1-3) or minJSW 1-3mm (or 0-3mm) may therefore represent a suitable compromise for one-year MRI trials.

REFERENCES: [1] Wirth, OARSI, 2019

3D STRUCTURAL PARAMETERS PREDICT FUTURE TOTAL HIP REPLACEMENT BETTER THAN CURRENT 2D RADIOGRAPHIC STANDARDS: AN AGES-REYKJAVIK STUDY

*Turmezei T.D., **Treece G.M., **Gee A.H., ***Sigurðsson S., ***Jónsson H., ****Aspelund T., ****Guðnason V., **Poole K.E.S.

*Norfolk and Norwich University Hospital, Norwich, UK
**University of Cambridge, Cambridge, UK
***Landspitalinn University Hospital, Reykjavík, Iceland
****Icelandic Heart Association, Kopavogur, Iceland

INTRODUCTION: 2D radiography has been the mainstay of imaging endpoint assessment in research trials, however the FDA recently published guidance recognising the importance of structural endpoints for accelerated therapeutic development. Here we show how a technically validated 3D imaging analysis technique using computed tomography (CT) imaging data called joint space mapping (JSM) can outperform the gold standard 2D radiographic approaches in prediction of total hip replacement (THR).

OBJECTIVE: To compare output from quantitative 3D structural analysis of hip CT data against gold standard 2D radiographic criteria in a predictive model of future THR in healthy older adults.

METHODS: We undertook a nested case-control study within the prospective AGES-REYKJAVIK cohort of 3133 healthy older adults. Standard clinical CT of both hips was performed at study baseline with 1mm slice thickness for all participants. After 2:1 matching of THR cases for age and gender, exclusion criteria applied were THR for fracture rather than osteoarthritis (16 hips), movement artefact (6 hips), incomplete joint coverage (2 hips), and joint ankylosis (1 hip), leaving 80 individuals with THR performed in the subsequent 5 years *versus* 187 controls. There was no significant difference between the two groups by age (74.3 ± 4.7 vs 74.4 ± 4.9 yrs), sex (30:50 vs 69:118 M:F), nor BMI (27.9 ± 4.3 vs 27.5 ± 4.2 kg/m^2). KLG and minimum 2D JSW were recorded for each hip from 2D radiographs digitally reconstructed from the CT imaging data. After performing JSM, statistical shape modelling determined 3D shape modes across all hips, the first 7 modes accounting for up to 90% of all shape variation. Statistical parametric mapping (SPM) was used to determine significantly different regions of 3D JSW between the two groups; any paired hips were averaged to account for cluster bias from within-subject correlation. The SPM general linear model included THR status, age, BMI, and the first 7 shape modes. Sex was highly correlated with shape mode 1 (scale) and therefore removed from all models. Receiver operating characteristic (ROC) curves with area under the curve (AUC) values were calculated using a leave-one-out cross-validation classifier predictive model for THR along with hip pain (HP, any pain in the index hip for more than one month in the last year), KLG, minimum 2D radiographic JSW (min2D), minimum 3D JSW from within the SPM significance region of interest (ROI) divided by mean global JSW (min3D), and 3D shape mode coefficients (SM).

RESULTS: SPM revealed a large area across the superior joint space in which JSW was dependent on future THR, being significantly narrower in THR cases compared to controls by up to 1 mm (p<0.05). This was the ROI from which a minimum 3D JSW value was taken at each hip to be used in the predictive model. Hip pain was the poorest predictor (AUC = 0.69), while KLG (0.72) and minimum 2D radiographic JSW (0.73) were outperformed by the first 7 3D shape modes (0.74) and minimum 3D JSW (0.79). AUC increased for the combination of 3D JSW and shape mode data (0.81), and was maximal when KLG was also included (0.86).

CONCLUSION: Quantitative output from 3D JSM of standard clinical CT imaging results in better prediction of THR than 2D radiographic gold standards in healthy older individuals. These findings support exploration of JSM application in clinical trials with potential for prediction, stratification, and monitoring of osteoarthritis.

HISTORY OF ACUTE KNEE INJURY AS AN INDICATOR FOR THE PROTECTIVE EFFECT OF BISPHOSPHONATES ON KNEE OSTEOARTHRITIS: A LONGITUDINAL PROPENSITY SCORE-MATCHED STUDY FROM THE OSTEOARTHRITIS INITIATIVE (OAI) COHORT

*Haj-Mirzaian A., **Guermazi A., **,***Roemer F.W., *Demehri S.

*Russell H. Morgan Department of Radiology and Radiological Science, Johns Hopkins University School of Medicine, Baltimore, Maryland, USA
**Department of Radiology, Boston University School of Medicine, Boston, Massachusetts, USA
***Department of Radiology, University of Erlangen-Nuremberg, Erlangen, Germany

BACKGROUND: Bisphosphonates (BPs) has gained much interest as potential disease-modifying osteoarthritis (OA) drugs, but findings about the possible effects of these drugs were conflicting. Due to the heterogeneous pathophysiology of knee OA (e.g., post-traumatic, genetic-based generalized, etc.), it might be possible that a subset of OA subject, not all of them, responds to BPs therapy.

OBJECTIVE: We aimed to evaluate whether BPs intake only in subjects with a positive history of acute knee injury (versus subjects with no history of acute injury) was associated with the lower risk of knee OA incidence/progression.

METHODS: We analyzed all data from the Osteoarthritis Initiative (OAI) cohort with more than 8-years follow-up (n= 9592 knees). Using baseline self-reports, included knees were categorized into two groups of with and without a history of acute injury and all analyses were performed in these two groups separately. In each group, subjects were classified as BPs user and non-user using baseline and annual self-reports. Next, to address confounding by indication bias and considering the potential relationship between OA and osteoporosis, BPs users and non-users were matched for potential confounding factors (defined based on FRAX tool) using 1:1 propensity score (PS) matching method. Using this method, 114:114 and 372:372 BPs users:non-users were selected in with and without acute injury groups, respectively. Cox proportional hazard regression was performed on BPs use for the prediction of longitudinal radiographic knee OA incidence (development of Kellgren-Lawrence (KL) grade ≥ 2), radiographic OA progression (worsening whole grade joint space narrowing score ≥ 1), and pain incidence or Non-Acceptable Symptom State (NASS). The mixed model analysis was also performed for evaluating the potential impact of BPs use on annual change of minimum medial joint space width (JSW) measures.

RESULTS: In subjects with a positive history of acute knee injury, BPs users had 68%, 9%, and 28% lower risk of radiographic OA incidence (HR: 0.32, 95%CI: 0.21-0.50), radiographic OA progression (HR: 0.91, 95%CI: 0.74-1.11), and NASS (HR: 0.72, 95%CI: 0.55-0.95) in comparison with non-users. In contrast, in knees with no history of acute injury, BPs use was associated with the higher risk of OA incidence (HR: 1.32, 95%CI: 1.03-1.70) and no significant associations for NASS and radiographic progression. Same results were obtained using mixed model analysis for JSW change; in knees with a history of acute injury, BPs use was associated with 52% lower risk of JSW loss in comparison with non-significant results for knees with no history of acute injury.

CONCLUSION: Using longitudinal analysis and new-user design, we showed that BPs use was associated with the lower risk of knee OA radiographic and symptomatic incidence as well as JSW loss only in knees with a positive history of an acute knee injury. Therefore, positive history of acute knee injury can be considered as an indicator of responding to BPs therapy regarding knee OA incidence.

THE ASSOCIATION BETWEEN MENISCAL VOLUME AND THE DEVELOPMENT OF KNEE OA IN SUBJECTS AT HIGH-RISK FOR OA DEVELOPMENT

*Xu D., **v.d. Voet J., **,***Hansson N., **,***Klein S., **Oei E., *Wagner F., *,****Bierma-Zeinstra S., *Runhaar J.

*Dept. of General Practice, Erasmus MC University Medical Center Rotterdam, the Netherlands
**Dept. of Radiology & Nuclear Medicine, Erasmus MC University Medical Center Rotterdam, the Netherlands
***Dept. of Medical Informatics, Erasmus MC University Medical Center Rotterdam, the Netherlands
****Dept. of Orthopedics, Erasmus MC University Medical Center Rotterdam, the Netherlands

INTRODUCTION: Literature showed that meniscal pathologies had a strong association to the structural progression of knee osteoarthritis (OA). However, whether the meniscus volume changes are related to the development of OA is unknown.

OBJECTIVE: To explore the association between meniscus volume and the development of knee osteoarthritis (OA) in overweight/obese women after 30 months.

METHODS: Data from the Prevention of knee Osteoarthritis in Overweight Females (PROOF) study were used. This cohort included 407 women free of knee OA symptoms and related complaints. Demographics were collected by questionnaires at baseline. Heberden's nodes, body weight and height, basic radiography and MRI were obtained at baseline and after 30 months. Menisci were segmented semi-automatically by using the programs ITK-SNAP and MeVisLab. Once the manual and automatic segmentation processes were complete, the meniscal volumes for all medial and lateral menisci at baseline and follow-up were calculated. The primary outcome measure was the incidence of knee OA, defined by: K&L ≥2, or the combined clinical and radiographic ACR criteria, or joint space narrowing (JSN) in the medial or lateral compartment ≥1.0 mm. The secondary outcomes were either of these items separately. Delta-volumes were calculated by distracting baseline volume for the follow-up volume. Generalized estimating equations (GEE) analysis was used to adjust for repeated measure within persons and for confounding factors: contralateral (delta-)volume and baseline BMI, age, knee injury, knee alignment, postmenopausal status, Heberden's nodes, meniscal pathologies, extrusion, osteophytes and cartilage defects. Subjects without MRI data at baseline and with missing data for the primary outcome were excluded; leaving 626 knees for analysis.

RESULTS: Medial and lateral baseline and delta-volume were not significantly associated to the primary outcome (see Table). Medial and lateral baseline volume were positively associated to incident K&L ≥2, while medial and lateral delta-volume were negatively associated to incident K&L ≥2. Only on the lateral side, baseline volume was significantly associated to JSN (OR= 0.865; 95%CI: 0.751-0.995), not medially and neither of the delta-volume measures were significantly associated to the JSN outcomes. None of the meniscal measures were significantly associated to the incidence of the ACR-criteria.

	Primary outcome		JSN medial		JSN lateral		K&L		ACR	
	OR	95%CI	OR	95%CI	OR	95%CI	OR	95%CI	OR	95%CI
Baseline Medial volume	1.044	0.972; 1.122	1.074	0.960; 1.202			1.316	1.152; 1.503	1.055	0.943; 1.180
Baseline Lateral volume	1.000	0.907; 1.103			0.865	0.751; 0.995	1.220	1.027; 1.448	0.944	0.826; 1.078
Delta Medial volume	1.000	0.999; 1.001	0.999	0.998; 1.001			0.998	0.997; 1.000	1.000	0.999; 1.001
Delta Lateral volume	1.000	0.999; 1.001			1.001	0.999; 1.002	0.997	0.996; 0.999	1.000	0.999; 1.002

CONCLUSION: Knees with higher baseline meniscal volume and a stronger decrease in meniscal volume over time were at increased risk for developing radiographic knee OA. Given the lack for an association or even a reversed association between meniscal measures and medial/lateral JSN, this indicates an association with osteophyte growth. Hence, meniscal volume might function as a prognostic biomarker for future structural knee OA.

DISCLOSURE STATEMENT: All authors declare no conflict of interest.
CORRESPONDENCE ADDRESS: j.runhaar@erasmusmc.nl

UTILITY OF MAGNETIC RESONANCE IMAGING QUANTITATIVE BIOMARKERS FOR EXPERIMENTAL MEDICINE STUDIES OF KNEE OA

*MacKay J.W., **Turmezei T.D., ***Sanaei F., *Kaggie J., *Khan W., *McDonnell S.M., ****Morgan-Roberts A.R., ****Janiczek R.L., ***Naish, J., ***Parker G.J.M., *Graves M.J., *Treece G.M., *McCaskie A.W., *Gilbert F.J.

*University of Cambridge, Cambridge, UK
**Norfolk and Norwich University Hospital, Norwich, UK
***BiOxyDyn, Manchester, UK
****GlaxoSmithKline, Stevenage, UK

INTRODUCTION: Multiple MR-based quantitative imaging biomarkers (QIBs) of knee OA have been described and implemented in phase II/III clinical trials. However, their utility in early-phase experimental medicine (EM) studies is uncertain due to the small participant numbers (typically ~10 per arm) and short follow-up periods ($\leq$ 6 months) involved.

OBJECTIVES: Determine the likely utility of candidate QIBs in EM studies by assessing (1) test-retest repeatability; (2) ability to discriminate between participants with knee OA and age-matched healthy controls (HC); (3) responsiveness to change over 6 months.

METHODS: We conducted a prospective observational study with 15 OA (KLG 2/3, medial compartment predominant disease) and 6 age-matched HC participants. Knee MR imaging was performed at baseline, 1 month and 6 months on a 3T platform (GE 750) using an 8-channel transmit/receive knee coil (Invivo). MR sequences included a high-spatial resolution 3D fat-suppressed SPGR sequence for assessment of bone and cartilage morphology, T1rho and T2 mapping sequences for assessment of cartilage composition, and dynamic contrast-enhanced (DCE) sequences for assessment of synovitis. Candidate QIBs for subchondral bone (femoral bone area, i.e. tAB including osteophytes), cartilage (femoral thickness, T1rho and T2) and synovium (K^{trans}, the volume transfer coefficient between the plasma and the extracellular extravascular space) were derived from the MR data. We determined test-retest repeatability using baseline and 1-month data and calculating root-mean-square coefficients of variation (RMSCV). We assessed discrimination between OA and HC groups using baseline data and calculating standardized mean differences (SMD, analogous to effect size). We evaluated 6-month responsiveness to change by comparing baseline and 6-month data and determining the number of OA participants with changes greater than the smallest detectable change (SDC). The SDC was calculated from test-retest data and represents the 95% confidence interval for genuine change for an individual participant.

RESULTS: Results are summarized in the table below. Bone area was the most repeatable QIB (RMSCV 1.9%). K^{trans} demonstrated the greatest difference between OA and HC groups at baseline (SMD [90% CI] = 0.94 [0.10, 1.78]). The number of participants with significant (> SDC) changes at 6 months was greatest for femoral bone area (11 out of 13 participants with analyzable 6-month follow-up bone area data).

Biomarker	Test-retest RMSCV (%)	Difference OA-HC (SMD, 90% CI)	No. (%) OA participants with 6-month Δ > SDC
Bone area	1.9	0.33 (-0.53,1.18)	11/13 (85%)
Cartilage thickness	3.8	0.06 (-0.74, 0.86)	8/13 (62%)
Cartilage T1rho	4.9	0.35 (-0.46, 1.16)	8/12 (67%)
Cartilage T2	4.4	0.37 (-0.44, 1.18)	9/11 (82%)
Synovium K^{trans}	22.2	0.94 (0.10, 1.78)	8/12 (67%)

CONCLUSION: The majority of OA participants demonstrated changes greater than the SDC at 6 months for all included QIBs, suggesting adequate responsiveness for EM studies. Although test-retest repeatability was worse for K^{trans} compared to bone/cartilage QIBs, the comparison is somewhat biased due to the higher likelihood of biological fluctuations in synovitis when compared to cartilage or bone over the test-retest interval. Inclusion of MR QIBs in EM studies could help inform decisions on whether to progress novel therapies into later stage studies by providing early evidence of efficacy or lack thereof.

24-MONTH RESPONSIVENESS OF TIBIOFEMORAL 3D JOINT SPACE NARROWING MEASURED WITH STANDING CT IN THE MOST STUDY

*Segal N.A., **Ho M, *Rabe K.R., **Lynch, J.A., **Nevitt M.C., ***Anderson D.D.

*University of Kansas Medical Center, Kansas City, KS, USA
**University of California-San Francisco, San Francisco, CA, USA
***University of Iowa, Iowa City, IA, USA

INTRODUCTION: Joint space width (JSW) measured on weight-bearing radiographs suffers from poor sensitivity in detection of knee OA and correlates poorly with symptom progression. Limitations of 2D radiographic JSW, such as the dependence on x-ray beam alignment with the medial tibial plateau, along with the temporal and spatial heterogeneity of structural progression of knee OA, limits the responsiveness of 2D radiographic JSW to disease progression (3-year standardized response means (SRM) range from -0.03 to -0.74). In contrast, quantitative cartilage thickness on 3D MRI has greater responsiveness to disease progression, with SRM as high as -0.84 over 1 year. However, MRI generally is non-weight-bearing, which may hinder responsiveness due to cartilage swelling and altered position of the menisci. 3D JSW measured on standing CT (SCT) images holds potential to overcome these limitations and enhance responsiveness through measuring JSW in a loaded position, while avoiding bony overlap and error due to beam angle.

OBJECTIVE: To provide preliminary data for the responsiveness of 3D JSW on SCT over 24 months.

METHODS: SCT images of the knee were acquired using a commercial scanner (InLine, CurveBeam, Warrington, PA) while participants stood in fixed-flexion. The scanner produced pulsed cone-beam x-ray on a 30×30 cm amorphous silicon flat-panel detector over a 360° projection angle (total scan time 32 seconds; effective radiation dose 0.1 mSv). A 3D dataset with an isotropic resolution of 0.37mm and field of view of 350mm was reconstructed from cone beam projections. Tibiofemoral bony geometries were obtained through semi-automated segmentation of the SCT images as triangulated 3D surface meshes (Seg3D Version 2.4.0). The meshes were minimally smoothed to remove voxellation artifact using Geomagic Design X (3D systems). The 3D JSW was then defined as the Euclidean distance from the center of each triangulated face to the opposing surface along its normal direction. The mean JSW over each tibiofemoral surface was calculated and t-test was used to assess the change. The SRM (mean change/SD change) was calculated to assess the responsiveness of 3D JSW to detecting change over 24 months.

RESULTS: 3D JSW was calculated for 639 participants at the 144-month Multicenter Osteoarthritis Study (MOST) clinic visit. At the time of this analysis, 67 of these participants had returned for 168-month follow-up and had 3D JSW measured from SCT images (71.6% women; mean±SD age 71.3±5.9; BMI 28.8±5.0 kg/m^2). Mean Change and Responsiveness to Change in 3D JSW over 24 months presented in the table below.

Tibiofemoral Compartment	Mean Change in JSW Over the Joint Surface (mm)	Standard Deviation of Change in Mean JSW Over the Joint Surface	p-value for Change	SRM
Medial	-0.298	0.368	<0.001	-0.81
Lateral	-0.105	0.496	0.089	-0.21

CONCLUSION: These preliminary data support the hypothesis that 3D JSW is more responsive to 24-month change in medial tibiofemoral JSW than has been reported for radiographic JSW over 36 months and similar to that for quantitative cartilage thickness measured on MRI over 12 months. Completion of 24-month follow-up JSW measurements in this cohort will add clinical value through allowing determination of responsiveness in sub-groups (e.g. by baseline KLG, injury history, sex) and the extent to which change in 3D JSW corresponds with changes in knee symptoms and other clinically-relevant outcomes.

DISCLOSURE STATEMENT: The authors have no conflict of interest to disclose.
CORRESPONDENCE ADDRESS: nsegal@kumc.edu

A NOVEL METHOD TO CHARACTERIZE TOPOGRAPHY OF CARTILAGE CHANGE ON MRI

*Mathiessen A, **Ashbeck E.L., *Huang E., ** Bedrick E.J., **Kwoh C.K., *Duryea J.

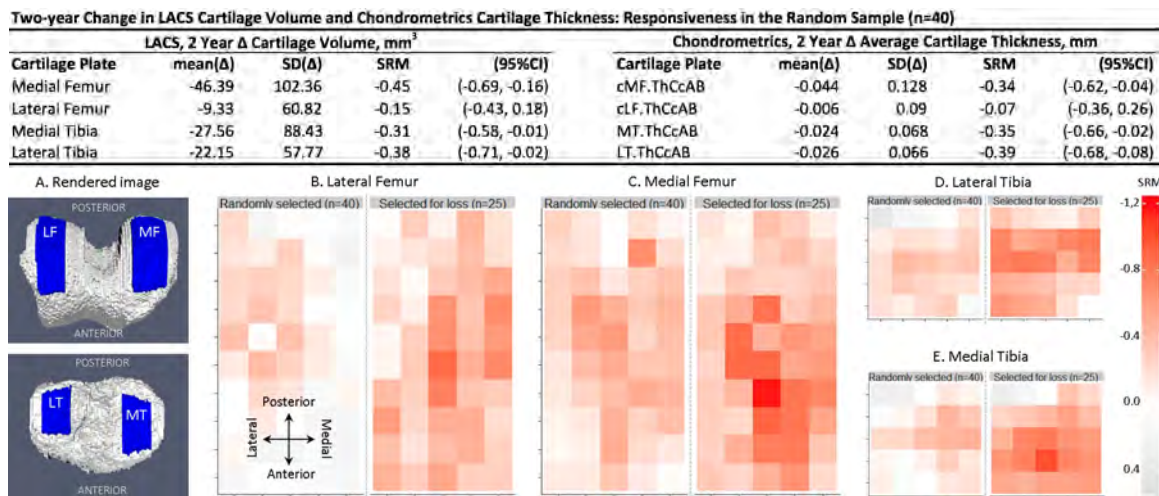*Brigham and Women's Hospital, Harvard Medical School, Boston, MA, USA
**University of Arizona Arthritis Center, the Univ. of Arizona College of Medicine, Tucson, AZ, USA

INTRODUCTION: Semi-automated Local Area Cartilage Segmentation (LACS) software for measuring medial femur cartilage has been demonstrated to be fast, responsive to change, and associated with radiographic and pain progression. However, LACS was initially developed to segment MF cartilage only.

OBJECTIVE: 1) Extend LACS to the LF, MT, and LT; 2) estimate correlation between LACS VC and measures of ThC from manual segmentation (Chondrometrics); 3) explore a novel method to characterize change in cartilage volume over defined subregions.

METHODS: 126 OAI participants with symptomatic knee OA were selected, including 40 randomly knees as well as knees selected for excessive 2-year cartilage loss in the MF, LF, MT and LT based on Chondrometrics measures. VC in each plate was measured with LACS on unilateral knee MRI scans (sagittal 3D DESS) at 0 and 2-year visits. Briefly, a non-expert reader identified anatomical femur/tibia landmarks. Automated edge detection algorithms outlined cartilage areas, followed by margin correction by an expert reader if necessary. Pearson correlation between LACS VC and Chondrometrics ThC was estimated in the full sample (n=126). 2-year cartilage change was calculated as standardized response mean (SRM = mean(ΔVol)/SD(ΔVol)) in the random sample (n=40) for LACS and Chondrometrics. 95% CI for correlation and SRM estimates were obtained with bias-corrected accelerated bootstrap. Finally, LACS SRM was estimated over grids in the random sample and knees selected for cartilage loss and displayed in the form of responsiveness heat-maps, showing change over a grid (topography) of each cartilage plate. The mathematical nature of the LACS method permits any grid location to be determined consistently.

RESULTS: Correlation between LACS and Chondrometrics; LF r=0.75 (95%CI: 0.65, 0.81); MF r=0.87 (95%CI: 0.81, 0.90); LT r=0.89 (95%CI: 0.84, 0.92); MT r=0.71 (95%CI: 0.62, 0.78). Estimated SRMs for LACS and Chondrometrics were similar (Table). Figure A shows renderings of segmented cartilage (blue). Subregions with the greatest magnitude of loss are identified in responsiveness heat-maps corresponding to rendered cartilage plates for knees selected randomly (left) and for loss (right) (Figures B-E).

Two-year Change in LACS Cartilage Volume and Chondrometrics Cartilage Thickness: Responsiveness in the Random Sample (n=40)

	LACS, 2 Year Δ Cartilage Volume, mm³					Chondrometrics, 2 Year Δ Average Cartilage Thickness, mm			
Cartilage Plate	mean(Δ)	SD(Δ)	SRM	(95%CI)	Cartilage Plate	mean(Δ)	SD(Δ)	SRM	(95%CI)
Medial Femur	-46.39	102.36	-0.45	(-0.69, -0.16)	cMF.ThCcAB	-0.044	0.128	-0.34	(-0.62, -0.04)
Lateral Femur	-9.33	60.82	-0.15	(-0.43, 0.18)	cLF.ThCcAB	-0.006	0.09	-0.07	(-0.36, 0.26)
Medial Tibia	-27.56	88.43	-0.31	(-0.58, -0.01)	MT.ThCcAB	-0.024	0.068	-0.35	(-0.66, -0.02)
Lateral Tibia	-22.15	57.77	-0.38	(-0.71, -0.02)	LT.ThCcAB	-0.026	0.066	-0.39	(-0.68, -0.08)

CONCLUSION: We found favorable SRM for VC change and good correlation with established ThC measurements. Following full-region cartilage segmentation, LACS software enables measurement of cartilage volume over a grid, with heat-map visualization. Parameterization of cartilage plate topography could be used as a novel method to characterize cartilage loss over time in future OA studies.

CORRESPONDENCE ADDRESS: jduryea@bwh.harvard.edu

Poster Presentations

EVALUATE THE EFFICACY OF AN 'E'-TRIAGE TOOL, INCORPORATING RAGIOGRAPHIC GRADING, TO IMPROVE THE REFERRAL PROCESS FOR KNEE OA SURGERY

*Dervin G., *Vogel K., **Dombrowski J., **Sly-Haven M., **Moon L., ***Cooke T.D.

*Division Orthopedics, University Ottawa, Ottawa, ON, Canada
**Regional MSK Assessment Centre, Queensway Carlton Hospital, Ottawa, ON, Canada
***School of Rehabilitation, Queens University, Kingston and OAISYS Inc, Maberly, ON, Canada

INTRODUCTION: Regional Assessment Clinics (RAC) for musculoskeletal care are now mandated in many Canadian provinces as the means to triage patients referred for total joint arthroplasty. Their use underscores the limitations of Primary Care Physicians (PCP) to appropriately refer patients. Problems arise when patients with severe Osteoarthritis (OA) are subject to this significant extra step while those seen with insufficient limitations contribute to costs and crowd the access portal for surgery. We postulated that patient reported disability, readiness for surgery and validated grading of a standing knee X-ray would provide an inexpensive yet effective tool to improve the referral process for Knee OA patients.

OBJECTIVE: Evaluate the efficacy for an eTriage tool, based on radiographic grading, disability score and surgery readiness to appropriately identify Knee OA cases warranting surgical evaluation.

METHODS: 245 consenting patients, all referred by their PCP to the RAC with a diagnosis of symptomatic Knee OA, were enrolled in the study. All patients were evaluated as per the current RAC protocol including a medical history, physical examination and an X-ray (standing AP, lateral and patella-femoral skyline). Prior to the visit, subjects were sent a copy of the Oxford Knee Score (OKS) and requested to answer whether their current clinical status was acceptable YES (PASS 1) or NO (PASS 2), not acceptable. The PASS 1 patient data set was set aside for separate analysis. All PASS 2 cases are included here. All X-rays were scored for OA severity using the validated compartmental grading from 0 – 13 (Sheehy et al: Validity and sensitivity to change of three scales for the radiographic assessment of knee osteoarthritis using images from the Multicenter Osteoarthritis Study (MOST). Osteoarthritis and Cartilage 2015).

RESULTS: Of the 245 cases, 200 declared themselves 'NO', PASS 2, completed the OKS questionnaires and had standing X-rays for evaluation. Of the 200 included cases, 104 were referred by RAC to see a surgeon. In analysis, we found that a self-reported PASS 2 'NO' and X-rays graded at 6 or above predicted over 75% of those patients that were referred. This represents a 3.4 greater likelihood of referral using this simple analysis. The OKS score did not modify this prediction.
On review of the remaining 25% the majority of those referred by RAC with low X-Ray grades could have waited without worsening and a small proportion might be considered inappropriate. Many of the cases with high grades and significant symptoms were delayed because they had not received alternative care; all subsequently went on to surgery. A few of the more severe grades but with less limitations were considered for timely future referral.

CONCLUSION: The use of a validated X-ray grading with 'readiness for surgery' appropriately triaged 75 % of patients for surgical consideration. The review identified opportunities for improvement at either end of the X-ray severity spectrum: some patients with less severe gradings were being unnecessarily referred to RAC and then on for surgery, leading to overuse resources, crowding the access to surgery and adding to costs; whereas others, with higher grades, were being needlessly delayed. Use of eTriage tool, based on validated X-ray gradings in concert with the patient's surgical readiness and disability level will lead to improved use of expensive resources, improve patient care and satisfaction with the provision of tools that the PCP and RAC may adopt for appropriate referral.

PRELIMINARY STUDIES OF MACHINE LEARNING APPLICATIONS FOR AUTOMATED SEVERITY GRADING OF RADIOGRAPHIC KNEE OSTEOARTHRITIS

*Stewart J., **Cooke T. D.

*School of Computing Science, Queens University, Kingston, ON, Canada
**School of Rehabilitation, Queens University, Kingston, and OAISYS Inc, Maberly, ON, Canada

INTRODUCTION: While Kellgren-Lawrence (KL) grading is widely used to measure severity of radiographic Knee Osteoarthritis (OA) it is with limitations (need for training, observer variation, lack of clinical impact, limited range and relevance to alignment). A validated Compartmental Grading (CG) (Cooke et al J. Rheumatol 1999. 26, 3: 641, Sheehy L. et al. Osteoarthritis and Cartilage 2015, 23(9):1491-8) has shown promise for improvement, compared with KL. Neither scale is widely employed in clinical scenarios. Recently, the CG grading has shown promise in evaluating appropriateness for surgical referral for knee OA. Our interest is to explore the role that Machine Learning (ML) approaches may offer to improve radiographic grading of knee OA, compared to current use of KL and CG, in both research and clinical settings.

OBJECTIVE: Develop an automated radiographic grading method for Knee OA using Machine Learning approaches for Kellgren-Lawrence (KL) and Compartmental Grading (CG) schemes.

METHODS: We have graded and annotated 950 AP semi-flexed standing knee images from the MOST database. Each image was graded for most severe damage (Medial or Lateral) using the Compartmental Grading (CG) scheme from 0-13 (Cooke et al) for Joint Space (JS 0-3), Femoral Osteophytes (FO 0-3), Tibial Erosion (TE 0-4) and Subluxation (SU 0-3). Each image was annotated with the position of the most superior points of the intercondylar femur notch and of the intercondylar tibial eminence, as well as the centers of the femur and tibia at the top and bottom of the image, respectively, so that tibial-femoral alignment could be estimated.

In preparation for input to the ML algorithm, each of the 950 images image was manually cropped to a square region that was (a) centred at the midpoint between the intercondylar notch and intercondylar eminence and (b) sized to contain the femur and tibia within the middle 80% of the box width. Histogram equalization was applied to each cropped image in order to have an even distribution of grey levels while maintaining contrast of detailed features.

The Keras Python toolkit was used to build a convolutional neural network (CNN) consisting of three convolutional layers and a final dense layer. The cropped images were paired with their joint space (JS 0-3) classifications and used as input. Eighty percent were used for training and twenty percent for validation.

RESULTS: Initial results were poor, with the CNN achieving less than 0.50 accuracy. We expect that refinements to the CNN structure should substantially improve this measure. Other future work will consist of applying the CNN to the other measures of Femoral Osteophytes, Tibial Erosion, and Sublaxation, with the expectation of deriving an overall Compartmental Grading score.

CONCLUSIONS: We have built a dataset of 950 CG-classified knee images for input to a machine learning algorithm and have made a preliminary investigation into using a CNN to classify those images.

FUTURE PLANS: Following a successful CNN design, we plan to include alignment parameters in future training and explore the utility of these methods for other knee images (Skyline Patello-femoral, etc). In addition, we plan to develop automated approaches for the manual image cropping step. Our longer term interest is the provision of improved automated image analyses for both research and clinical applications.

IONIC AND NON-IONIC CLINICAL CONTRAST AGENTS AND THEIR EFFECTS ON THE SWELLING BEHAVIOR OF SHEEP MENISCUS FIBROCARTILAGE

*Crowder H.A., *Martin C, **Baylon E.G., *Gold GE, *Levenston M.

*Stanford University, Stanford, CA, USA
**University of California at San Francisco, San Francisco, CA, USA

INTRODUCTION: Although MRI is the most accurate and least invasive method for assessing lesions in the knee joint, some patients are ineligible for MRI, and CT is a common alternative. Contrast agents at clinically-relevant dilutions were recently shown to induce transient swelling and deswelling of articular cartilage, but the effects on joint tissues, such as the meniscus, are not yet fully understood.

OBJECTIVE: This study examined the mechanical effects of two iodinated contrast agents (non-ionic Omnipaque 350 (Iohexol) and ionic Cysto-Conray II) on sheep meniscus explants.

METHODS: Meniscus explants were taken from the surface of four immature sheep stifles using an 8mm biopsy punch and trimmed to 2mm thickness, surface intact. Explants were stored at -20°C in Phosphate Buffered Saline (PBS) until mechanical testing. Before testing, samples were thawed to 25°C, trimmed to 6mm, and randomly assigned to one of five testing groups: 1XPBS, 0.1XPBS, 10XPBS, 100% Omnipaque (Omni), 100% Cysto-Conray II (Conray). Samples (n=3/group) were placed in a rubber confining ring and tested on an Instron 5940 microtester using a 10N load cell and an hemispherical indenter tip (radius 1mm). Once in the rubber ring, samples were placed in a 1XPBS bath and pre-loaded to 0.02N. Samples were loaded at 0.002mm/s to 15% strain followed immediately by unloading at the same rate and a 15-minute recovery period. After 3 cycles in 1XPBS the bath was changed to the assigned solution group, and the sample was indented for 4 more cycles to monitor the equilibrium response of the tissue. The bath was then changed back to 1XPBS and indented for 4 cycles to monitor tissue recovery. The peak force from each cycle was normalized by the peak force value of the third initial cycle in 1XPBS. Data were analyzed using one-way ANOVA followed by Bonferroni post-hoc test for pairwise comparisons. Results are presented as mean+/-SEM.

RESULTS: Normalized peak force (N) in the control (1XPBS) group did not vary (Figure 2), which indicates the testing protocol did not damage the meniscus tissue. Normalized peak force data for cycle 4 contrast agent equilibrium show the Omni group (0.1178N/N+/-0.04996) to be significantly lower than all other groups, Conray (0.7142N/N+/-0.2940) to be significantly lower than 0.1XPBS (1.2321N/N+/-0.0516), and 0.1XPBS to be significantly higher than 1XPBS (0.9738N/N+/-0.0306) and 10XPBS (0.5170N/N+/-0.0278) (Figure 3). No significant difference was detected between Conray and 1XPBS. Normalized peak force data for recovery equilibrium show Omni (0.2915N/N+/-0.2137) to be significantly lower than all other groups and no other significant differences between groups (1.0059N/N+/-0.0553) (Figure 3).

CONCLUSION: Exposure to iodinated CT contrast agents has a significant and varied mechanical effect on meniscus tissue in the knee. In addition, there was an incomplete recovery of meniscus tissue in 1XPBS within one hour post-contrast agent equilibrium, which bears clinical consideration. This illustrates the need for the development of robust clinical protocols to prevent damage to the meniscus surface after exposure to iodinated contrast agents.
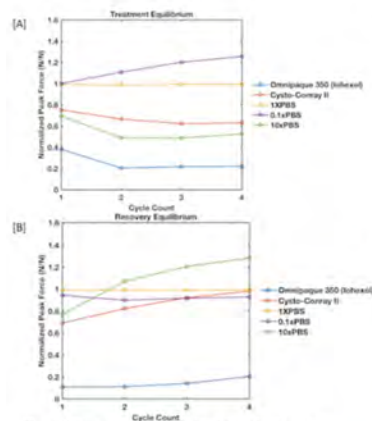
Figure 2: Representative normalized peak force data (points) of samples in [A] contrast agent equilibrium and [B] recovery in PBS.
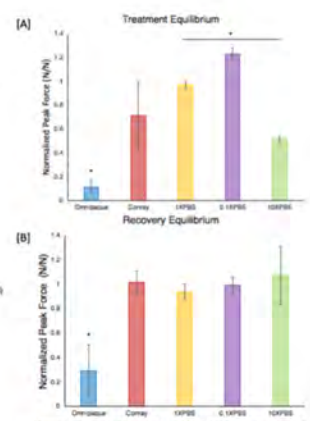
Figure 3: Normalized peak force data for cycle 4 for [A] contrast agent equilibrium and [B] recovery equilibrium.

HIGH-RESOLUTION QUANTITATIVE IMAGING WITH DEEP LEARNING-ENHANCED MRI

*Desai A.D., *Gold G.E., *Hargreaves B.A., *Chaudhari A.S.

*Radiology, Stanford University, Stanford, USA

INTRODUCTION: High-resolution knee MRI is crucial for qualifying small morphological changes in the cartilage and meniscus to measure OA progression. Additionally, quantitative MRI parameters such as T_2 and $T_1\rho$ have shown promise for measuring early compositional changes associated with tissue degeneration prior to the manifestation of morphological changes[1,2]. The quantitative double-echo steady-state sequence (qDESS) can simultaneously produce accurate morphometry and T_2 measures for cartilage and meniscus[3]. However, conventional qMRI sequences are often limited to lower resolutions due to signal-to-noise ratio (SNR) constraints. The availability of high-resolution qMRI may be beneficial for evaluating both the subtle morphological and quantitative changes seen in OA. Deep-learning-based super-resolution (DLSR) techniques have enabled further enhancement of the resolution of MRI without increasing scan time or decreasing SNR[4]. While DLSR can enhance the morphological image quality, its impact on quantitative parameter accuracy is still unknown.

OBJECTIVE: To compare the quantitative T_2 accuracy of DLSR-enhanced qDESS MRI scans compared to original acquisitions scans. Specifically, we generate high-resolution qDESS images from 2x lower resolution (low-res) images using DeepResolve[4], a state-of-the-art DLSR algorithm, to compare T_2 estimates from the two scans in femoral cartilage.

METHODS: We utilized DeepResolve, pretrained on DESS images from the OAI[5], to super-resolve low-res (1.6mm slice thickness) qDESS scans into twofold higher resolution (0.7mm slice thickness) in 51 consecutive patients referred for a clinical MRI scan. Subsequently, DOSMA[6], a fully-automated MSK pipeline, was used to segment and subdivide the femoral cartilage into six regions: the medial and lateral condyles, each with anterior, central, and posterior compartments[3,7]. Segmentation was performed on high-resolution DLSR scans and mapped to the corresponding low-res scans to standardize the region-of-interest between scans. Statistical comparisons between the DLSR scans and the low-res scans were assessed using pairwise Kruskal-Wallis tests and corresponding Dunn posthoc tests (α=0.05). The root-mean-squared coefficient of variation (rms-CV) and Lin's concordance correlation coefficient between T_2 estimates from the two scans were measured.

RESULTS & DISCUSSION: Differences in T_2 estimates from DLSR scans and low-res scans were insignificant (p>0.50) for all six sub-regions of femoral cartilage. High concordance between the two estimates was indicated by high Lin's concordance (0.996) and low rms-CV (0.58%). Estimates from DLSR scans negligibly overestimated that of interpolated scans (Fig. 1), and the range of difference in estimates between the two scans was comparable to that of scan/rescan for qDESS[7] (Fig. 2).

Figure 1: T_2 estimates from low-resolution and deep-learning super-resolved (DLSR) scans for six sub-regions of femoral cartilage.

CONCLUSION: Deep-learning super-resolution can enhance MRI resolution and preserve the quantitative accuracy of the T_2 relaxation time, allowing for high-resolution morphological and quantitative imaging.

REFERENCES: [1] Li, MRM, 2009 [2] Williams, OAC, 2012 [3] Chaudhari, JMRI, 2018 [4] Chaudhari, MRM, 2018 [5] Peterfy, OAC, 2008 [6] Desai, ISMRM, 2019 [7] Barbieri, ISMRM, 2019
DISCLOSURE STATEMENT: AC has provided consulting services to Subtle Medical, Skope MR, Chondrometrics GmBH.
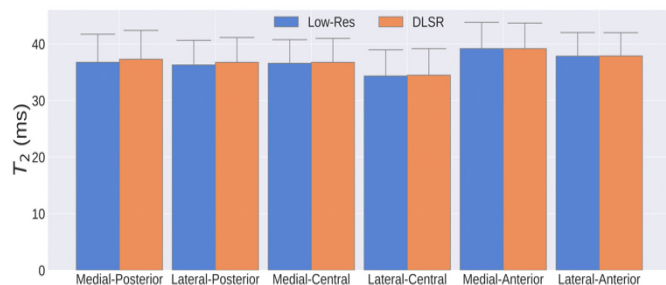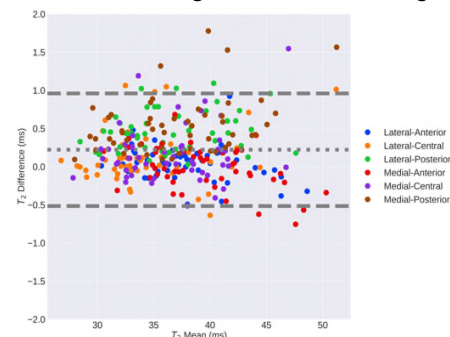CORRESPONDENCE ADDRESS: arjundd@stanford.edu

Figure 2: Bland-Altman analysis of T_2 estimates from deep-learning super-resolved scan shows minimal bias (~0.25 ms) and strong concordance to ground truth.

DESIGN OF A NOVEL MRI-SAFE PHYSICAL ACTIVITY SIMULATOR FOR CADAVER KNEES

*Espinosa Maldonado A.A., *Johnston J.D., *McWalter E.J.

*Mechanical Engineering, University of Saskatchewan, Saskatoon, Canada

INTRODUCTION: Quantitative MRI can be used non-invasively to assess articular cartilage and meniscus biochemical content and mechanical integrity at an early disease stage. Preliminary studies of T2 and T1ρ relaxation times have shown correlations with cartilage and meniscus health condition. However, most cadaver studies are carried out without loads or under simplified (axial) loading conditions. Since mechanical loading contributes to OA progression, it is important to study knee soft tissue structure under true physiologic loading conditions.

OBJECTIVE: To design a MRI-safe loading simulator that applies three-dimensional loading (knee forces, moments and muscle tension) of physiologic magnitude to cadaver knees.

METHODS: The simulator must meet a set of design criteria. For example, only MRI-compatible materials can be used, the size is constrained to the MR scanner bore (0.45m max diameter), the knee capsule must be kept intact to emulate the in-vivo knee, and constant loads (not constant displacements) must be applied to account for soft tissue viscoelasticity (time-varying response of tissue to load). Physically realistic three-dimensional loading data was acquired from musculoskeletal modelling software (OpenSim, https://opensim.stanford.edu/), instrumented implant data (OrthoLoad, http://orthoload.com) and custom algorithms (MATLAB, the Mathworks, Natick, MA). In terms of final design operation, a statically equivalent multiaxial loading scenario was achieved by tensile/compressive actuators and cables oriented in different directions, with rig actuators being powered by a portable pneumatic compressor, and bending moments applied by off-axis forces. For initial design purposes, we simulated internal knee joint loading for walking (stance and swing) prior to considering different physical activities (e.g., stair climbing).

RESULTS: A simulator (Fig. 1) and companion algorithms have been developed, which allowed determining the system settings to deliver the mean loading regime for a 100kg subject.
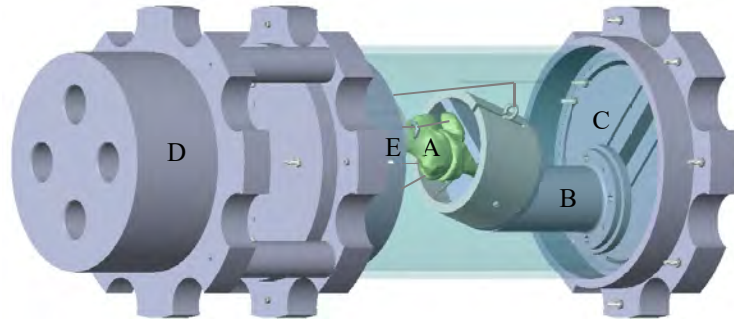
Fig.1: MR-safe knee loading rig: Potted specimen (A), compressive actuator (B), r-θ positioning stage (C), tensile actuators block (D), load cell (E)

CONCLUSION: This design can simulate loading conditions similar to those experienced during activities of daily living without complex controls systems used with other loading rigs and in-vivo setups for closed bore MRI systems. This simulator can be used to carry out quantitative MRI assessments of knee soft tissue health in cadaver specimens under physiologic loads. Ultimately, this may improve our understanding of the relationship between function and structure in healthy and osteoarthritic soft tissues.

CORRESPONDENCE ADDRESS: aae619@mail.usask.ca

BONE AND CARTILAGE SEGMENTATION FROM MULTIPLANAR MR IMAGES USING STATE-OF-THE-ART CONVOLUTIONAL NEURAL NETWORK

*Felfeliyan B., *, **Küpper J.C., ***Forkert N., *, **Ronsky J.

*McCaig Institute for Bone and Joint Health University of Calgary, Calgary, AB, Canada
**Mechanical and Manufacturing Engineering, University of Calgary, Calgary, AB, Canada
***Hotchkiss Brain Institute, Department of Radiology and Clinical Neurosciences, University of Calgary, Calgary, AB, Canada

INTRODUCTION: Three-dimensional (3D) bone and cartilage segmentation is a necessary component for the study of in-vivo musculoskeletal structures and joint interactions associated with osteoarthritis (OA). Specifically, high speed biplanar videoradiography (HSVB) is a low-dose technology that requires 3D bone models as an essential step in the intricate post processing pipeline. HSBV enables the observation of in vivo 3D dynamic bone movement with unparalleled precision and accuracy (0.08 mm) [1]. Variables that are potentially related to OA such as joint cartilage contact or deformation can be identified with HSBV. These outcomes require segmentation of both bone and cartilage, typically obtained from MR images.

OBJECTIVE: The aim of this project is to 1) deploy two U-nets (well-known encoder-decoder convolutional neural network (CNN) architectures [2]) for sagittal and coronal planes MRI data and generate 3D models of bone and cartilage, and 2) compare the bone and cartilage surfaces acquired through the automatic approach to the baseline (manual approach).

METHODS: The CNN automatic segmentation method was trained on a T1 MRI dataset collected using a 3T 750 GE scanner (Ethics ID #REB15-0554). The dataset (n=19 for training, n=2 for validation and test) was acquired from knees of healthy and ACL deficient male participants. Structures in the MR images (femur, tibia, femoral and tibial cartilages were manually segmented by trained users. The MR image volumes were disassembled and augmented (by mirroring) to separate stacks of 2D images in the sagittal and coronal planes. Two separate U-nets with 5 layers and 32 feature maps were designed for each coronal and sagittal plane. Using different planes for segmentation enables optimization of information in both views, particularly for areas with rapid changes in curvature. To solve the high-class imbalance problem, the weighted cross entropy cost function was used (i.e., weighting is inversely related to the probability of each class). The final convolutional layer is a $1{\times}1$ convolutional kernel which reduces the 32 features to the final probability maps of the four-channel feature maps (background, bone, femoral cartilage and tibial cartilage). The average outcome of two networks was used to calculate the probability of belonging to each class (per voxel). Voxels are assigned to specific tissues when the probability exceeds a threshold defined for each tissue. Small artifacts are removed, and 3D bone and cartilage models are generated (marching-cubes algorithm). To quantify the surface distance between the 3D models arising between the predicted output and the labeled output, the maximum and average Hausdorff distances were calculated.

RESULTS: The maximum Hausdorff distance for all the surfaces was between 13 to 13.5 pixels. However, the average Hausdorff distance for the bone surfaces was 0.08 pixels (0.04 mm) and for the cartilage surfaces was 0.3 pixels (0.15 mm). The Dice coefficient was > 0.9 for bones and was >0.8 for cartilages. In Fig. 1 the qualitative result of the algorithm is shown.

CONCLUSION: The bone and cartilage models were shown to be within a subpixel range of the manual approach. Therefore, the CNN automatic approach is acceptable for application to HSBV and OA studies, as differences between surfaces are on the order of or less than the HSBV accuracy.

REFERENCES: [1] Sharma, J Biomech, 2015 [2] Ronneberger, MICCAI, 2019
DISCLOSURE STATEMENT: None
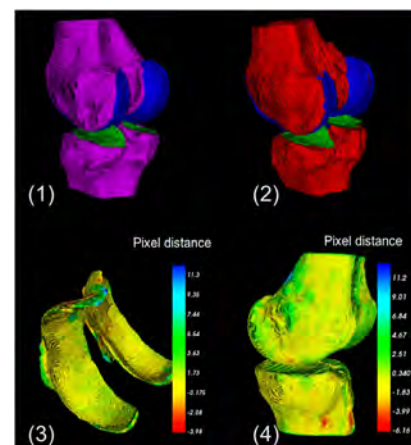CORRESPONDENCE ADDRESS: banafshe.felfeliyan@ucalgary.ca

Fig1. (1) manual segmentation (2) automatic segmentation, (3) The pixel distance between manual and automatic segmentation for cartilages and (4) for bones.

CURRENT METHODOLOGIES IN PATELLOFEMORAL JOINT RADIOGRAPHY AND GRADING OF PATELLOFEMORAL OSTEOARTHRITIS: A SYSTEMATIC REVIEW

*Hill J.R., **Oei E.H.G., ***Crossley K.M., ***Menz H.B., ****Macri E.M., *****Smith M.D., ***Wyndow N., *****Collins N.J.

*Faculty of Medicine, The University of Queensland, Brisbane, Australia & School of Health and Rehabilitation Services, The University of Queensland, Brisbane, Australia & Ochsner Clinical School, New Orleans, LA, USA
**Department of Radiology and Nuclear Medicine, Erasmus MC University Medical Center, Rotterdam, Netherlands
***La Trobe Sport and Exercise Medicine Research Centre, School of Allied Health, La Trobe University, Melbourne, Australia
****Department of General Practice, Erasmus MC University Medical Center, Rotterdam, Netherlands
*****School of Health and Rehabilitation Services, The University of Queensland, Brisbane, Australia

INTRODUCTION: The patellofemoral joint (PFJ) is the most commonly affected compartment in knee OA, and patellofemoral OA (PFOA) tends to affect a younger, more active population than tibiofemoral OA. Radiographs are currently the most widely used imaging modality in OA evaluation and management, and the only modality accepted by the FDA for assessment of OA structural change. Despite this, a variety of radiographic techniques are used to image the PFJ and no consensus exists on how to grade radiographic features of PFOA. Standardized methods of acquiring radiographs of the PFJ have yet to be adopted, resulting in variances in patient positioning, weight-bearing status, flexion angle, and beam direction. Furthermore, the literature is characterized by multiple radiographic grading systems used to assess PFOA, and a consensus on optimal radiographic measures and thresholds for PFJ alignment has yet to be reached.

OBJECTIVE: To conduct a systematic review of the literature published since January 2000 to:
1) provide an overview of contemporary methods of acquiring radiographs of the PFJ;
2) describe current methods of radiographic grading of PFOA and their measurement properties; and
3) summarize PFJ alignment and bony morphology measures as identified on radiography.

METHODS: The methods of this systematic review were developed in accordance with PRISMA guidelines. Electronic searches of PubMed, CiNAHL, SPORTDiscus, SCOPUS, EMBASE, PsycInfo, Cochrane Central Register of Controlled Trials (CENTRAL), and Web of Science were conducted from January 1, 2000 to December 31, 2018. Keywords related to the concepts of 'patellofemoral' and 'radiograph' were used to form the search. Records identified by the search strategy were screened for eligibility by two independent assessors using Covidence software. Inclusion criteria included primary studies with mention of radiography of the knee, grading of radiographic features of PFOA, and measures of alignment or bony morphology of the PFJ. Studies were excluded if they were non-human studies, cadaver studies, consisted of only a pediatric population (age <10 years), or were single-subject studies. For studies that evaluate measurement properties of radiographic OA grading scales, methodological quality was assessed by two independent assessors using the COSMIN Risk of Bias checklist. As this review is a qualitative synthesis of radiographic methods, meta-analyses are not appropriate.

RESULTS: The database search generated 18,678 records with 15,139 unique records identified after removal of duplicates. Article screening, quality rating, data extraction and synthesis are currently ongoing. Outcomes addressing the three aims will be presented.

CONCLUSION: Findings of this systematic review will inform the development of guidelines regarding radiographic acquisition methods, as well as development of a revised radiographic atlas for clinical and research evaluation of the PFJ.

"PROJECTED CARTILAGE AREA RATIO" BY 3D MRI ANALYSIS DETECTS DECREASES IN CARTILAGE AMOUNTS OVER SEVERAL MONTHS IN PATIENTS COMPLAINING OF KNEE PAIN

*Hyodo A., *Ozeki N., *Aoki H., **Suzuki K., **Itai Y., **Masumoto J., *Sekiya I.

*Center for Stem Cell and Regenerative Medicine, Tokyo Medical and Dental University, Tokyo, Japan
**Fujifilm Corporation, Tokyo, Japan.

INTRODUCTION: We have been developing 3D MRI analysis software that enables a semi-automatic reconstruction of 3D images of the cartilage in the knee joint. This software allows measurement of the "projected cartilage area ratio" with the intended thickness to quantitate the cartilage.

OBJECTIVE: In this study, we examined the measurement error associated with the "projected cartilage area ratio" of the knee in volunteers. We also examined temporal alterations of the "projected cartilage area ratio" of the knee in patients complaining of knee pain.

METHODS: MRI was performed with an MRI system (Achieva 3.0TX, Philips) at 3.0 T. After 3D reconstruction, the femoral cartilage was projected onto a flat surface. The "projected cartilage area ratio" shows the ratio of the projected cartilage area to the total area in the anterolateral (AL), anteromedial (AM), posterolateral (PL), and posteromedial (PM) segments. In this study, a "projected cartilage area ratio" for a cartilage thickness $\geq$1.5 mm was evaluated. For measurement error, 10 volunteers aged 32–52 years old were included and underwent two MRI examinations. For measurements of temporal alterations, we screened 1039 knees that had undergone MRI examinations. Of these, 411 knees had undergone MRI at least twice; however, 395 knees were excluded because of history of knee trauma, patellofemoral joint osteoarthritis, rheumatoid arthritis, osteonecrosis, or surgical indications. Ultimately, 16 knees (8 patients) were selected. These 8 patients were 22–68 years old, complained of knee pain, and had undergone MRI examination twice at 3–21 (10 ± 5) month intervals.

RESULTS: For the projected cartilage area ratio, the intra-reader intraclass correlation coefficient (ICC) was almost 1.0 and the inter-reader ICC was 0.9–1.0 in each segment. The intra-reader coefficient of variation (CoV) was between 1.0 and 1.4 and the inter-reader CoV was between 1.0 and 2.2. The intra-measurement ICC was 0.9–1.0, except for the posterolateral segment (0.8), and the intra-measurement CoV was between 0.8 and 1.7. For measurement of temporal alteration, the most affected segment was the posteromedial segment in 4 patients and the posterolateral segment in 4 patients. In all patients, the projected cartilage area ratio at the most affected segment decreased during the time interval from the first MRI to the second MRI. The projected cartilage area ratio at the most affected segment decreased by an average of 13% per year.

CONCLUSION: We proposed a novel evaluation method to quantify the amount of cartilage in the knee by 3D MRI analysis. This method had a low measurement error and was highly sensitive for quantifying cartilage. The "projected cartilage area ratio" provides the possibility of detecting a decrease in the amount of cartilage over several months in patients with osteoarthritis of the knee.

CORRESPONDENCE ADDRESS: hyodo.arm@tmd.ac.jp
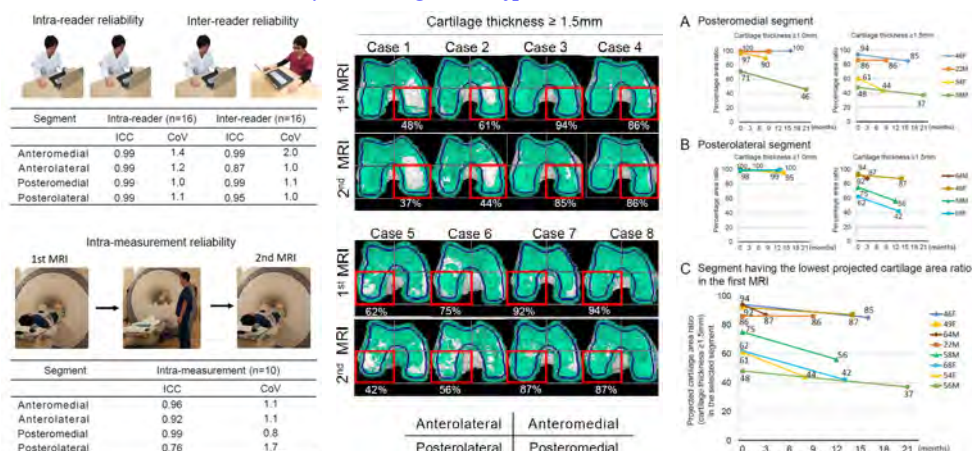
INTRODUCING A NEW SCORING SYSTEM FOR INTRAARTICULAR MINERALIZATION OF THE KNEE: BUCKS (BOSTON UNIVERSITY CALCIUM KNEE SCORE)

*Jarraya M., **Neogi T, ***Lynch J.A., **Felson D., **Clancy M., ***Nevitt M., ****Lewis C.E., *****Torner J., *Guermazi A.

*Department of Radiology, Boston University School of Medicine, Boston, MA
**Department of Medicine, Boston University School of Medicine, Boston, MA
*** Department of Epidemiology, University of California San Francisco, San Francisco, CA
****Department of Epidemiology, University of Alabama at Birmingham, AL
*****Department of Epidemiology, College of Public Health, University of Iowa, IA

INTRODUCTION: The role of intra-articular mineralization in OA is unclear and underestimated by radiography and MRI. Computed tomography (CT) has higher sensitivity than radiography and MRI for the detection of soft tissue mineralization.

OBJECTIVE: To describe and assess the reliability of a novel CT scoring system, the BUCKS (Boston University Calcium Knee Score) method, for evaluating intra-articular mineralization.

METHODS: We included both knees from subjects from the most recent visit of the Multicenter Osteoarthritis Study (MOST) Study, which is a NIH-funded longitudinal cohort of community-dwelling older adults with or at risk of knee OA. All subjects underwent CT scans of bilateral knees. Each knee was divided into 14 WORMS subregions and each subregion was read for the presence and severity of mineralization in cartilage by a musculoskeletal radiologist. We assessed the presence and severity of mineralization in menisci, capsule and ligaments. To assess reliability, readings of a sample of 30 participants by the same reader and a second reader were repeated 12 weeks later.

RESULTS: The BUCKS method assesses 28 locations for mineralization: 14 cartilaginous and 6 meniscal subregions (each meniscus was subdivided into 3 subregions: anterior horn, body and posterior horn). Each subregion was assigned a score ranging from 0-3 reflecting greater quantity with higher scores). The joint capsule, 2 posterior meniscal roots (medial and lateral), 2 cruciate (ACL/PCL) and 2 collateral ligaments (MCL/LCL) were each scored 0 or 1 for absence or presence of mineralization. Vascular calcifications were scored 0-3. The intra-reader reliability (weighted-kappa) ranged from 0.93 for ligaments to 1.0 for joint capsule (table 1). The inter-reader reliability (weighted-kappa) ranged from 0.92 for cartilage to 1.0 for joint capsule.

CONCLUSION: BUCKS demonstrated excellent reliability, and is therefore a potentially useful tool for studying the role of calcium crystals in knee OA assessed using CT.

Table 1. Intra-rater and inter-rater reliability (weighted kappa) for different locations in the knee joint.

	Cartilage (14 locations)	Meniscal* (8 locations)	Vascular (1 location)	Capsule (1 location)	Ligament (4 locations)
Intra-rater	0.94	0.98	0.97	1.0	0.93
Inter-rater	0.92	0.95	0.95	1.00	1.00

*Including posterior meniscal roots

CORRESPONDENCE: mohamedjarraya@gmail.com

RAPID WHOLE-LEG MRI FOR ASSESSMENT OF LEG ALIGNMENT

*Kogan F., **Uhlrich S. D., ***Berkson M., *Chaudhari A., *Black M., *Mazzoli V., *Gold G.E., *Hargreaves B.A.

*Stanford University Departments of Radiology, Stanford, CA, USA
**Stanford University Department of Mechanical Engineering, Stanford, CA, USA
***Palo Alto Veterans Affairs Hospital, Palo Alto, CA

INTRODUCTION: Varus and valgus alignment are associated with the presence and progression of knee osteoarthritis. Knee alignment is most commonly assessed with a full lower-limb radiograph. However, there is concern about the radiation of these exams to the pelvic regions. Further, there is increasing application of MRI to studying OA in research and clinical settings.

OBJECTIVE: To develop and assess a rapid method to assess leg alignment on MRI that can be incorporated into all knee MRI exams.

MATERIALS & METHODS: 5 patients underwent a whole-leg radiograph as well as a knee MRI on a 3T whole-body scanner. Whole-leg MRI was performed using a 3-station single-shot fast spin-echo (SSFSE) using the scanner transmit/receive body coil and imaging parameters. For each station, maximum-intensity projections of the bone were created and stitched together to create whole-leg projections. On radiographs and MRI, alignment was measured as the angle from the center of the femoral head to the midpoint of the tibial plateau to the midpoint of line from the lateral fibula to the medial tibia at the height of the tibial plafond(Fig 1). Differences between measures were assessed by Bland-Altman analysis and concordance correlations.

RESULTS: The mean difference in alignment between MRI and radiograph measurements was -0.01±1.31 degrees (95% Limits of Agreement: -2.6 to 2.6 degrees) [0.01 degrees more varus] with a high concordance correlation of 0.94 (Figure 2). Three station scanning was performed in 45-90 seconds.

Figure 1: Leg alignment from 3-station MRI (left) MIP and X-ray (Right).

DISCUSSION: MRI alignment scans can replace the typical localizer for the individual clinical and quantitative knee MRI that is previously performed (usually on the order of 20-45 seconds). It should be noted that MRI scanning in our study was not under load while radiographs are performed in a weight-bearing position. Nevertheless, it appears that that unloaded MRI assessment can be used to approximate measures of knee alignment, with minimal scan time. Future work can identify whether specific positioning of the patient in the scanner can further improve the MRI-based measurement of static limb alignment.

CONCLUSIONS: We present a new method for rapid measurement of knee alignment on MRI which showed good agreement with radiographic measures. This technique can easily be incorporated into routine MRI knee scans to add important knee alignment information and remove the need for additional scanning.

Figure 2: Bland-Altman Analysis of Knee Alignment measures between MRI and Radiographs.
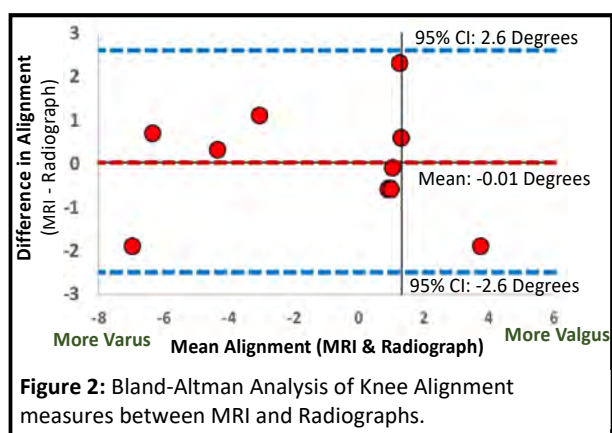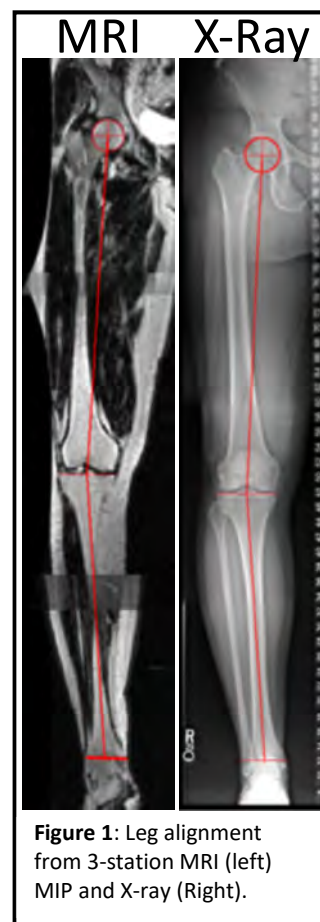
A MACHINE LEARNING METHOD FOR AUTOMATICALLY SCORING KNEE MRI-DETECTED EFFUSION-SYNOVITIS

*Liu H., *Ge Y., **.***Roemer F.W., **Guermazi A., ****Kwoh C.K.

*Department of Management Information Systems, The University of Arizona, Tucson, AZ, USA
**Department of Radiology, Boston University, Boston, MA
***Department of Radiology, University of Erlangen, Nuremberg, Erlangen, Germany
****The University of Arizona Arthritis Center, The University of Arizona, Tucson, AZ, USA & College of Medicine, University of Arizona, Tucson, AZ, USA

INTRODUCTION: Magnetic resonance imaging (MRI) has been recognized as an important tool for the diagnosis of knee osteoarthritis (OA) because MRI detects various knee structure features that may be early signals of knee OA. Effusion-synovitis (ES), as one MRI-detected feature, is associated with the development of incident radiographic knee OA and is also correlated with pain and other clinical outcomes. The Osteoarthritis Initiative (OAI) has the availability of MOAKS (MRI Osteoarthritis Knee Score) scores of ES by experienced musculoskeletal radiologists. Such a scoring method has been proven to be a valuable approach for performing knee OA assessment based on MRI images. However, such manual readings are both time and resource intensive, with high resultant costs. Thus, it is very difficult to scale these semi-quantitative MRI readings to large amounts of MRI data. For example, to date, of the over 50,000 knee MRIs available on 4800 participants in the OAI, less than 5,000 have had semi-quantitative MRI readings.

OBJECTIVE: To build a deep learning model using MOAKS scores of ES and their associated MRIs to automatically classify knee ES into different categories of severity.

METHODS: We collected 4993 records of 1652 patients with annual visits from baseline to 48 months. Basis for assessment were a bag of Axial DESS MRIs, each bag has 30-90 images with size 384x384 pixels. A MOAKS score of ES is provided by a group of experienced musculoskeletal radiologists for each record after reading the associated axial MRIs. The MOAKS score reflects the severity of knee MRI-detected ES from 0) physiologic amount; 1) small – fluid continuous in the retropatellar space; 2) medium – with slight convexity of the suprapatellar bursa; 3) large – evidence of capsular distention. There are 1971 records for grade 0, 1911 for grade 1, 823 for grade 2 and 288 for grade 3. We developed a Multi-Instance Convolutional Neural Network (MICNN) for both binary (i.e., 0/1 versus 2/3) and four-class (i.e., 0, 1, 2, 3) classification and compared with CNN model as a benchmark method. The dataset was randomly split into training (60%), validation (20%) and testing (20%) datasets. MICNN and CNN models were trained on the training dataset, hyper-parameters of the models were tuned on validation dataset and both models were evaluated on testing dataset using classic classification evaluation metrics including Accuracy, Macro AUC, Macro F1 score (i.e., the harmonic mean of the precision and recall).

RESULTS: Our MICNN classifier achieved Accuracy (0.590), Macro AUC (0.814) and Macro F1 score (0.536) for multi-class classification, compared to CNN with Accuracy (0.555), Macro AUC (0.762) and Macro F1 score (0.492). For binary classification, our MICNN achieved Accuracy (0.844), Macro AUC (0.881) and Macro F1 score (0.765) compared to CNN with accuracy (0.976), Macro AUC (0.861) and Macro F1 score (0.601).

CONCLUSION: The MICNN has much better performance than the CNN for multi-class classification. For binary classification, the CNN model has high accuracy but low macro F1 score because it predicted most records as class 0/1. Overall the MICNN classifier performs better than CNN method. These models will be fine-tuned on additional datasets of MOAKS readings of ES and different classification of severity.

IMAGING OF BONE-SYNOVIUM INTERACTIONS USING DYNAMIC CONTRAST ENHANCED MRI AND SODIUM FLUORIDE PET

*MacKay J.W., **Watkins L.E., **Kogan F., ***Sanaei F., *Kaggie J., *Khan W., *McDonnell S.M., ****Morgan-Roberts A.R., ****Janiczek R.L., ***Naish J., ***Parker G.J.M., *Graves M.J., *McCaskie A.W., *Gilbert F.J., **Gold, G.E.

*University of Cambridge, Cambridge, UK
**Stanford University, Stanford, CA, USA
***BiOxyDyn, Manchester, UK
****GlaxoSmithKline, Stevenage, UK

INTRODUCTION: Evidence from in-vitro and animal studies suggests that synovitis plays a role in osteophyte (OP) development and progression in OA via paracrine effects on the adjacent bone and periosteum. Evidence of this phenomenon in humans would improve understanding of OA development and support the targeting of synovial inflammation to achieve disease modification.

OBJECTIVES: (1) Determine whether synovitis adjacent to OPs is more intense than the whole-joint average; (2) Assess the relationship between OP metabolic activity (assessed using Sodium Fluoride PET) and intensity of adjacent synovitis; (3) Assess whether intensity of synovitis is greater adjacent to OPs which progress over 1 year compared with those which do not.

METHODS: We included a total of 23 participants (32 knees). 14 participants with knee OA had MR imaging of a single knee at baseline and 1 year on a 3T platform (GE 750). We also performed simultaneous PET-MR imaging (GE Signa) of both knees of another 9 OA participants at a single timepoint with administration of 2.5 mCi of Sodium Fluoride (NaF) to assess OP metabolic activity. MR examinations for both groups included standard morphological sequences, pre-contrast T1 mapping, dynamic contrast-enhanced (DCE) sequences acquired during the administration of gadolinium-based contrast agent, and matching pre and post contrast 3D fat-suppressed (FS) SPGR images for synovial segmentation. OPs were graded according to the MRI Osteoarthritis Knee Score (MOAKS). Synovium was semi-automatically segmented via shuffle subtraction of the pre and post contrast 3D FS SPGR sequences. Regions of interest (ROIs) adjacent to each OP were defined by the intersection of a manually drawn region around the OP and the semi-automatic synovial segmentation. DCE data were processed to yield maps of K^{trans}, the volume transfer coefficient between the plasma and the extracellular extravascular space which reflects intensity of synovitis. For objective (1), we assessed whether the K^{trans} ratio (KTR: ratio of median K^{trans} adjacent to OP: whole synovium median K^{trans}) was significantly different to 1 using a one-sample t-test. For objective (2), we assessed the association between OP SUV_{max} and adjacent K^{trans} using a linear mixed model adjusted for OP MOAKS grade and participant. For objective (3), we compared K^{trans} ratio adjacent to OPs which increased in MOAKS grade over 1 year vs those which did not, stratified by baseline MOAKS grade and assessed statistically using a two-sample Wilcoxon signed rank test.

RESULTS: A total of 117 OPs were detected (68 grade 1, 43 grade 2, 6 grade 3). Of 37 OPs which had 1-year follow-up imaging, 6 (16%) progressed: five from grade 1 to grade 2, one from grade 2 to grade 3. Of the 80 OPs which had NaF PET data available, 49 (61%) demonstrated increased NaF uptake ($SUV_{max} > 5$ x background bone SUV_{max}). Mean KTR for all OPs was 1.43 (95% CI 1.25 to 1.60, p < 0.001). There was a significant positive association between OP SUV_{max} and adjacent K^{trans} ($R^2 = 0.50$, p = 0.006). Figure 1 shows an example MR image with overlaid PET and K^{trans} data. KTR adjacent to MOAKS grade 1 OP which progressed over 1 year was higher (1.28, 1.04 to 1.53) than adjacent to OPs which did not progress (1.19, 1.02 to 1.35), but with highly overlapping CIs (p = 0.35).

CONCLUSION: Synovitis is more intense adjacent to OPs than the whole-joint average and is more intense adjacent to more metabolically active OPs. The association between intensity of synovitis and OP progression remains uncertain, with a very limited number of OPs progressing in our cohort based on semi-quantitative grading. The combination of PET with DCE-MR provides a unique opportunity to examine the temporal relationship between synovitis and OP development in detail, and to examine whether interventions leading to improvements in synovitis also reduce adjacent OP activity and progression.
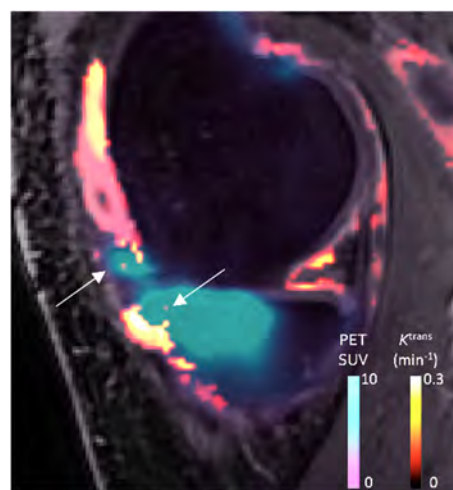

Figure 1. Sagittal 3D fat-suppressed SPGR image through the medial compartment of the knee with overlaid PET and DCE-MR data. White arrows indicate osteophytes – note PET uptake and high K^{trans} values adjacent to medial tibial osteophyte.

PRECISE PRESSURE-CONTROLLED LOADING TO QUANTIFY CARTILAGE AND MENISCUS FUNCTIONALITY BASED ON ADVANCED MRI TECHNIQUES

*Nebelung S., *Thüring J., *Kuhl C., *Truhn D.

*Department of Diagnostic and Interventional Radiology, Aachen University Hospital, Aachen, Germany

INTRODUCTION: Cartilage and meniscus pathologies are closely intertwined in osteoarthritis (OA). The study of these tissues by advanced MRI techniques such as T1ρ, T2 and T2* mapping in dynamic contexts reveals functional tissue features beyond (statically obtained) structural and compositional features. However, to date, adequately precise devices to study cartilage and meniscus functionality in basic research contexts are lacking.

OBJECTIVE: The aim of this study was to design, manufacture and validate an MRI-compatible pressure-controlled device capable of loading both meniscus and cartilage samples in a standardized and reproducible manner and under simultaneous MR Imaging to further explore the basic mechanisms involved in load transmission and its failure that ultimately lead to the development of OA.

METHODS: The device was manufactured using MRI-compatible materials. Force transmission was realized via an externally controllable digital pneumatic that generated pre-programmed loading regimes. Its reproducibility was tested using dedicated pressure-sensitive sensors (K-Scan 4000, Tekscan, Boston, US). At three pressure levels, i.e. 0, 2 and 4 bar [meniscus] and 0, 0.75 and 1.5 bar [cartilage], serial MRI measurements were performed on $n=5$ macroscopically structurally grossly intact meniscus (lateral meniscus body region) and cartilage samples (lateral femoral condyle) using standard PDw and T1ρ mapping sequences for morphological and compositional assessment, respectively. In this regard, samples were subject to direct indentation (cartilage) and torque-induced compression using a lever device (meniscus) (Fig. 1a, b).
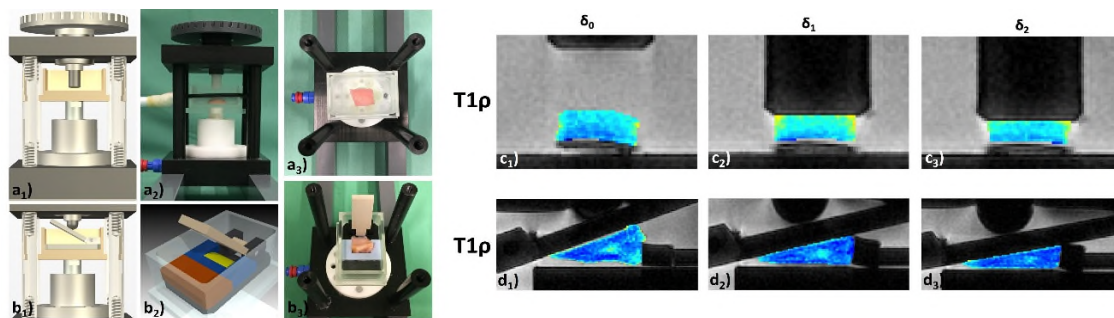
Figure 1: Cross-sectional CAD image (a_1, b_1) and photographs (a_{2-3}, b_{2-3}) of the pressure-controlled loading device containing a representative cartilage (a) and meniscus (b) sample. Cartilage was directly loaded by indentation, while meniscus was loaded using a compressive lever device. Serial T1ρ maps of cartilage (c) and meniscus (d) as a function of increased loading (δ_0 unloaded; δ_1 loaded to 0.75/2 bar; δ_2 loaded to 1.5/4 bar). T1ρ maps were overlaid onto the corresponding PDw images.

RESULTS: The force-pressure calibration revealed a perfect linear dependency of set pressure levels versus measured forces ($r=1.0$, $p<0.001$). Repeated force measurements at set pressure levels were highly reproducible with a standard deviation of 2.7%. Qualitatively, Fig. 1c, d show serial T1ρ measurements of representative cartilage and meniscus samples. Quantitatively, T1ρ values in cartilage increased from 53.9 ± 8.5 ms to 65.4 ± 4.5 ms in response to loading ($p=0.07$) and remained about constant in meniscus (69.7 ± 7.7 ms vs. 71.3 ± 8.8 ms, $p=0.74$). Histological analysis revealed all samples to be grossly intact.

CONCLUSION: The MRI-compatible pressure-controlled loading device allows for precise and standardized loading of cartilage and meniscus samples with excellent reproducibility. This study was exploratory with only limited numbers of samples included, thus future studies are necessary to establish a reliable baseline for the image-based response-to-loading assessment of soft tissues using advanced MRI techniques.

ADVANCED MACHINE LEARNING AND MRI TECHNIQUES TO NON-INVASIVELY PREDICT HUMAN ARTICULAR CARTILAGE COMPOSITION

*Nebelung S., **Linka K., ***Rieppo L., *Thüring J., *Kuhl C., *Truhn D.

*Department of Diagnostic and Interventional Radiology, Aachen University Hospital, Aachen, Germany
**Department of Continuum and Materials Mechanics, Hamburg University of Technology, Germany
***Research Unit of Medical Imaging, Physics and Technology, University of Oulu, Finland

INTRODUCTION: Cartilage degeneration is the hallmark change of osteoarthritis (OA). Early, potentially reversible cartilage degeneration is characterized by distinct changes in cartilage composition and ultrastructure, while the tissue's morphology remains largely unaltered. Hence, early degenerative changes may not be diagnosed by current clinical standard diagnostic tools.

OBJECTIVE: The aim of this study was to determine the tissue's compositional features non-invasively by bringing together a set of established quantitative MRI (qMRI) parameters of cartilage (i.e. T1, T1ρ, T2 and T2* maps), spatially resolved compositional reference measurements (i.e. local proteoglycan [PG] and collagen [CO] contents as determined by Fourier-Transform Infrared Microspectroscopy [FTIR-MS]) and an advanced machine learning technique (i.e. an artificial neural network [ANN]) (Fig. 1). We hypothesized that -following comprehensive training- the prediction of the tissue's composition based on qMRI parameters alone is possible with high precision and accuracy.

METHODS: 11 grossly intact (as controlled by histology) human articular cartilage samples were included to undergo MRI measurements on a clinical 3T scanner (Achieva, Philips) using high-resolution T1 (inversion recovery sequence), T1ρ (spin-lock multigradient echo sequence), T2 (multi-spin echo sequence) and T2* (multi-gradient echo sequence) sequences. Reference FTIR-MS measurements were performed using the 1064 cm^{-1} and 1202 cm^{-1} peaks of the second derivative of the spectra to determine local PG and collagen contents. An ANN consisting of 4 layers and 8 neurons per layer was established and trained using leave-one-out cross validation. Root-mean-square errors (RMSE) and relative-percentage errors (RPE) were calculated to determine the model's predictive accuracy.
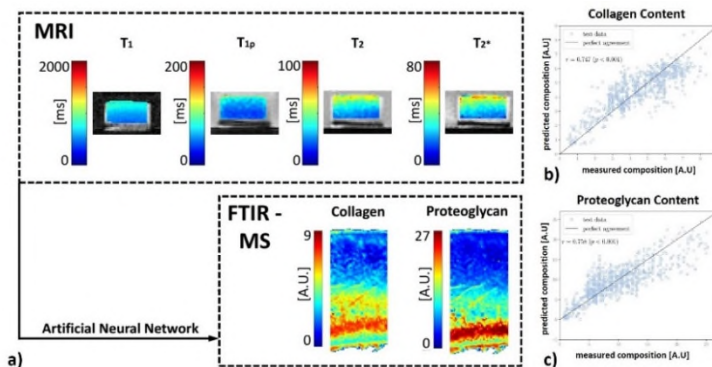

Figure 1. a) Color-coded representative quantitative MRI parameter (upper row) and compositional content maps (lower row) of a representative human articular cartilage sample. Using spatially resolved quantitative MRI parameters (i.e. T1, T1ρ, T2 and T2* maps) as input, collagen and proteoglycan contents (as referenced by microspectroscopic measurements) were predicted based on an artificial neural network. b, c) Detailed voxel-wise relations of measured versus predicted compositional features, i.e. collagen (b) and proteoglycan contents (c). A.U. = Absorption unit.

RESULTS: Correlations between measured and predicted compositional features was strong with r_{CO}=0.75 (p<0.001) and r_{PG}=0.76 (p<0.001). Consequently, correspondence between these features was high and resultant errors low (RSME / RPE: 2.8 Absorption Units [A.U.] / 4.8 % [PG], 0.88 A.U. / 2.1 % [CO]).

CONCLUSION: Once modified for the clinical setting, sophisticated machine learning approaches may be used to predict compositional features of cartilage based on qMRI parameters alone with potential implications for the diagnosis of (early) degeneration and for the monitoring of therapeutic outcomes.

QUANTIFICATION OF FAT FRACTION IN SUBCHONDRAL BONE MARROW OEDEMA-LIKE LESIONS OF KNEE OSTEOARTHRITIS USING DIXON MR IMAGING

*Noorveriandi H., *Cootes T.F., **Felson D., ***O'Neill T.W., *Hodgson R.

*Centre for Imaging Sciences, University of Manchester, UK
**Boston University School of Medicine, Boston, Massachusetts, USA &
Arthritis Research UK Centre for Epidemiology, University of Manchester, UK
***Arthritis Research UK Centre for Epidemiology, Division of Musculoskeletal & Dermatological Sciences, Faculty of Biology, Medicine and Health, Manchester Academic Health Science Centre, The University of Manchester, UK; NIHR, Manchester Biomedical Research Centre, Manchester University NHS Foundation Trust, Manchester Academic Health Sciences Centre, Manchester, UK; Department of Rheumatology, Salford Royal NHS Foundation Trust, Manchester, UK

INTRODUCTION: Subchondral bone marrow oedema-like lesions (BMLs) which are observed on MRI of knee OA have been linked to pain, progression of cartilage loss, and progression to joint replacement. There are, however, challenges in quantifying BMLs size and change. Poorly-defined boundaries of BMLs can lead to inconsistency in quantifying lesion volume and detecting changes in size over time. Further, BMLs are treated as similar when their compositions may differ. The assessment of change in lesion volume is affected by the accuracy and reliability of the segmenting approach in capturing small changes in BML volume. Quantitative MRI techniques, such as Dixon imaging, provide an alternative approach for characterisation of BMLs based on their fat and water composition.

OBJECTIVE: (1) To compare fat fraction of subchondral BMLs and surrounding normal-appearing marrow in subjects with symptomatic knee OA using 3D gradient echo Dixon imaging and (2) To determine the association between changes in fat fraction and BML volume.

METHODS: We analysed images from 18 symptomatic knee OA subjects with subchondral BMLs taken from a clinical trial. Subjects were imaged using a 3.0 T Philips MR scanner. A single observer manually segmented subchondral BMLs volume using sagittal FSE SPAIR sequences (TR 2900/TE 30 ms) at 2 visits separated by approximately 8 weeks. Region of interest (ROI) of BMLs and nearby normal appearing marrow were segmented on Dixon water images (mDixon Quant) (TR 15 ms, 6 echoes, TE minimum 1.4 ms, echo spacing 1.1 ms, 3° flip angle) at baseline. In addition, ROIs of BMLs were segmented on either the baseline or follow-up Dixon water images to determine the association between changes in BMLs volume and fat fraction; image registration was performed to register the ROIs of BML at one visit onto the other visit. The average fat fraction within the ROIs at both time points was recorded. The fat fraction of BMLs and normal appearing nearby marrow on the baseline image was compared using paired t-test. The change in BML volume between the baseline and follow up image was determined and also the change in fat fraction of the BML ROI between baseline and follow up. Spearman's correlation coefficient was used to assess the association between change in BML volume and change in fat fraction.

RESULTS: At baseline, the fraction of fat within the BMLs was significantly lower than that of nearby normal-appearing marrow ($72.4\pm8.4\%$ vs $92.1\pm2.8\%$, $p<0.005$). The change in size of BMLs over time was negatively correlated with the change in fat fraction ($r=-0.58$, $p=0.013$).

CONCLUSION: BMLs of subjects with symptomatic knee OA had a significantly lower fat fraction than normal-appearing marrow. Changes in fat fraction correlated with change in BMLs volume. Estimation of BML fat fraction avoids some of the variability inherent in measuring change in BML size and provides an alternative approach for BML assessment requiring segmentation at a single time point only.

3D MRI ANALYSIS FOR CARTILAGE IN ANTERIOR CRUCIATE LIGAMENT INJURED KNEES

*Ozeki N., **Koga H., *Aoki H., *Hyodo A, ***Suzuki K., ***Itai Y., ***Masumoto J., *Sekiya I.

*Center for Stem Cell and Regenerative Medicine, Tokyo Medical and Dental University, Tokyo, Japan
**Department of Joint Surgery and Sports Medicine, Tokyo Medical and Dental University, Tokyo, Japan
***Fujifilm Corporation, Tokyo, Japan

INTRODUCTION: It has been reported that knee instability or duration from injury to surgery affects the incidence of cartilage injury in anterior cruciate ligament (ACL) injured patients. Cartilage condition is often evaluated by arthroscopy as a gold standard. However, it would be better if it is evaluated in detail by MRI non-invasively. We have been developing a 3D MRI analysis system that enables to reconstruct 3D images of the cartilage in the knee joint automatically (Figure 1). To quantitate the cartilage condition, projected cartilage area ratio with intended thickness can be measured with this system.

OBJECTIVE: To examine the projected cartilage area ratio in ACL injured knees and to investigate the factors that were correlated with cartilage injury.

METHODS: Thirty-two patients who had 3T MRI (Achieva 3.0TX, Philips, pixel spacing: 0.31mm×0.31mm, slice thickness: 0.6mm) before ACL reconstruction were included in this study. After 3D reconstruction, femoral cartilage was projected to a flat surface, and ROI was defined to 4 segments; anteromedial (AM), posteromedial (PM), anterolateral (AL) and posterolateral (PL) segments. In this study, the projected cartilage area ratio with cartilage thickness of 1.5 mm and over was evaluated. Correlations between the cartilage area ratio and the following factors were evaluated; age, duration from injury to surgery, incidence of giving way, anterior instability measured by knee arthrometer (mm) , pivot shift test grade (0-6), Lysholm score (1-100), and Tegner Activity Scale (1-10). We also investigated the correlation between the cartilage area ratio by MRI and the cartilage grading by arthroscopy as validation. Simple linear regression analysis was used for statistical analysis.

RESULTS: Projected cartilage area ratio was 0.96±0.04 in AM, 0.92±0.07 in PM, 0.95±0.93 in AL, and 0.97±0.05 in PL. Projected cartilage area ratio in PM correlated with duration from injury to the surgery ($p < 0.0001$), the incidence of giving way (p=0.003), and the pivot shift test grade（p=0.009）(Fig 2, 3). Cartilage area ratio in PM was correlated with cartilage grading by arthroscopy (Figure 4).

CONCLUSION: Projected cartilage area ratio by MRI was useful to evaluate cartilage status after ACL injury. Cartilage injury in ACL deficient knees evaluated by projected cartilage area ratio was correlated with the duration from injury to surgery, the incidence of giving way, and the pivot shift test grade.

Figure 1
Projected Cartilage Area Ratio (≧1.5mm)
AM: 0.79   AL: 0.93   PM: 0.82   PL: 0.98

Figure 2

Figure 3

Figure 4
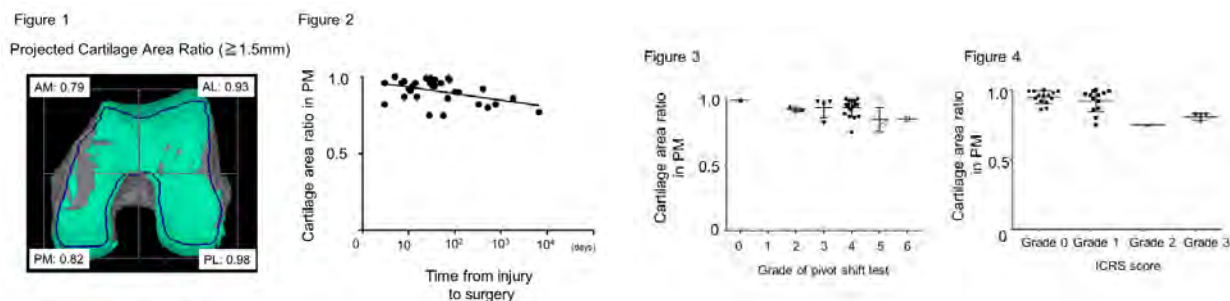
MACHINE LEARNING PREDICTS RAPID RATE OF CARTILAGE LOSS: DATA FROM THE OSTEOARTHRITIS INITIATIVE

*Paixao T., *Goetz C., *Bertalan Z., *Ljhuar R., **Nehrer S.

*Imagebiopsy Lab, Vienna, Austria
**Danube University Krems, Center for Regenerative Medicine, Krems, Austria

INTRODUCTION: Measurement of Joint Space Width (JSW) by radiographic means remains the gold standard for assessment of cartilage loss. However, this rate can vary widely between patients at risk or suffering from knee OA. The causes for these differences in cartilage loss rates remain unknown.

OBJECTIVE: Here, we investigate whether quantitative and semi-quantitative radiographic features can be used to predict the rate of Joint Space Width (JSW) loss.

METHODS: We collected bilateral knee radiographs, acquired in the context of the OAI study, from 4100 patients (2383 female, 1717 male). Each patient was imaged up to 7 times, separated by at least 12 months, across a time span of 8 years. Each radiograph was analyzed by software to obtain Kellgren-Lawrence (KL) and OARSI grades for Osteophytes, Sclerosis and Joint Space Narrowing (JSN) readings, as well as JSW measurements for each individual knee. Linear regressions of JSW were performed per individual knee compartment (medial or lateral) to estimate the rate of JSW loss per month. Individual knees with rate of JSW loss above 0.072 mm/year (the average yearly loss within JSN grade) were classified as progressors (956 knees). From these, knees in the top 10% of JSW loss rate were classified as fast progressors (91 knees). A logistic regression model was used to predict the fast progressor phenotype with KL and OARSI grades at baseline as independent variables. Model performance was estimated using 10-fold cross-validation training/testing dataset splits and used area under the curve (AUC) as performance criteria.
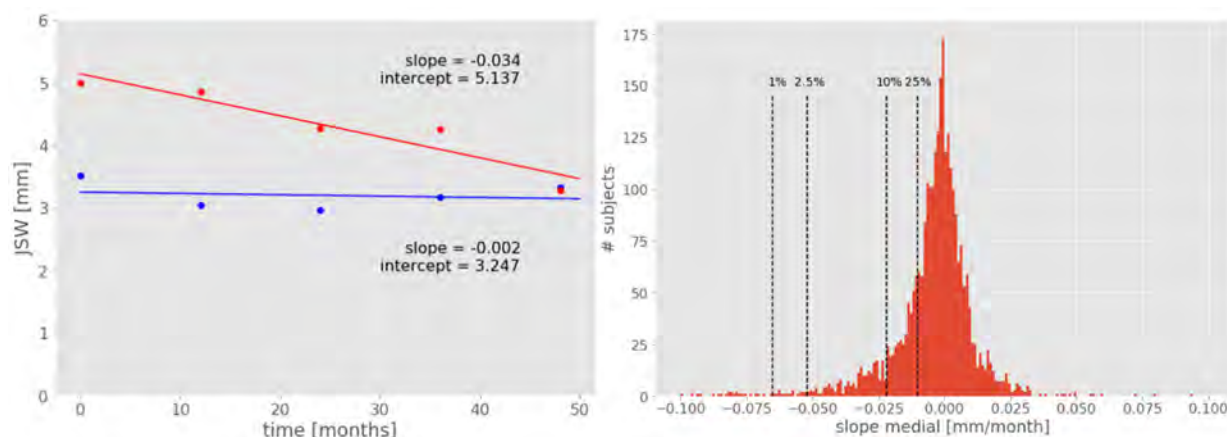
RESULTS: The logistic regression classifiers achieved AUCs of 0.71 (SE 0.015) and 0.66 (SE 0.013) at classifying individual knees as fast progressors for medial and lateral compartments, respectively. Analysis of the individual coefficients of the classifiers reveals that JSN and Sclerosis OARSI grades are the main predictors of rapid cartilage loss.

CONCLUSION: Our results show that it is possible to predict future rapid cartilage loss from quantitative and semi-quantitative readings from a single plain radiograph. Interestingly, neither KL grade nor Osteophytes OARSI grade contributed greatly to this prediction. Instead, Sclerosis and JSN grade seem to be the major predictors of rapid cartilage loss, suggesting a non-canonical mode of OA progression.

EFFECT OF CONTRALATERAL RADIOGRAPHIC STATUS ON THE PREVALENCE AND PROGRESSION OF SYNOVIAL TISSUE PATHOLOGY IN KNEES WITHOUT ESTABLISHED OSTEOARTHRITIS

*,**Roemer F.W., ***Eckstein F., *Guermazi A., ****Duda G., ***Maschek S., *****Sharma L.,***Wirth W.

*Quantitative Imaging Center (QIC), Department of Radiology, Boston University School of Medicine, Boston, MA
**Department of Radiology, Friedrich-Alexander University Erlangen-Nürnberg & Universitätsklinikum Erlangen, Erlangen, Germany
***Department of Imaging and Functional Musculoskeletal Research, Institute of Anatomy, Paracelsus Medical University Salzburg & Nuremberg, Salzburg, Austria & Chondrometrics GmbH, Ainring, Germany
****Julius Wolff Institute, Charité-Universitätsmedizin, Berlin, Germany
*****Division of Rheumatology, Feinberg School of Medicine, Northwestern University, Chicago, IL

INTRODUCTION: Structural MRI-defined pathology of the knee joint has been observed in a large proportion of the population, including subjects without radiographic abnormalities or knee pain. Cartilage transverse relaxation time (T2) has been suggested as a compositional endpoint for measuring progression of knee OA at its earliest stages. However, it is currently unknown whether structural pathology drives T2 changes in knees without radiographic signs of OA or pain.

OBJECTIVE: To test whether radiographically normal knees (K-L 0) with definite contralateral radiographic knee OA (K-L 2 to 4), but without contralateral trauma history (i.e. an 'early OA model'), exhibit greater prevalence and progression of structural joint pathology as defined by MRI than those with bilateral radiographically normal knees (K-L 0) without risk factors ('healthy reference'). In another step we compared the prevalence and progression rates with those previously reported for bilateral K-L 0 knees with risk factors.

METHODS: We included 154 knees from the Osteoarthritis Initiative (OAI) without ROA (K-L=0), but with definite ROA (K-L$\geq$2) in the contralateral knee, and 78 participants from the OAI healthy reference cohort (without any signs of radiographic OA, knee pain or risk factors in either knee). Effusion-synovitis, Hoffa-synovitis, bone marrow lesions (BMLs), cartilage lesions, meniscus morphology and - extrusion and osteophytes were assessed at year 1 (Y1) and year 4 (Y4). Frequencies of features for both groups at Y1 and rates of worsening from Y1 to Y4 were compared using Fisher's exact test.

RESULTS: At year 1, the early OA model group exhibited more structural pathology in their radiographically normal (K-L 0) knee than the healthy reference group. This applied for all features apart from effusion synovitis, which had a similar prevalence in both groups (19.2% vs 26.0%, p=0.33). Femorotibial cartilage damage was seen in 77.3% vs. 50%, femorotibial BMLs in 27.3% vs 12.8% and meniscal damage in 35.7% vs. 9.0% in the early OA model vs. healthy reference.Femorotibial cartilage damage worsening was seen in 34.4% in the early OA model groups over 3 years, vs. 20.5% in the healthy reference group (p=0.03). Other structural features also showed more frequent worsening in the early OA model, but only for femorotibial osteophytes, and osteophytes in either compartment, the difference attained statistical significance. Concerning development of new damage (i.e. incident features), femorotibial osteophytes, and osteophytes in either compartment, were more commonly seen in the early OA model than in healthy reference knees (9.1% vs 1.3%, p=0.02 and 9.7% vs 1.3%, p=0.01). When looking at different BMI strata in the early OA model group, significantly more incident cartilage damage was seen in the obese group compared to the overweight and normal subgroups (21.3% vs. 13.2% and 2.6%, p=0.01). No differences between the groups were seen for number of lesions present at year 1 or for increase of number of lesion over three years Additional sensitivity analyses, stratifying the early OA model into three different age groups (<60, 60-70, >70 years), did not reveal any difference in the frequencies of features at year 1, nor in the number of lesions present at year 1, nor worsening in number over 3 years the different age groups (data not shown).

CONCLUSION: We found that MRI synovial tissue structural pathology is far more prevalent in an early OA model of KLG0 knees with contralateral ROA, compared with a healthy reference sample. This applied for all features, apart from effusion-synovitis. Regarding longitudinal change, incident cartilage damage was more common in the early OA model group, supporting the assumption that patients with a radiographically normal knee but contralateral ROA represent an attractive model for testing DMOADs in clinical trials of early, non-radiographic osteoarthritis.

MULTI-PARAMETRIC ASSESSMENT OF KNEE JOINT SYNOVITIS AT ULTRA-HIGH FIELD (7T) MRI USING CONTRAST-ENHANCED AND NON CONTRAST-ENHANCED SEQUENCES

*,**Roemer F.W., **Treutlein C., *Guermazi A., **Nagel A., ***Schett G., **Uder M., **Bäuerle T.

*Quantitative Imaging Center (QIC), Department of Radiology, Boston University School of Medicine, Boston, MA
**Department of Radiology, Friedrich-Alexander University Erlangen-Nürnberg & Universitätsklinikum Erlangen, Erlangen, Germany
***Department of Medicine 3, Rheumatology and Immunology, Friedrich-Alexander University Erlangen-Nürnberg & Universitätsklinikum Erlangen, Erlangen, Germany

INTRODUCTION: With clearance for clinical use recently, 7T systems are already used clinically and will potentially become more widely available. MRI has made an important clinical impact in the assessment of inflammatory arthritis particularly since the introduction of effective anti-rheumatic therapies. However, to date no clinical studies are available that have assessed the feasibility of 7T MRI for evaluation of inflammatory arthritis. Recommended imaging protocols on standard 1.5T and 3T systems include T1- and T2-weighted fat suppressed spin echo sequences and the use of contrast-enhanced (CE) MRI for the evaluation of synovitis. Experience regarding feasibility of CE imaging at 7T to date is limited. In addition, novel non-enhanced techniques replacing CE imaging are desirable that enable differentiation of intraarticular joint fluid from synovial thickening and inflammation

OBJECTIVE: To investigate the feasibility of contrast-enhanced (CE) and non-enhanced MRI at 7T for the assessment of knee joint synovitis.

METHODS: 10 patients with an established diagnosis of psoriatic or rheumatoid arthritis underwent 7T MRI. Our study protocol consisted of sagittal intermediate-weighted fat-suppressed (FS), axial fluid-attenuated inversion recovery (FLAIR) FS, sagittal 3D T1-weighted dynamic contrast enhanced (DCE) and an axial static 2D T1-weighted FS contrast-enhanced sequence (T1-FS CE). Ordinal grading on non-enhanced (Hoffa- and effusion-synovitis) and enhanced images (11-point synovitis score), comparison between FLAIR-FS and static T1-FS CE imaging using semiquantitative (SQ) and volume assessment was performed. Inter- and intra-reader reliability was determined. For reliability assessment weighted kappa statistics for ordinal scores and intraclass correlation coefficients (ICC) for continuous variables were applied.

RESULTS: Total duration of study protocol was 15 min 38 s. Synovitis was detected in all patients (mild: n=3; moderate: n=5; severe: n=2). SQ assessment yielded significantly lower peripatellar summed synovitis scores for FLAIR-FS compared to CE T1-FS ($p<0.01$). Peripatellar synovial volume between CE T1-FS and FLAIR-FS was comparable with FLAIR-FS showing significantly lower volumes ($p<0.01$) with a mean percentage difference of $18.6 \pm 9.5\%$. Inter- and intra-reader agreement for SQ scoring ranged from 0.21 (inter-reader Hoffa-synovitis) to 1.00 (inter-reader effusion-synovitis). Inter- and intra-reader agreement of SQ 3D-DCE parameters ranged from 0.86 to 0.99.

CONCLUSION: CE MRI of knee synovitis at 7T is clinically feasible. 7T FLAIR-FS imaging is a potential non-enhanced imaging method visualizing synovial inflammation with high conspicuity and holds promise for further application in research endeavors and clinical routine by trained readers.

A. B. C.
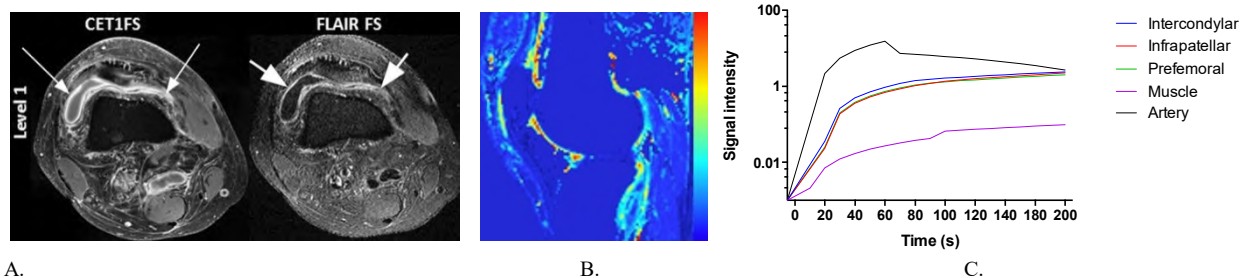
A. Image pair of contrast-enhanced T1-weighted fat suppressed (T1-FS CE) and non-enhanced fluid attenuated inversion recovery fat suppressed (FLAIR-FS) sequences. Left figure column depicts the T1-weighted enhanced images with synovial thickening and contrast-enhancement at all levels (long arrows). Figure parts in the right figure column show corresponding FLAIR-FS images with synovitis being depicted in similar fashion as hyperintense with corresponding thickening of the synovial tissue at all levels (short arrows). B. Dynamic contrast enhanced MRI. iAUC based calculation of parametric maps over time (red depicts high uptake of contrast agent; blue represents low uptake of contrast agent). **C.** Typical enhancement curves from a single patient for the different ROIs show steep enhancement between 20 and 40 sec followed by continued but much slower enhancement after 40 sec. Maximum enhancement is reached at about 200 sec post contrast administration.

JOINT INFLAMMATION ON MRI PREDICTS INCIDENT KNEE OA, BUT CAN'T WE USE PATIENT-REPORTED MEASURES?

*Runhaar J., *Landsmeer M.L.A., *van Middelkoop M., **van der Plas P., **Vroegindeweij D., ***Oei E.H.G., *Bindels P.J.E., *,****Bierma-Zeinstra S.M.A.

*Erasmus MC University Medical Center Rotterdam, Dept. of General Practice
**Maasstad Hospital, Dept. of Radiology
***Erasmus MC University Medical Center Rotterdam, Dept. of Radiology & Nuclear Medicine
****Erasmus MC University Medical Center Rotterdam, Dept. of Orthopedics

INTRODUCTION: Joint inflammation seen on MRI is an independent risk factor for incident radiographic knee OA, for radiographic and symptomatic progression. However, given the high costs for MRI, single questionnaires items will be preferred to screen for individuals at high risk for knee OA development.

OBJECTIVE: To compare the predictive value of 1) inflammation on MRI, 2) patient-reported swelling of the knee, and 3) patient-reported morning stiffness of the knee for the incidence of clinical and radiographic knee OA in a high-risk cohort of middle-aged overweight/obese women free of knee OA at baseline.

METHODS: 407 middle-aged women with a BMI$\geq$27 kg/m^2, free of clinical and radiographic knee OA had radiography and MRI of both knees taken and filled-in the KOOS questionnaire at baseline, 2.5 and 6.5 years. Primary outcome measures were incident clinical knee OA ('clinical and radiographic' ACR criteria) and incident radiographic knee OA (KL$\geq$2). For baseline presence of inflammation on MRI (score $\geq$1 for either effusion/synovitis or Hoffa-synovitis using MOAKS), patient-reported swelling (score $\geq$1 on 0-4 scale for item on KOOS symptom subscale), and patient-reported morning stiffness (score $\geq$2 on 0-4 scale for item on KOOS stiffness subscale), sensitivity, specificity, and pre- and post-test probabilities were calculated.

RESULTS: 345 women (85%) had complete data available at 2.5 years and 227 (56%) at 6.5 years and were included in the analyses. At baseline, women had a median age of 55.2 years and a median BMI of 31.1 kg/m^2. Baseline prevalence of inflammation on MRI was 15% and patient-reported swelling and stiffness were present in 12.0% and 14.3% of the knees, respectively. Incidence of clinical knee OA was 7.0% after 2.5 and 11.7% after 6.5 years and incidence of radiographic knee OA was 4.7% after 2.5 and 15.5% after 6.5 years. Predictive abilities of the three baseline criteria are presented in the Table.

Incident clinical knee OA						
	Time point	Pre-test probability (%) (95% CI)	Sensitivity (%) (95% CI)	Specificity (%) (95% CI)	Post-test probability+ (%) (95% CI)	Post-test probability- (%) (95% CI)
Inflammation on MRI	@2.5 yr.	7.0 (5.2-9.3)	17.4 (7.8-31.4)	86.0 (83.0-88.7)	8.6 (4.6-15.4)	93.2 (92.3-94.0)
	@6.5 yr.	11.7 (10.3-15.2)	19.6 (9.8-33.1)	85.4 (81.5-88.8)	15.2 (7.9-26.6)	88.9 (85.1-91.8)
Morning stiffness	@2.5 yr.	7.0 (5.2-9.3)	32.6 (19.5-48.0)	88.7 (86.0-91.1)	17.9 (12.0-25.8)	94.6 (93.4-95.5)
	@6.5 yr.	11.7 (10.3-15.2)	23.5 (12.8-37.5)	90.4 (87.0-93.1)	24.5 (15.3-36.7)	89.9 (88.4-91.2)
Swelling	@2.5 yr.	7.0 (5.2-9.3)	17.4 (7.8-31.4)	89.5 (86.8-91.8)	11.1 (6.0-19.7)	93.5 (92.6-94.3)
	@6.5 yr.	11.7 (10.3-15.2)	9.8 (3.3-21.4)	88.8 (85.2-91.8)	10.4 (4.6-21.9)	88.1 (87.1-89.1)
Incident radiographic knee OA						
Inflammation on MRI	@2.5 yr.	4.7 (3.2-6.7)	40.0 (22.7-59.4)	88.1 (85.3-90.6)	14.1 (9.2-21.1)	96.8 (95.7-97.6)
	@6.5 yr.	15.5 (12.3-19.4)	32.8 (21.8-45.4)	89.3 (85.7-92.3)	36.1 (26.4-47.0)	87.9 (85.9-89.6)
Morning stiffness	@2.5 yr.	4.7 (3.2-6.7)	13.3 (3.8-30.7)	86.2 (83.2-88.8)	4.5 (1.8-10.7)	95.3 (94.6-96.0)
	@6.5 yr.	15.5 (12.3-19.4)	20.9 (11.9-32.6)	89.3 (85.7-92.3)	26.4 (17.1-38.4)	86.0 (84.0-87.5)
Swelling	@2.5 yr.	4.7 (3.2-6.7)	23.3 (9.9-42.3)	90.1 (87.4-92.3)	10.3 (5.4-18.6)	96.0 (95.2-96.7)
	@6.5 yr.	15.5 (12.3-19.4)	19.4 (10.8-30.9)	90.7 (87.2-93.5)	27.7 (17.6-40.7)	86.0 (84.4-87.4)

CONCLUSION: Patient-reported morning stiffness better predicted incident clinical knee OA than inflammation on MRI. Inflammation on MRI slightly better predicted incident radiographic knee OA. However, for patients' convenience and costs for society, the advantage of a patient-reported feature over MRI might be much larger.

DISCLOSURE STATEMENT: All authors declare no conflicts of interest.
CORRESPONDENCE ADDRESS: j.runhaar@erasmusmc.nl

FACTORS ASSOCIATED WITH LONGITUDINAL CHANGE OF MENISCAL EXTRUSION IN OVERWEIGHT WOMEN WITHOUT CLINICAL SIGNS OF KNEE OA

*,**,***Voet van der J.A., ***Wesselius D., ****Zhang F., **Vroegindeweij D., *Oei E.H., ***,*****Bierma-Zeinstra S.M.A., ****Englund M., ***Runhaar J.

*Dept. of Radiology & Nuclear Medicine, Erasmus MC University Medical Center, Rotterdam, The Netherlands
**Dept. of Radiology, Maasstad Hospital, Rotterdam, The Netherlands
***Dept. of General Practice, Erasmus MC University Medical Center, Rotterdam, The Netherlands
****Lund University, Faculty of Medicine, Department of Clinical Sciences Lund, Orthopaedics, Clinical Epidemiology Unit, Lund, Sweden
*****Dept. of Orthopaedics, Erasmus MC University Medical Center, Rotterdam, The Netherlands

INTRODUCTION: Previously, we showed a significantly increased risk for incident knee osteoarthritis (KOA) after 2.5 years in knees with meniscal extrusion in a high-risk population of overweight and obese middle-aged women, free of OA at baseline[1.]

OBJECTIVE: In the present study, we aimed to identify variables associated with longitudinal change in meniscal extrusion, which might be used as possible targets for the prevention of KOA.

METHODS: We used data from the PROOF study, an RCT evaluating a high-risk population of middle-aged overweight and obese women (BMI $\geq$ 27 kg/m^2), free of clinical and radiographic KOA at baseline. Meniscal extrusion was assessed on the mid-coronal slice of an MRI at baseline and after 30 months. Outcomes were the absolute change in medial and lateral meniscal extrusion (mm) and the absolute change in relative extrusion (%). Based upon literature, several factors were hypothesized to be associated with longitudinal change in meniscal extrusion, including baseline age, baseline BMI, change in BMI over 30 months, postmenopausal status, malalignment, quadriceps strength, physical activity, baseline meniscal tears, incident meniscal tears, a history of knee injury and the presence of Heberden's nodes. Linear GEEs were used to model the effect of these covariates on the change in extrusion, adjusted for tibial width, to take differences in knee size into account.

RESULTS: 786 knees were available for analysis. The greatest change in medial meniscus extrusion was seen in menisci with an incident meniscal tear (absolute: 0.88 mm, 95% CI: 0.28, 1.47; relative 14.52%, 95% CI: 4.38, 24.66). Tears at baseline only led to an absolute increase in extrusion in the lateral meniscus: 0.65 mm, 95% CI: 0.13, 1.16. Varus malalignment resulted in a significant increase of medial extrusion of 0.57 mm (95% CI: 0.14, 1.00). A 5 kg/m^2 increase in baseline BMI led to an absolute and relative increase of medial extrusion of 0.21 mm and 2.96% (95% CI: 0.10, 0.33; 1.32, 4.79). Change in BMI during follow-up (per 1 point) also resulted in a significant increase in extrusion (absolute: 0.06 mm, 95% CI: 0.02, 0.09; relative: 0.6%, 95% CI: 0.05, 1.15). Interestingly, a higher baseline value of extrusion resulted in a slight decrease of extrusion during the 30 months follow-up. Adjusting for tibial width and the intervention groups of the original trial did not influence the results.

CONCLUSION: Of all the studied variables, meniscal tears, malalignment and BMI showed the strongest association with change in meniscal extrusion. They might be used as a target to prevent or reduce extrusion and by that decelerate the development of knee OA.

REFERENCES: [1] von der Voet, OAC, 2017 [2] Runhaar, Am J Med, 2015
CORRESPONDENCE ADDRESS: j.a.vandervoet@erasmusmc.nl

T2 CHANGES IN LOADED CADAVERIC TIBIOFEMORAL CARTILAGE IN 0.5T MROpen AND 7T MRI

*,**,***Stockton D.J., *,**Desrochers J., *,****Yung, A.C., *,**Wilson D.R.

*Centre for Hip Health and Mobility, UBC, Vancouver, Canada
**Department of Orthopaedics, UBC, Vancouver, Canada
***Clinician Investigator Program, UBC, Vancouver, Canada
****MRI Research Center, UBC, Vancouver, Canada
 Dr. Desrochers and Dr. Stockton contributed equally to this work

INTRODUCTION: Upright open MRI allows articular cartilage imaging in functionally relevant postures, which introduces the possibility of measuring cartilage mechanics directly. The resolution of weightbearing images is not sufficient to measure cartilage strain accurately, but cartilage T2 has the potential to yield indirect measurements of cartilage mechanics because of the association of T2 with load. However, high resolution MRI studies of cartilage have shown that the response of T2 to load depends on the depth of the cartilage layer and the load magnitude. It is not clear how these effects would affect weightbearing measurements of cartilage T2 in upright open MR.

OBJECTIVE: Therefore, the objective of the current study was to investigate whether 0.5T upright open MRI of loaded knee cartilage could detect the depth and load dependent changes in T2 visible on 7T MRI.

METHODS: Two cadaveric knees were prepared and bony ends were mounted in a custom designed, MRI-compatible loading rig. MR image volumes of unloaded and loaded tibiofemoral cartilage were acquired first in upright open MRI (MROpen, Paramed) using the 3D STSS sequence and subsequently on a Bruker Biospec 7T MRI using the 3D DESS sequence. Acquisition parameters included:

Image Data		**T2 3D DESS parameters 7T**		**T2 3D STSS parameters MROpen**	
Voxel size MROpen	860×860 μm	Flip angle	$30°$	Flip angle	$30°$
Voxel size 7T	208×208 μm	Repetition time (TR)	17 ms	Repetition time (TR)	16 ms
Slice thickness MROpen	2500 μm	Echo time (TE)	4.5 ms	Echo time (TE)	6 ms
Slice thickness 7T	800 μm				

Cartilage in contact was segmented for three conditions in both the 0.5T and 7T scans: unloaded, ~15% strain; and ~25% strain. Tibiofemoral cartilage was divided into 4 regions: medial-tibial (MTC), lateral-tibial (LTC), medial-femoral (MFC) and lateral-femoral (LFC). For MROpen cartilage, surface zone cartilage (SZ) was defined as the first row within the segmented volume for each slice; middle zone cartilage (MZ) was the second row and deep zone cartilage (DZ) an average of the remaining voxels. 7T image volumes were downsampled to yield voxel sizes of approximately equal dimensions as the MROpen and then downsampled voxels were assigned to zones as for MROpen. T2 values for each zone, region, and load were calculated in MATLAB (R2018b, Mathworks, Natick, MA). One-way ANOVA with Tukey's honest significant difference correction for multiple comparisons was used to test for differences in mean T2 across zone depths and loads for 7T and MROpen. Multivariable linear regression models for 7T and MROpen data were built to test for the effect of load on T2, controlling for cartilage region and zone. Statistics were performed using R (R Core Team 2018, Vienna, Austria) with significance set at $p < 0.05$.

RESULTS: At 7T, region-specific and depth-dependent changes in T2 were observed. Relative to the SZ, mean T2 was lower in the MZ ($P<0.001$) and DZ ($P<0.001$), (Table 1). In the multivariable model, relative to the unloaded state and controlling for region and zone depth, 15% strain and 25% strain were associated with mean decreases in T2 of 0.4 ± 0.2ms ($P = 0.01$), and 0.7 ± 0.2ms ($P<0.001$), respectively. The model explained 70% of the variation in T2. Similar depth- and load-dependent changes were observed in the MROpen. Relative to SZ, mean T2 was lower in the MZ ($P<0.001$) and DZ ($P<0.001$), (Table 1). In the multivariable model, relative to the unloaded state and controlling for region and zone depth, 15% strain and 25% strain were associated with mean changes in T2 of $+2.6 \pm 0.8$ms ($P<0.001$), and -5.7 ± 0.8ms ($P<0.001$). However, this model explained only 24% of the variation in T2.

Table 1: Comparison of T2 for Loaded Knee Cartilage in the Three Zones for High Resolution vs. MROpen MRI

Zone	T2, 7T (mean ± SD, ms)	T2, MROpen (mean ± SD, ms)
Bulk Average	17.0 ± 9.0	39.4 ± 15.3
SZ	21.2 ± 10.6	45.7 ± 14.3
MD	15.6 ± 7.0	39.1 ± 14.3
DZ	12.1 ± 4.4	29.9 ± 12.9

CONCLUSIONS: Upright open MRI detects depth- and load-dependent changes in tibiofemoral cartilage T2, which have been shown in high resolution MRI, suggesting that T2 has the potential for use as an indirect index of cartilage strain. However, the low (24%) proportion of variation explained by the model for MROpen data indicates that further work must examine the additional sources of variability in T2 in the MROpen before T2 can be used as an indirect measure of cartilage mechanics.

FEASBILITY AND REPRODUCIBILITY OF 3D JOINT SPACE MAPPING AT THE KNEE WITH STANDING CT DATA FROM THE MULTICENTER OSTEOARTHRITIS STUDY

*Turmezei T.D., *Low S.B., **Segal N.A., ***Treece G.M., ***Gee A.H., ****Lynch J.A., ***Poole K.E.S.

*Norfolk and Norwich University Hospital, Norwich, UK
**University of Kansas Medical Center, USA
***University of Cambridge, Cambridge, UK
****University of California San Francisco, USA

INTRODUCTION: Joint space mapping (JSM) is a 3D image analysis technique that can deliver structural parameters such as 3D JSW distribution and shape from computed tomography (CT) imaging data. The ability to acquire CT at the knee in a fixed-flexion standing position now presents the opportunity for the application of JSM at this joint.

OBJECTIVE: To demonstrate 1) feasibility and 2) interoperator reproducibility of JSM at the knee in a convenience sample of standing CT data from Multicenter Osteoarthritis Study (MOST).

METHODS: A convenience sample of standing CT data from both knees in 23 individuals was selected from MOST with the full KLG range. A prototype commercial CT scanner (LineUp, CurveBeam, Warrington, PA) took weight-bearing images of both knees in a fixed-flexed stance. Data sets with isotropic voxels at 0.37 mm were reconstructed from cone beam projections. JSM was performed at each knee to measure JSW in 3D at the tibiofemoral compartments using a hybrid full-width-half-maximum/threshold measurement technique. Femoral and tibial joint surfaces and JSW as the distance between them were defined by the JSM measurement algorithm. JSM output "halfway" joint surfaces were then registered to their average, with JSW data mapped onto the average surfaces for statistical analysis and presentation of results. For feasibility, the side with the worse KLG was chosen from each individual, randomly if equal, giving 23 knees for statistical parametric mapping (SPM), performed to look for dependence of 3D JSW on KLG. For reproducibility, 3 bilateral knee sets with KLG 0-3 were used for training of a novice, followed by comparison of the remaining 20 bilateral knee sets against an expert.

1) JSW dependence on KL
(inferior view, right knee)

2) RMSCV (%)
(inferior view, right knee)
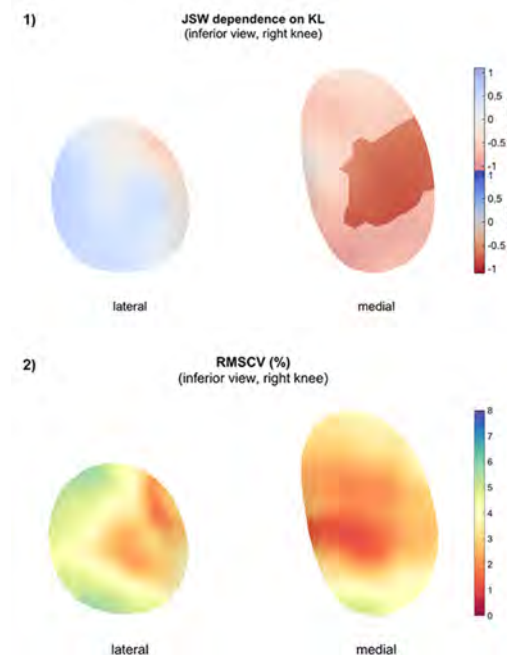
RESULTS: SPM showed that for each increment in KLG, there was a significant reduction in JSW of up to 0.75 mm at the medial tibiofemoral compartment ($p<0.05$), and a non-significant trend for an increase in JSW up to 0.5 mm at the lateral tibiofemoral compartment (Figure 1). Global interoperator bias was near zero at −0.02 mm, global limits of agreement ±0.33 mm, and global root mean square coefficient of variation (RMSCV) 3.45%. Results were even better in the central joint regions with limits of agreement down to 0.1 mm and RMSCV down to 1% in the central medial tibiofemoral compartment (Figure 2). There was negligible difference for global reproducibility values when the medial and lateral tibiofemoral compartments were analysed separately.

CONCLUSION: JSM at the knee is feasible, reproducible, and readily learned, meaning it could have an important role in the structural assessment of knee osteoarthritis in future research studies. The next stage will be to apply JSM in larger numbers to explore the relationship of 3D JSW distribution with clinical outcome measures such as pain and disability.

MULTIPARAMETRIC 3D IMAGING OF THE KNEE USING STANDING CT DATA FROM THE MULTICENTER OSTEOARTHRITIS STUDY

*Turmezei T.D., *Low S.B., **Segal N.A., ***Treece G.M., ***Gee A.H., ****Lynch J.A., ***Poole K.E.S.

*Norfolk and Norwich University Hospital, Norwich, UK
**University of Kansas Medical Center, USA
***University of Cambridge, Cambridge, UK
****University of California San Francisco, USA

INTRODUCTION: Multiparametric imaging of joint tissues is normally considered the reserve of MRI. However, CT imaging is being used increasingly to enhance our understanding of the relationship between mineralised structural features and OA disease status. Imaging analysis techniques such as joint space mapping (JSM) and cortical bone mapping (CBM) deliver multiple parameters that can be analysed in 3D with statistical parametric mapping (SPM) to look for significant associations with disease.

OBJECTIVE: To demonstrate the potential for 3D multiparametric imaging and statistical analysis in a convenience sample of standing CT (SCT) data from the Multicenter Osteoarthritis Study (MOST).
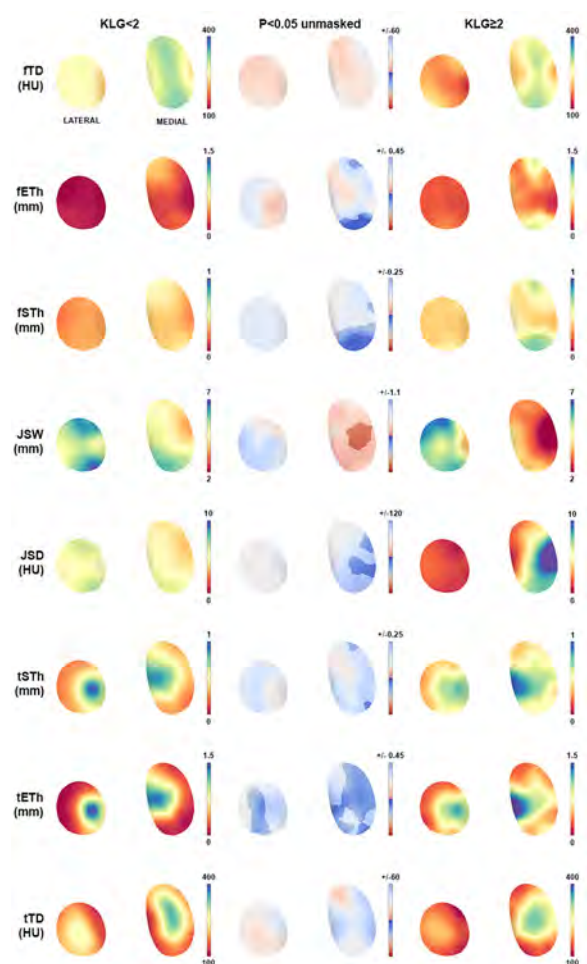
METHODS: A convenience sample of standing CT data from both knees in 23 individuals was selected from MOST with full KLG range (KLG0 n=27, KLG1 n=9, KLG2 n=7, KLG3 n=2, KLG4 n=1). A prototype commercial CT scanner (LineUp, CurveBeam, Warrington, PA) took weight-bearing images of both knees in a fixed-flexed stance. Data sets with isotropic voxels at 0.37 mm were reconstructed from cone beam projections. JSM was performed at each knee to measure JSW in 3D at the tibiofemoral compartments using a hybrid full-width-half-maximum/ threshold measurement technique. Femoral and tibial joint surfaces and JSW as the distance between them were defined by the JSM algorithm. CBM was performed at each joint surface to automatically map subchondral bone plate thickness, endocortical bone thickness, and subarticular bone trabecular density for the femur and tibia. A new concept of joint space density (JSD) was also developed, calculating mean density values between femoral and tibial surfaces. Average "halfway" joint surfaces comprised of medial and lateral patches were then registered to each individual knee patch set, with multiparametric data mapped onto the average for presentation of mean values for KLG<2 *vs* KLG≥2 and SPM results by KLG.

RESULTS: SPM results for the 8 parameters are shown in the figure: femoral/tibial trabecular density (f/tTD), femoral/tibial endocortical bone thickness (f/tETh), femoral/tibial subchondral plate thickness (f/tSTh), JSW, and JSD. Regions of significant dependence on KLG (P<0.05) were identified for all but trabecular density parameters.

CONCLUSION: Multiparametric analysis of SCT knee imaging data with JSM and CBM brings a novel quantitative 3D approach to imaging assessment of OA. This will now be applied throughout the MOST cohort to establish the relationship of these parameters with clinical measures of disease such as pain and function, and to look at whether they have greater sensitivity than current imaging standards.

RELIABILITY OF PQCT IMAGING OF SUBCHONDRAL TIBIA AND FEMUR BONE QUALITY OF THE KNEE IN A HEALTHY PILOT STUDY

*Whyte R., **Mathur S., ***Haroon N., *Naraghi A., *Probyn L., *Mohankummar R., *Linda D., ****McDonald-Blumer H., ***Chahal J., *****Johnston J.D., *Wong A.K.

*Joint Department of Medical Imaging, University Health Network, Toronto, ON
**Department of Physical Therapy, University of Toronto, Toronto, ON
***Orthopedics Division, Arthritis Program, Krembil Research Institute, Toronto, ON
****Centre for Arthritis and Autoimmune Disease, Mount Sinai Hospital, Toronto, ON
*****Department of Mechanical Engineering, University of Saskatchewan, Saskatoon, SK

INTRODUCTION: Knee Osteoarthritis (OA) has been associated with obesity but there is a sizeable proportion of individuals who are not even overweight (over 20% in our clinics receiving knee replacement). This is particularly apparent in Asian cohorts wherein the mean BMI is well under 25 kg/m^2 (Muraki et al 2015). We previously found that among 37% of a postmenopausal cohort with OA, 20% of them also had osteoporosis. It was proposed that knee OA damage could stem from bone abnormalities. We therefore developed methods for quantifying subchondral bone quality.

OBJECTIVE: To determine the test-retest reliability of measuring medial and lateral subchondral tibial and femoral bone properties using peripheral quantitative computed tomography (pQCT).

METHODS: A convenience sample of healthy volunteers without knee pain was recruited through poster advertisements and word of mouth (N=11) and individuals were excluded if pregnant or if calves or knees were larger than 430 mm in circumference. This is an ongoing study that is part of a larger knee OA study of subchondral bone fluid dynamics. Participants completed a pQCT (XCT2000) scan of the knee from the non-dominant leg with 4 different reference landmarks placed tangential to the outer cortex of each knee compartment in a coronal scout view. A single slice was obtained (scan speed 10 mm/s, 38 kVp, 0.3 mA, 2.3±0.5mm thick, 200 μm pixel size) for each compartment at 1% of tibial length distal to medial and lateral tibial plateaus; and at 2% of femoral length proximal to medial and lateral femoral condyles (modified from Bennell et al 2008). Participants were positioned with knees straight and leg aligned parallel to the scanner's z-axis. Two scans were obtained with repositioning in between. Images from each compartment were analyzed separately with regions of interests (ROI) defined by a threshold-guided periosteal contour around the entire bone, which was then reduced by 20% to represent the weight-bearing region. For the tibia, medial and lateral compartments were separated by half of the tibial width. Threshold-based segmentation was performed within these ROIs with contour mode 2, peel mode 2, and an inner threshold of 100 mg/cm^3. The cortical-subcortical component represented the subchondral bone and trabecular component represented marrow. Test-retest reliability was evaluated by root-mean-square (RMS) coefficients of variation (CV) and standard deviation (SD), including Bland-Altman limits of agreement (LOA) and short-test least significant change (LSC). A benchmark of 5% RMSCV was used to assess a parameter as being reliable.

RESULTS: In 8 women and 3 men, mean age was 33.4 ± 16.2 (range 22-69) years, height was 1.65 ± 0.10 m, weight was 63.1 ± 9.4 kg, and BMI was 23.1 ± 2.2 (range 20.0-25.1) kg/m^2. All compartments in general had similar parameters that showed RMSCV well within 5%, with subchondral BMD (1.1% at MF, 1.5% LF, 2.8% at MT, and 3.0% at LT) and marrow density (3.1% at MF, 1.8% at LF, 1.6% at MT, and 1.9% at LT) being the most consistent across compartments. ROI size was more reproducible in the medial compartment than lateral compartment. Subchondral BMD when calculated by including marrow (305.24±49.23 mg/cm^3) versus when excluding marrow (349.77±38.85 mg/cm^3) was significantly different (p<0.001). Overall, the mean subchondral BMD and marrow density to exceed before being considered clinically significant was 39.75 mg/cm^3 and 17.24 mg/cm^3, respectively.

CONCLUSION: pQCT measurement of subchondral bone density and marrow density in the 4 compartments of the knee are deemed consistently reliable. While sample size is smaller, the continued expansion of this cohort will yield a reasonable reference for clinically significant change in future studies. Imaging of OA knees may be challenged by difficulty discerning outer cortex boundaries for each compartment when bone-on-bone is present. This study should be repeated in KL 2 to 4 knees.

DICLOSURE STATEMENT: None of the authors have any conflicts of interests to declare.
CORRESPONDENCE ADDRESS: andy.wong@uhnresearch.ca

EFFECT OF UNDIFFERENTIATED ARTHRITIS AND PRECLINICAL RHEUMATOID ARTHRITIS ON THE RADIOGRAPHIC INCIDENCE AND PROGRESSION OF KNEE OSTEOARTHRITIS AND PATIENTS' SYMPTOMS

*Haj-Mirzaian A., **Mohajer B., ***Guermazi A., ***,****Roemer F.W., *Demehri S.

*Russell H. Morgan Department of Radiology and Radiological Science, Johns Hopkins University School of Medicine, Baltimore, Maryland, USA
**Tehran University of Medical Sciences, Tehran, Iran
***Department of Radiology, Boston University School of Medicine, Boston, Massachusetts, USA
****Department of Radiology, University of Erlangen-Nuremberg, Erlangen, Germany

BACKGROUND: Undifferentiated Arthritis (UA) and Preclinical Rheumatoid Arthritis (Pre-RA) are considered as early stage inflammatory arthropathy before RA occurrence. However, UA and Pre-RA may persist without ultimate progression to RA, and they may lead to other degenerative joint diseases.

OBJECTIVE: To assess the predictive ability of UA and Pre-RA in future radiographic and symptomatic incidence and progression of knee osteoarthritis (OA).

METHODS: 9062 knees from the Osteoarthritis Initiative (OAI) dataset were included in the study for follow-up time of 8 years. Subjects were categorized into UA, Pre-RA, and control groups based on the self-reported history of physician-diagnosed arthritis, connective tissue disease (CTD) questionnaire score, radiographic findings, and RA development (physician-diagnosed) in baseline and follow-up visits. Cox regression model, adjusted for relevant covariates, was performed to assess influence of the presence of arthritis (UA or Pre-RA) on hazard ratios (HR) for OA radiographic incidence (development of Kellgren-Lawrence grade$\geq$2) and progression (worsening medial joint space narrowing score$\geq$1) as well as symptomatic incidence assessed with Western Ontario and McMaster Universities Arthritis Index (WOMAC) scores.

RESULTS: Presence of arthritis was significantly associated with the higher risk of symptomatic and radiographic OA incidence in both UA and Pre-RA subjects, and radiographic OA progression only in Pre-RA subjects. Adjusted HR and 95%CI of radiographic incidence for subjects with Pre-RA and UA were 1.63 (1.02 – 2.60) and 1.48 (0.95 – 2.29), respectively; comparing to HRs for symptomatic incidence (HR (95%CI): 3.46 (2.47 – 4.83) and 1.86 (1.29 – 2.68)), respectively.

CONCLUSION: Presence of pre-clinical arthritis (UA and Pre-RA) can be predictive of future knee OA incidence and progression, regardless of RA development. This may be indicative of a shared inflammatory process in the early steps of disease.

HAND OSTEOARTHRITIS AND ITS ASSOCIATION WITH WORSENING OF MRI-BASED TIBIOFEMORAL OSTEOARTHRITIS

*Haj-Mirzaian A., *Kwee R., **Guermazi A., **,***Roemer F.W., *Demehri S.

*Russell H. Morgan Department of Radiology and Radiological Science, Johns Hopkins University School of Medicine, Baltimore, Maryland, USA
**Department of Radiology, Boston University School of Medicine, Boston, Massachusetts, USA
***Department of Radiology, University of Erlangen-Nuremberg, Erlangen, Germany

BACKGROUND: The association between the hand osteoarthritis (OA) and knee OA has been suggested by some reports, and OA has been considered as a generalized disorder in some cases. However, the exact relationship between these two medical conditions has not been studied using advanced imaging modalities to discover the underlying pathophysiological mechanism.

OBJECTIVE: To determine whether the presence of hand osteoarthritis (OA) is associated with radiographic knee OA progression (over 48-months) and MRI-based knee OA structural damage worsening (over 24-months).

METHODS: 600 subjects from the Foundation for the National Institute of Health (FNIH) project which is an IRB approved HIPAA compliant study were included (one index knee and hand in each subject). Baseline hand radiography of all subjects was measured for the presence of hand OA (modified Kellgren and Lawrence (mKL) grade >2 in each hand joints). Baseline and follow-up knee radiographic measurements and MRI OA Knee Score (MOAKS) variables for cartilage damage, bone marrow lesions, osteophytes, effusion, and Hoffa-synovitis as well as MRI-based knee periarticular bone area measurements were extracted. The association between the presence of hand OA (presence vs. absence of hand OA in each hand joint) and 48-months radiographic knee OA progression (>0.7mm reduction in medial tibiofemoral joint space width) as well as 24-months change in knee MOAKS and periarticular bone measurements were analyzed using regression model (adjusted for age and sex).

RESULTS: Presence of any carpometacarpal (CMC) OA (OR 95%CI: 1.58(0.96–2.62)) and overall hand OA (presence of any mKL>2 in all hand joints) (OR 95%CI: 1.44(0.97–2.07)) was associated with 48-month radiographic knee OA progression (approached but not reached significance). In comparison with controls, subjects with hand OA showed higher odds of worsening tibial/femoral cartilage damage (OR 95%CI: 1.38(0.95–2.01) and 1.79(1.24–2.58)) and femoral periarticular bone area expansion (Beta 95%CI: 10.54(1.40–19.69)) over 24-months. CMC OA and 24-months worsening of MRI-based tibiofemoral cartilage damage and periarticular bone area expansion were also showed approached significant associations.

CONCLUSION: Presence of hand OA, especially in CMC joint, is associated with longitudinal MRI-based knee OA-related structural damage worsening including tibial/femoral cartilage damage and periarticular bone area expansion. Hand OA (specifically CMC OA), as a marker of generalized OA, may be considered a predictor of more rapid progression of knee OA compared to patients without hand OA, which might be of relevance for inclusion in clinical trials of disease-modifying OA drug development.

STATIN THERAPY AND NODAL KNEE OSTEOARTHRITIS: RADIOGRAPHIC AND CLINICAL EVALUATION USING LONGITUDINAL PROPENSITY SCORE-MATCHED STUDY FROM THE OSTEOARTHRITIS INITIATIVE (OAI)

*Haj-Mirzaian A., **Mohajer B., ***Guermazi A., ****Conaghan P., *****Lima J., *****Blaha M., ******Bingham C., ***,*******Roemer F.W., ********Cao X., *Demehri S.

*Russell H. Morgan Department of Radiology and Radiological Science, Johns Hopkins University School of Medicine, Baltimore, Maryland, USA
**Tehran University of Medical Sciences, Tehran, Iran
***Department of Radiology, Boston University School of Medicine, Boston, Massachusetts, USA
****Leeds Institute of Rheumatic and Musculoskeletal Medicine, University of Leeds and NIHR Leeds Biomedical Research Centre, Leeds, UK
*****Division of Cardiology, Department of Medicine, Johns Hopkins University School of Medicine, Baltimore, Maryland
******Divisions of Rheumatology and Allergy and Clinical Immunology, Johns Hopkins University, Baltimore, MD, USA
*******Department of Radiology, University of Erlangen-Nuremberg, Erlangen, Germany
********Department of Orthopedic Surgery, Johns Hopkins University School of Medicine, Baltimore, MD, USA

BACKGROUND: Statins are mainstay lipid-lowering drugs and are known for their pleiotropic effects. However, the exact contribution of statins in knee osteoarthritis (OA) radiographic outcomes and characteristics of OA patients as potential responders to statin therapy is still unclear.

OBJECTIVE: To evaluate the effect of statin therapy on radiographic knee OA incidence (development of Kellgren Lawrence [KL] grade $\geq$2) and progression in joint space narrowing (JSN) according to the nodal OA status defined as the presence of Heberden's nodes (HN).

METHODS: Institutional review boards approved the HIPAA-compliant protocol, and all participants gave informed consent. Using the Osteoarthritis Initiative (OAI) cohort, we conducted a longitudinal 1:1 propensity-score (PS) matched study and defined two HN+ and HN- subcohorts considering the presence of HNs during baseline physical examination. Using per-protocol and new-user design, in each subcohort statins initiators (<1-year of intake before enrollment) and non-initiators (no intake before enrollment and during the cohort) were matched for variables concerning confounding by indication bias for OA and cardiovascular diseases. Participants were annually followed over 8-years while being monitored for adherence to statin. Association between statin use and longitudinal knee OA radiographic incidence JSN progression and nonacceptable symptomatic state (NASS) incidence were assessed using hazard ratios (HRs) of Cox regression.

RESULTS: 832-knees (416 pair matched knees of statin initiators and non-initiators) and 386-knees (193 pair matched knees) were enrolled in HN+ and HN- subcohorts, respectively. In HN+ subcohort, statin users had a 46% lower risk of OA progression in comparison with matched non-users (HR:0.54, 95%CI:0.36–0.93). In contrast, in HN- subcohort, statin use had no association with radiographic JSN progression (HR: 1.37, 95%CI: 0.74–2.53). No significant associations between statin use and radiographic incidence were detected in either subcohort.

CONCLUSION: Statin therapy may reduce the risk of radiographic knee OA JSN progression, only in subjects with nodal OA.

ASSOCIATION OF CIGARETTE SMOKING WITH MRI CARTILAGE DAMAGE OF THE KNEE: A META-ANALYSIS OF OBSERVATIONAL STUDIES

*Shakoor D., **Aghaie Meybodi M., ***Guermazi A., ****Roemer F.W., *Demehri S.

*Russell H. Morgan Department of Radiology, Johns Hopkins University, Baltimore, Maryland, USA
**Division of Gastroenterology and Hepatology, Johns Hopkins University, Baltimore, Maryland, USA
***Department of Radiology, Boston University School of Medicine, Boston, Massachusetts, USA
****Department of Radiology, University of Erlangen-Nuremberg, Erlangen, Germany

INTRODUCTION: Cigarette smoking has been associated with several musculoskeletal conditions including increased fracture risk, rheumatoid arthritis and degenerative disc disease. However, the impact of smoking on the development and progression of knee osteoarthritis (KOA) is still unclear. While there are a number of radiographic studies, suggesting a protective association between smoking and osteoarthritis, new evidence suggests detrimental effect of smoking on cartilage metabolism.

OBJECTIVE: To perform a meta-analysis of observational studies to determine the association between smoking and cartilage damage of the knee, detected by MRI.

METHODS: Observational studies describing the cross-sectional association between smoking and MRI cartilage damages of the knee were systematically searched through Medline, Embase and Scopus. Odds ratios (OR) along with their 95% confidence intervals (CI) were retrieved to calculate the weighted pooled odds ratio, using random effects model.

RESULTS: Our systematic review revealed 260 relevant records, 20 studies were reviewed at the level of full text and five studies consisting of 4078 participants were included. Two studies were performed on cohorts of patients with KOA, while the remaining were performed on healthy subjects. Pooled odds ratio between smoking and cartilage damage were 1.9 (95% CI: 1.27, 2.82) and 1.81 (95% CI: 1.17, 2.80) in healthy and KOA subjects, respectively. Low level of heterogeneity was observed in both groups. When the results were stratified based on the location of cartilage damage, the pooled odds ratio were not statistically significant (Table 1).

CONCLUSION: The findings of this study suggest a positive cross-sectional association between smoking and cartilage damages of the knee, detected by MRI, in both healthy and KOA subjects. Further studies are required to determine the causal relationship between smoking and development and progression of knee cartilage damage, since cigarette smoking could be a potentially modifiable risk factor for the development and progression of cartilage damage with significant public health implication.

Table 1. Sensitivity analysis, displaying the pooled OR based on the location of cartilage damage

	No of studies	No. of subjects	Pooled OR (95% CI)	I^2 for heterogeneity	P-value for heterogeneity
Medial tibiofemoral	3	755	2.75 (0.84-9.00)	64%	0.06
Lateral tibiofemoral	3	755	1.30 (0.74-2.28)	0	0.71
Patellofemoral	2	430	2.38 (1.00-5.66)	0	0.73
Whole	3	3648	1.77 (1.02-3.06)	47%	0.15

DO PATIENTS WITH KNEE, HIP OR HND OSTEOARTHRITIS HAVE HIGHER BONE MINERAL DENSITY? A SYSTEMATIC REVIEW AND METAANALYSIS OF OBSERVATIONAL STUDIES

*Shakoor D., **Aghaie Meybodi M, ***Guermazi A., ***,****Roemer F.W., *Demehri S.

*Russell H. Morgan Department of Radiology and Radiological Sciences, Johns Hopkins University, Baltimore, Maryland, USA
**Division of Gastroenterology and Hepatology, Johns Hopkins University, Baltimore, Maryland, USA
***Quantitative Imaging Center, Department of Radiology, Boston University School of Medicine, Boston, Massachusetts, USA
****Department of Radiology, University of Erlangen-Nuremberg, Erlangen, Germany

INTRODUCTION: Osteoporosis and osteoarthritis (OA) are two common musculoskeletal disorders in the elderly population. Several studies have indicated that high bone mineral density (BMD) is associated with higher risk of osteoarthritis at different joints including knee, hip and hand. However, some studies have suggested that patients with osteoarthritis are at risk of developing osteoporosis. Therefore, the association between BMD and OA remains unclear.

OBJECTIVE: To perform a systematic review and meta-analysis of observational studies to compare the BMD of lumbar spine (LS) and femoral neck (FN) of patients with knee OA (KOA), hip OA (HOA), hand OA (HAOA) with the healthy control without OA and determine the association between BMD and presence of OA in the mentioned joints.

METHODS: Our systematic review was performed to identify cross-sectional, case-control and cohort studies, which evaluated the relationship between KOA, HOA, HAOA and BMD. Pooled mean difference (MD) of BMD levels were calculated between subjects with HOA and control. Where possible, pooled odds ratio (OR) was calculated to determine the association of BMD and presence of HOA. Based on the level of heterogeneity, fixed or random effects model were used to calculate the pooled effect size.

RESULTS: Our systematic review included 20 studies on KOA, 9 studies on HOA and 12 studies on HAOA. Comparing KOA and control groups, pooled MD for LS and FN were 0.03 (95% CI: 0.01, 0.05, P-value=0.0004) and 0.01 (95% CI: 0, 0.02, P-value=0.006), respectively, implying a significantly higher BMD in the KOA group. Comparing HOA and control groups, pooled MD for LS and FN were 0.08 (95% CI: 0.04, 0.12, P-value=0.002) and 0.05 (95% CI: 0.03,0.08, P-value=0.002), respectively, implying a significantly higher BMD in the HOA group. Comparing HAOA and control groups, pooled MD for LS, FN were 0.04 (95% CI: 0.01, 0.07, P-value=0.02) and 0.01 (95% CI: 0.00, 0.02, P-value=0.04), respectively, implying statistically significantly higher BMD values in the HAOA group. A statistically significant association was observed between BMD and KOA (Pooled OR: 1.37,(95% CI:1.21, 1.55)), as well as BMD and HOA (Pooled OR: 1.98 (95% CI:1.49-2.64)).

CONCLUSION: Subjects with OA have higher level of BMD, in lumbar spine as well as femoral neck suggesting a systemic role rather than local biomechanical role of BMD in OA pathogenesis.

THE ASSOCIATION BETWEEN HIP OSTEOARTHRITIS AND HCV VIREMIA: A CROSS-SECTIONAL ANALYSIS USING THE ALIVE BONE COHORT

*Shakoor D., *Haj-Mirzaian A., **Brown T.T., *Demehri S.

*Russell H. Morgan Department of Radiology and Radiological Sciences, Johns Hopkins University, Baltimore, Maryland, USA
**Department of Endocrinology, Diabetes and Metabolism, Johns Hopkins University, Baltimore, Maryland, USA

INTRODUCTION: Systemic inflammatory biomarkers has been considered as key elements and potentially modifiable risk factors in the pathogenesis of osteoarthritis (OA) in subjects with chronic inflammatory conditions. In this regard, chronic viral infections such as HCV viremia is highly associated with the elevated level of systemic inflammatory cytokines. However, the possible deteriorative impact of chronic viral infections on hip OA has not been studied.

OBJECTIVE: To assess the association HCV infection status with the presence of hip osteoarthritis (including imaging and clinical features) using an available cross-sectional database

METHODS: In this prospective IRB-approved study (NIH funded ALIVE Bone cohort), four groups of patients according the status of HCV infections were included in this ancillary analysis. As part of the primary protocol, all subjects underwent non-contrast abdominopelvic CT scan, and the status of hip OA was assessed by a musculoskeletal radiologist using Kellgren-Lawrence (KL) grade. All OA-related demographic data and symptomatic finings including hip pain and stiffness using WOMAC scale were also obtained by the research coordinator during site visit. The association between the above OA features and HIV/HCV status were assessed using regression models adjusted for age, gender, BMI and concurrent methadone use (adjusted only for symptoms).

RESULT: Of the total 259 patients in the cohort, 224 had available CT scan. 75 patients (M/F: 39/36, mean age: 56.69±6.1, mean BMI: 29.46±7.1) had undetectable level of HCV viral load and were determined as control group and 184 patients had detectable level of HCV viral load and were defined as case group (m/f: 129/55, age: 56.05±6.2, BMI: 26.68±12.4). Comparing case group with the control, there was a statistically significant association between presence of HCV viremia and higher level of morning stiffness (Beta:0.149, SE:0.40, P-value=0.005) as well as stiffness throughout the day (Beta: 1.20, SE:0.43, P-value=0.006). No statistically significant association was observed between presence of HCV viremia and CT-based KL Grading of the hip joints (Beta: -0.32, SE: 0.32,P-value=0.3).

CONCLUSION: Using cross-sectional analysis in this ancillary study higher level of joint stiffness is observed in patients with the detectable HCV viral load, without associated worse hip OA features evaluated using CT examinations. Worse joint stiffness is observed in patients with the detectable HCV viral load may not be justifiable by worse hip OA status; other etiologies such as myopathy remain to be investigated.

Table 1. Association between pain under different conditions and HCV viral status.

	BETA (SE)	P-VALUE
BOTH SIDES		
PAIN IN STAIR	0.75 (0.38)	0.051
PAIN IN BED	0.87(0.39)	0.4
PAIN WHILE SITTING	0.31 (0.36)	0.3
PAIN WHILE STANDING	0.51 (0.37)	0.1
PAIN WHILE WALKING	0.56 (0.37)	0.1

TALAR OSTEOCHONDRAL LESION OF THE ANKLE: A METANALYSIS OF DIAGNOSTIC PERFORMANCE OF MAGNETIC RESONANCE IMAGING

*Shakoor D., **de Cesar Netto C., **Schon L.C., ***Osgood G., ***Shafiq B., *Demehri S.

*Russell H. Morgan Department of Radiology and Radiological Sciences, Johns Hopkins University, Baltimore, Maryland, USA
**Department of Orthopedic Surgery, Union Memorial Hospital, Baltimore, Maryland, USA
***Department of Orthopedic Surgery, Johns Hopkins University, Baltimore, Maryland, USA

INTRODUCTION: Osteochondral lesions of the talus (OLT) is defined as a separation of a fragment of articular cartilage which could be accompanied by the underlying subchondral bone. Previous studies have reported that magnetic resonance imaging (MRI) could offer comprehensive evaluation of the intra-articular lesions of the ankle. However, the overall evidence regarding the performance of MRI in diagnosing OLTs remains to be determined.

OBJECTIVE: To investigate diagnostic performance of MRI in diagnosing OLTs, using arthroscopy or surgery as the standard of reference

METHODS: A comprehensive literature search (until March 2019) was performed and original research studies reporting diagnostic performance of MRI and magnetic resonance arthrography (MRA) in the detection of OLTs were included. Pooled values of sensitivity and specificity were calculated using fixed or random effect models based on the level of heterogeneity

RESULTS: Out of 887 identified records, 9 studies (424 MRI examinations) were included. No studies have reported the diagnostic performance of MRA or 3T MRI. One study was performed with 1 T scanner and the rest were performed by 1.5 T scanner. Pooled values of sensitivity, specificity and diagnostic odds ratio (DOR) were 74.9% (95% confidence interval (CI): 57.8%-86.7%), 94.9% (95% CI: 57.3%-99.6%) and 56.0 (95% CI: 3.58-875.9), respectively. Pooled estimates of positive and negative likelihood ratios were 14,7 (1.2-181.6) and 0.26 (0.14-0.48), respectively. High degree of heterogeneity was observed for sensitivity ($I2 =88\%$) and specificity ($I2 =88\%$)

CONCLUSION: MRI has high level of specificity in detecting abnormality in a normal cartilage, however this modality doesn't have high sensitivity to rule out osteochondral lesions of talus. MRI exams performed with 1.5 T or lower scanners are limited in providing data for correct diagnosis of OLTs, thus, the decision to perform surgery should not be solely based on MRI findings. Given the paucity of current literatures, future investigation of the diagnostic performance for other advanced imaging modalities such as MRA and 3 T MRI for OLT diagnosis are warranted in future studies.

WEIGHT-BEARING SYNDESMOTIC MEASUREMENTS IN ANKLE INJURIES: COMPARISON WITH THE NORMAL SIDE USING A SEMI-AUTOMATIC SOFTWARE

*Shakoor D., **Aghaie Meybodi M., ***de Cesar Netto C., ****Osgood G., ****Shafiq B., *****Brehler M., *****Zbijewski W., ***Schon LC., *Demehri S.

*Russell H. Morgan Department of Radiology and Radiological Sciences, Johns Hopkins University, Baltimore, Maryland, USA
**Division of Gastroenterology and Hepatology, Johns Hopkins University, Baltimore, Maryland, USA
***Department of Orthopedic Surgery, Union Memorial Hospital, Baltimore , Maryland, USA
****Department of Orthopedic Surgery, Johns Hopkins University, Baltimore, Maryland, USA
*****Department of Biomedical Engineering, Johns Hopkins University, Baltimore, Maryland, USA

INTRODUCTION: Assessment of syndesmotic injuries in ankle fractures can be a challenging task. Although CT images provide a comprehensive visualization of the ankle joint, prior reports on CT scan was not performed under weight bearing (WB). To optimize better evaluation of syndesmotic injuries, comparison of the injured side to the normal side is recommended, however, this approach has not fully addressed the challenges of syndesmotic assessment.

OBJECTIVE: To perform syndesmotic measurements on WB images and compare the results with the normal contralateral side, using a semi-automatic software on images obtained from Cone Beam CT (CBCT)

METHODS: Patients with prior unilateral ankle injuries were recruited and were bilaterally scanned 12 weeks following the injury in both WB and non-weight-bearing (NWB) conditions.Twelve syndesmosis measurements were obtained by two readers using JMAT (Brehler et al SPIE Med Im 2017).This software package was developed to provide multi-planar rendering of the CBCT volumes to guide the user through selection of anatomical points and compute the measurements.At 10 mm above tibial plafond, 5 diastasis measurements including ATFD, PTFD,TFCS,diastasis and angular measurements,3 rotation and 2 translation measurements were performed. At 5 mm below talar dome, medial and lateral clear space (MCS and LCS) were obtained. WB and NWB measurements were compared between injured and normal ankles using paired t-test.

RESULTS: Nine men and 16 women with mean age of 45 years were included.Fourteen patients underwent operative treatment for their ankle fracture without receiving syndesmotic fixation and the rest received non-operative treatment. In WB images, mean values of Tang rotation and MCS were significantly higher in the injured side than the normal ankle (P-value<0.05). In NWB images,mean values of Tang rotation were significantly higher in the injured ankle than the normal side (P-value<0.05).Mean values of angular measurement in both WB images(P-value<0.001) and NWB images (P-value=0.01) were significantly lower on the injured side.

CONCLUSION: Comparison with the contralateral asymptomatic ankles,the ankles with fractures have distinct tibiofibular syndesmotic measurement differences between WB and NWB scan acquisitions. In order to improve the detectibility of syndesmotic injuries, distinct tibiofibular syndesmosis measurements may be used in clinical practice according to the weight bearing mode of image acquisition (WB vs NWB) using dedicated extremity CBCT.

DIAGNOSTIC PERFORMANCE OF DIFFERENT IMAGING MODALITIES FOR THE DETECTION OF CHONDRAL LOSS OF THE WRIST

*Shakoor D., **Aghaie Meybodi M., ***Shores J.T., ****Lifchez S.D., *Demehri S.

*Russell H. Morgan Department of Radiology and Radiological Sciences, Johns Hopkins University, Baltimore, Maryland, USA
**Department of Gastroenterology and Hepatology, Johns Hopkins University, Baltimore, Maryland, USA
***Department of Plastic and Reconstructive Surgery, Johns Hopkins Univeristy. Baltimore, Maryland, USA
****Department of Orthopedic Surgery, Johns Hopkins University, Baltimore, Maryland, USA

INTRODUCTION: Due to the complex anatomy of the wrist joint, wrist arthroscopy is often required for the assessment of patients with wrist pain. Advanced imaging modalities such as magnetic resonance imaging (MRI), MR arthrography (MRA), and CT arthrography (CTA) have shown promising results in detecting chondral lesions of the wrist. However, the optimal imaging modality remains to be determined.

OBJECTIVE: To evaluate the diagnostic performance of MRA, MRI and CTA in detecting chondral lesions of the wrist, with arthroscopy as the standard of reference.

METHODS: A comprehensive literature search (until March 2019) was performed by two investigators independently and original studies on diagnostic performance of MRI, MRA or CTA in detecting chondral lesions of the wrist were included. Pooled values of sensitivity and specificity were obtained using fixed or random effect models based on the level of heterogeneity. To compare the diagnostic odds ratio (DOR) of these three modalities, DOR was regressed against their category and relative DOR (rDOR) was obtained.

RESULTS: Our literature search yielded 767 related records. Of these, 15 eligible studies were read at the level of full text and 7 studies were included. Results of 109 CTA exams, 241 MRA exams and 191 MRI exams were pooled in three separate categories. All MRI were performed by 1.5 T scanners. The pooled estimates of sensitivity of CTA, MRA and MRI were 94% (95% confidence interval: 80%-99%), 63% (49%-75%) and 45% (35%-55%), respectively. The pooled estimates of specificity of CTA, MRA and MRI were 98% (94%-100%), 97% (94%-99%) and 83% (79%-87%), respectively. A high degree of heterogeneity was observed ($I^2>50\%$). Comparing DOR of all 3 modalities, CTA provided the highest performance (rDOR=3.2, P-value=0.006). MRA performed better than MRI (rDOR=9.1 P=0.04).

CONCLUSION: For detection of chondral lesions of the wrist, CTA appears to be more accurate than MRA and MRI utilizing 1.5 T scanners. MRA was more accurate than MRI performed with similar magnetic field. Further studies are warranted to determine the accuracy of 3T MRA/MRI and compare its performance with CTA.

WHAT DOES IT FEEL LIKE TO MAKE A DIFFERENCE?

Our scientific team understands the therapeutic and support needs of our patients, which allows them to better discover and develop meaningful therapies. Can you imagine a place where passion and collaboration can change patients' lives? **We can.**

EMD SERONO

Curiosity Drives Our Innovation

US/NPR/0318/0117